Copyright Warning & Restrictions

The copyright law of the United States (Title 17, United States Code) governs the making of photocopies or other reproductions of copyrighted material.

Under certain conditions specified in the law, libraries and archives are authorized to furnish a photocopy or other reproduction. One of these specified conditions is that the photocopy or reproduction is not to be "used for any purpose other than private study, scholarship, or research." If a, user makes a request for, or later uses, a photocopy or reproduction for purposes in excess of "fair use" that user may be liable for copyright infringement,

This institution reserves the right to refuse to accept a copying order if, in its judgment, fulfillment of the order would involve violation of copyright law.

Please Note: The author retains the copyright while the New Jersey Institute of Technology reserves the right to distribute this thesis or dissertation

Printing note: If you do not wish to print this page, then select "Pages from: first page # to: last page #" on the print dialog screen

INFORMATION TO USERS

This manuscript has been reproduced from the microfilm master. UMI films the text directly from the original or copy submitted. Thus, some thesis and dissertation copies are in typewriter face, while others may be from any type of computer printer.

The quality of this reproduction is dependent upon the quality of the copy submitted. Broken or indistinct print, colored or poor quality illustrations and photographs, print bleedthrough, substandard margins, and improper alignment can adversely affect reproduction.

In the unlikely event that the author did not send UMI a complete manuscript and there are missing pages, these will be noted. Also, if unauthorized copyright material had to be removed, a note will indicate the deletion.

Oversize materials (e.g., maps, drawings, charts) are reproduced by sectioning the original, beginning at the upper left-hand corner and continuing from left to right in equal sections with small overlaps. Each original is also photographed in one exposure and is included in reduced form at the back of the book.

Photographs included in the original manuscript have been reproduced xerographically in this copy. Higher quality 6" x 9" black and white photographic prints are available for any photographs or illustrations appearing in this copy for an additional charge. Contact UMI directly to order.

UMI

A Bell & Howell Information Company
300 North Zeeb Road, Ann Arbor MI 48106-1346 USA
313/761-4700 800/521-0600

ABSTRACT

REMOVAL OF VAPORS FROM AIR BY SELECTIVE MEMBRANE PROCESSES

by
Junseok Cha

The behaviors of different membrane modules for the selective removal and recovery of water vapor and some volatile organic compounds (VOCs) from N_2 have been studied. For the selective permeation-based removal of water vapor from N_2, a polymeric water-swollen gel membrane in the form of Cuprophan hollow fiber was employed. A thin film composite type rubbery membrane module was studied for the selective removal of VOCs like toluene or methanol from N_2 by permeation. The usefulness of pore-condensation phenomenon-based removal of toluene or xylene from N_2 was explored using a microporous ceramic tubular membrane.

The experimental performance of Cuprophan hollow fiber membrane module was studied for the permeation removal of water vapor from N_2. A simple model was developed taking into account the observed exponential dependence of moisture permeance on relative humidity. Water vapor was removed continuously and efficiently through the Cuprophan hollow fiber membrane; the experimentally obtained performances were well described by the model. The membrane showed considerable selectivity for water vapor over N_2 and water vapor over toluene vapor.

Short hollow fiber modules employing an ultrathin nonporous silicone coating membrane on a porous substrate were found to be extremely productive in removing toluene or methanol from N_2 at atmospheric pressure by an applied permeate-side vacuum. Removal of 90-99 % of VOC was achieved at low feed gas flow rates over a

wide range of VOC concentrations. The membrane exhibited high selectivities for the VOC over N_2; VOC permeance was extremely concentration-dependent.

Selective removal of toluene or xylene from N_2 via pore-condensation in a microporous tubular ceramic membrane having 50 Å pores was not found to be as efficient. This is likely to be due to the difficulty of achieving pore condensation in larger pores and at lower VOC partial pressures.

REMOVAL OF VAPORS FROM AIR BY SELECTIVE MEMBRANE PROCESSES

by
Junseok Cha

A Dissertation
Submitted to the Faculty of
New Jersey Institute of Technology
in Partial Fulfillment of the Requirements for the Degree of
Doctor of Philosophy

Department of Chemical Engineering,
Chemistry and Environmental Science

May 1994

APPROVAL PAGE

REMOVAL OF VAPORS FROM AIR BY SELECTIVE MEMBRANE PROCESSES

Junseok Cha

Dr. Kamalesh K. Sirkar, Dissertation Advisor — Date
Professor of Chemical Engineering and Sponsored
Chair in Membrane Separations and Biotechnology
New Jersey Institute of Technology

Dr. Henry Shaw, Committee Member — Date
Professor of Chemical Engineering
New Jersey Institute of Technology

Dr. Piero Armenante, Committee Member — Date
Professor of Chemical Engineering
New Jersey Institute of Technology

Dr. Demetri Petrides, Committee Member — Date
Assistant Professor of Chemical Engineering
New Jersey Institute of Technology

Dr. Namunu Meegoda, Committee Member — Date
Associate Professor of Civil and Environmental Engineering
New Jersey Institute of Technology

BIOGRAPHICAL SKETCH

Author: Junseok Cha

Degree: Doctor of Philosophy in Chemical Engineering

Date: May 1994

Undergraduate and Graduate Education:

- Doctor of Philosophy in Chemical Engineering, New Jersey Institute of Technology, Newark, NJ, 1994
- Master of Science in Chemical Engineering, Seoul National University, Seoul, Korea, 1984
- Bachelor of Science in Chemical Engineering, Seoul National University, Seoul, Korea, 1980

Major: Chemical Engineering

Presentations and Publications:

1. Majumdar, S, Sengupta, A, Cha, J.S., Sirkar, K.K.,"Simultaneous SO_2/NO Separation from Flue Gas in a Contained Liquid Membrane Permeator", Ind. Eng. Chem. Res., Vol.33, No.3, 1994, 667-675.
2. Majumdar, S, Cha, J.S., Papadopoulos, T.H., Sirkar, K.K., "A Novel Liquid Membrane Technique for Removal of SO_2/NO_x from Flue Gas", ACS Preprints, Div. Petroleum Chemistry, 36 (1), 1992, 25-32.

3. Kim, E.Y., Kim, J.J, Cha, J.S., Seo, S.B., Ko, Y.H, "Outside Flow Type Hollow Fiber Membrane Blood Oxygenator with Built-in Blood Reservoir and Heat Exchanger", Korean Patent No. 35459, 1991.

4. Kim, S.S, Cha, J.S, Kim, J.J, Kim, E.Y, "Morphological Studies of Cellulose Acetate Hollow Fiber Membranes", J. Memb. Sci., 37, 1988, 113-129.

5. Kim, S.S, Cha, J.S, Kim, J.J, Kim, E.Y, "Morphological Studies on Melt Spun Cellulose Acetate Hollow Fiber Membranes", 86 Korean and Foreign Scientist Conference Summer Symposium Book, 1986, 235-240.

This dissertation is dedicated to
my wife Bokyung and daughter Jimin

ACKNOWLEDGMENT

I greatly express my gratitude to Prof. K. K. Sirkar for his constant help through many ideas, thoughtful comments, guidance and criticisms throughout this research. I am sure that his nourishing attitude and responsibility for research has influenced me considerably. I am also grateful to the members of the dissertation committee, Dr. H. Shaw, Dr. P. Armenante, Dr. D. Petrides and Dr. N. Meegoda for all the helpful suggestions made.

The financial supports during the earlier part of this research through Department of Energy (DOE), Center for Membranes and Separation Technologies at Stevens are gratefully appreciated. The financial support provided from Center for Waste Reduction Technology (CWRT) of American Institute of Chemical Engineers (AIChE) for the work reported here in chapter 3 is also greatly acknowledged.

I am really indebted to many people without whose help this work would not have been possible. I would like to thank especially Dr. Majumdar, Dr. Guha and Dr. Yang for many useful suggestions and friendship. Good advice from Dr. Bhaumik during hardtimes is also very much appreciated. Thanks are also due to Dr. Raphael Li who has made significant contributions in completing this research successfully. I would like to extend my thanks to Stephanie, Poddar, Shanbhag, Dilip and also our new members, Malik, Gordana and Sarma for friendship and sharing many pleasant times. Especially I wish to thank Shanbhag and Sarma for helping me in the technical editing of the manuscript. I express my thanks also to Mrs. Judy Kapp for her kind help in many ways and organizing many enjoyable parties.

A heartful gratitude is due to my wife Bokyung for her love, encouragement and patience and my beloved daughter Jimin whose cute playfulness has always given me a joy. Finally and most importantly, I express my sincere thanks to God.

TABLE OF CONTENTS

TABLE OF CONTENTS
(Continued)

TABLE OF CONTENTS
(Continued)

TABLE OF CONTENTS
(Continued)

LIST OF TABLES

LIST OF TABLES
(Continued)

LIST OF FIGURES

LIST OF FIGURES
(Continued)

LIST OF FIGURES
(Continued)

LIST OF FIGURES
(Continued)

LIST OF FIGURES
(Continued)

NOMENCLATURE

A	:	Membrane surface area in a module $\pi\ d_{lm}\ l\ N$, cm^2
a,b	:	Regression constants determined from experimental data
d_i, d_o	:	Inside and outside diameters of homogeneous Cuprophan hollow fiber membrane, cm
d_{lm}	:	Logarithmic mean diameter defined in equation (2.2), cm
dS	:	Differential surface area defined in equation (2.2), cm^2
F_i, F_o, F_p	:	Molar flow rate of water vapor/VOC at feed inlet end, at feed outlet end, and permeate, gmol/min
J_w, J_{VOC}	:	Flux of water vapor/VOC, gmol/min.cm^2
k	:	Constant defined by equation (2.7)
L, L_f, L_w	:	Total feed side molar flow rate per fiber at any location and at the feed inlet end, at the feed outlet end of the permeator, gmol/sec
l	:	Length of the permeator, cm
M	:	Molecular weight of the condensate, g/gmol
N	:	Number of fibers in a module
P, P_f, P_w	:	Feed side total pressure at any location, at the feed inlet end, at the feed outlet end of the permeator, cm Hg
p, p_l	:	Permeate side total pressure at any location, at the permeate outlet end, cm Hg
P_1	:	Gas phase pressure on upstream side of the membrane, cm Hg
P_2	:	Gas phase pressure on downstream side of the membrane,cmHg
P_c	:	Capillary pressure defined in equation (4.2), cm Hg
P_o	:	Saturated vapor pressure of planar surface, cm Hg
P_t	:	Saturated vapor pressure for capillary, cm Hg
$(\Delta p)_w$,$(\Delta p)_{VOC}$	:	Partial pressure difference of water vapor/VOC, cm Hg
Q_w	:	Permeability of water vapor, (gmol.cm)/(cm^2.sec.cm Hg)

NOMENCLATURE
(Continued)

Q_w/δ_m	:	Permeance of water vapor, gmol/(cm^2.sec.cm Hg)
r_p	:	Radius of the pore, cm
R	:	Gas constant, (atm.l)/(gmol.°K)
T	:	Absolute temperature, °K
V, V_l	:	Permeate side gas flow rate per fiber at any location, at the permeate outlet end, gmol/sec
x, x_f, x_w	:	Mole fraction of water vapor in the feed side gas mixture at any location, at the feed inlet end, and at the feed outlet end of the permeator
$x_{f,avg}$	:	Averaged mole fraction of water vapor in the feed side
x_i, x_o	:	Mole fraction of VOCs at the feed inlet and outlet end
y, y_l	:	Mole fraction of water vapor in the permeate side gas mixture at any location, at the permeate outlet end
z	:	Distance of any permeator location, starting from feed outlet end, cm

Greek Letters

α	:	Separation factor
δ_m	:	Wall thickness of the hollow fiber membrane, cm
ρ	:	Density of the condensate, g/cm^3
γ	:	Interfacial tension, dyne/cm
θ	:	Contact angle between the liquid-solid surface

CHAPTER 1

INTRODUCTION AND OBJECTIVES

1.1 Introduction

Volatile organic solvents are routinely used as carrier liquids and dissolving agents in many small and large industrial processes such as printing and coating, degreasing of metal parts, dry cleaning operations etc. During certain steps, these volatile organic compounds (VOCs) are vaporized into the air and finally escape into the atmosphere via process exhaust air stream. The solvents encountered in such air streams are toluene, xylene, acetone, trichloroethylene, ethanol, methanol etc. These organic vapors in atmosphere are a serious environmental problem. They react with nitrogen oxides and other airborne chemicals to form ground-level ozone which is a major component in the formation of smog (Ruddy et al., 1993). These VOCs in air are also a large financial loss. For a long time, these volatile organic compounds were simply discharged into the atmosphere. Stricter environmental regulations require currently some sort of treatment.

Various physical or chemical principles can be used to separate different kinds of industrially-emitted VOCs. The choice depends mostly on the chemical and physical properties of the species to be separated and on the technological conditions under which the VOCs are formed and emitted into the atmosphere. The most common methods of reducing emissions are : (i) adsorption on activated carbon; (ii) incineration; (iii) condensation; (iv) absorption in a liquid and so on. Among these methods, carbon adsorption and incineration are more popular and already in the marketplace.

In carbon adsorption processes, typically three large beds of activated carbon are used. Two of the beds are used usually for removing the organic solvents from the feed air and the third bed is utilized for stripping with steam. Although this process is more economical than the destructive incineration method, this process has the shortcoming of

being a cyclic batch operation due to the sorbent regeneration. Not all organic solvents are suitable for carbon adsorption. Some hydrocarbons which have low boiling points are not adsorbed by the carbon and some chlorinated solvents are not stable during the steam regeneration cycle. The incineration process is quite simple, reliable and inexpensive to install and since the process deals with the burning of the organic solvent vapors, this process is quite economical for relatively concentrated streams. For lower concentrations significant additional energy is needed; further new hazardous compounds such as dioxin, phosgene and hydrogen cyanide can be generated. Newer technologies are also being considered. Prominent among them are biofiltration, UV oxidation and membranes.

Membrane separation processes are being explored increasingly for removing VOCs from air. Membrane processes are simple and reliable. For the efficient performance of the process, the membrane, which is the key component in the membrane-based separation system, should ideally have the following properties : (i) high permeability for the vapor component; (ii) high selectivity between vapor/gas components; (iii) high chemical, thermal, and mechanical stability for the membrane-permeant system. This membrane technology can be expected to have a great potential in comparison with the conventional methods because it has many advantages. The modular nature and a high surface area per unit volume are unique advantages of membrane technology for the removal of VOCs from air/N_2.

The VOC in air is a vapor which is condensible unlike N_2,O_2,CO_2 etc. which are not condensible at room temperature and pressure. There is another species in atmosphere, namely, water vapor which is also condensible. There are then two classes of vapors in atmosphere, inorganic ones like H_2O,HCl,HNO_3, sometimes called volatile inorganic compounds (VICs) and organic ones like toluene, xylene, methanol, ethanol etc. identified as VOCs. Removal of both VOCs and VICs by membrane modules is the focus of this study. The separation of one gas from a gas mixture by preferential permeation has been investigated over the years (Sengupta and Sirkar, 1986). Membrane technologies for such

preferential permeation-based systems have been applied in large scale to industrial separations of gas mixtures because they offer low capital and operating costs as well as low energy consumption. However, only recently membrane technologies are becoming available for vapor removal.

A variety of membrane transport mechanisms and corresponding separation processes may be used to separate the vapor species from air. This will depend on the vapor species, nature of the membrane, conditions of separation etc. The transport-cum-separation mechanisms may be identified as follows [Sengupta and Sirkar, 1986; Koros, 1990] :

1. Poiseuille flow
2. Knudsen flow
3. Surface diffusion
4. Pore condensation
5. Pore blockage
6. Permeation (solution-diffusion).

Depending on the pore size, gas pressure, and temperature, membranes having mechanisms 1 to 5 are called either microporous or porous. Membranes having permeation are called nonporous. Of all these methods, the last three methods of membrane separation have been studied to a limited extent only for vapor removal. This thesis explores vapor separation processes and technologies using two different mechanisms, permeation and pore condensation, using a variety of membranes.

The focus here is on selective permeation-removal of vapor from air/N_2 through the membrane in a module. Since the amount of vapor in N_2/air is small, the membrane area required would be smaller than if N_2 or air were being selectively removed. On the other hand, the driving force for a vapor across the membrane is very small if a vacuum is maintained on the permeate side. The driving force for N_2/air can be much larger, but the vacuum pump capacity and power requirement would be much

greater by few orders of magnitude. Therefore selective vapor permeation is more desirable. The search is extended naturally to membranes and transport processes that yield very high permeabilities for vapors compared to the usually low membrane permeabilities for N_2 and O_2.

The permeation of a vapor by solution-diffusion through a nonporous polymeric membrane will depend amongst others on the nature of the membrane. The membrane may be glassy or rubbery or a gel. In a glassy polymeric membrane, the dimensions of the free volume containing regions are usually small enough to severely hinder the diffusion of larger solvent molecules (compared to the small molecules of the so-called permanent gases like He, N_2, O_2 etc.). Since there are stiff polymer backbones in glassy polymers, small molecules of gases like H_2 and He can diffuse much faster through the small openings between rigid polymer backbones than gaseous species having larger diameters like organic solvents. Therefore glassy polymeric membranes may not be used for selective VOC permeation-based separation. Of the other two, rubbery polymeric membranes are being explored for removing VOCs from air.

1.1.1 Gel Membranes

Polymeric gel membranes may have water or an organic solvent as the swelling agent. Cuprophan, a highly hydrophilic membrane, becomes a hydrogel by absorbing water/moisture from the ambient air. The water-swollen regenerated cellulose membrane of Cuprophan is an example of a gel membrane. A few studies have been carried out here using such a water-swollen gel membrane for gas/vapor separation.

The permeability coefficient of water vapor through a polymeric membrane is governed both by the diffusion coefficient and the solubility of water in the polymer. The sorption characteristics of water in various polymers depend not only on the nature of the polymers (hydrophilic or hydrophobic) but also on the polar groups of the polymer matrix. The sorption behavior of the water in cellulosic materials (a hydrophilic polymer)

was investigated by many researchers (Valentine, 1958; Urquhart, 1960). They showed that the typical equilibrium sorption was type II isotherm in the B.E.T. classification. The more hydrophobic polymers sorb minute quantities of water and it was reported that they obey Henry's law over the whole range of the relative pressure (Yasuda and Stannett, 1962). Here the relative pressure is defined as the partial pressure of water vapor divided by the saturation water vapor pressure.

The solubility tendency of water generally becomes higher when more polar groups are present in the polymer matrix. Usually the permeability of water vapor is not a constant but depends on the relative humidity (or partial pressure of water vapor). The relative permeability coefficient of regenerated cellulose film to oxygen as a function of the relative pressure was reported by Pilar (1960) at 25 °C in the presence of water vapor. It has an extreme sensitivity especially when the relative pressure was over 80%. Notley (1963) observed also large increases in the oxygen permeability of Cellophane film when water vapor was present. The permeability of water vapor can also be a function of temperature, membrane thickness, physical state of water, and the structure of the polymer (Barrie, 1968).

Bonne et al. (1990) invented a dehumidification process for the ambient atmosphere by means of a thin microporous membrane medium. They demonstrated two different methods of removing the water vapor from atmosphere using a hygroscopic collecting liquid (triethylene glycol, TEG) which has an affinity for the water vapor. In one method, the hygroscopic collecting liquid was immobilized in the pores of the microporous cellulose fibers and in the other method, the hygroscopic collecting liquid was flowing inside the polypropylene hollow fibers without wetting the fibers. They also attempted to remove the water vapor by the Kelvin effect using a porous membrane having sufficiently small pore size (< 30 Å).

There has been no systematic study of water vapor separation from air/N_2 by Cuprophan hollow fiber membranes. Such fibers are available in plenty and are probably

the cheapest of all hollow fibers. Further, since VOCs and VICs are present in air/N_2 an investigation of water vapor selectivity over such VOCs etc. through a Cuprophan hollow fiber would appear to be logical. Since these Cuprophan hollow fibers contain isopropylmyristate used as a spinning aid, special treatments were employed here to use such membranes for gas/vapor transport. Chapter 2 of this thesis reports experimental investigations of vapor separation through such a hollow fiber membrane. Water vapor transport has been studied extensively and a simplified model has been developed to describe the observed separation behavior in the permeator. The transport of VOCs (e.g. toluene, methanol) in the presence of water vapor has also been studied briefly.

1.1.2 Rubbery Membranes

For gas/vapor permeation through any dense polymeric membrane, the important parameters are diffusion and solubility coefficient of the gas/vapor in the polymer. The diffusion coefficient of a molecule decreases generally with increasing molecular size, but the solubility coefficient increases commonly with increasing molecular size. It also increases with the condensibility of the gas/vapor molecules (usually the species which has the higher critical temperature is more condensible). The transport of a gas/vapor through a rubbery polymeric membrane is determined more by its solubility coefficient than by its diffusion coefficient. The high solubility of organic vapors in rubbery polymers is the main reason for their high permeability. In addition, the permeabilities of simple gases are in almost all polymers independent of their partial pressure in the gas phase. On the other hand, the permeabilities of organic solvent vapors increase drastically with increasing solvent vapor pressure in the gas phase.

Baker et al. (1987) conducted a number of experiments for the separation of nitrogen and organic vapors using a variety of flat polymeric membranes having small areas. They showed that the permeability of the VOCs studied (e.g. octane, toluene, trichloroethane, acetone) depends on the vapor pressure (increasing solvent permeability

at higher solvent partial pressure). The permeabilities of the organic vapors were orders of magnitude higher than that of nitrogen for rubbery polymeric membranes. They have also plotted the permeability vs. selectivity for toluene and acetone in various rubbery membranes at 40 °C. Among these membranes, silicone rubber showed the highest VOC permeability and Neoprene rubber exhibited the highest selectivity for toluene/N_2 and acetone/N_2.

Strathmann et al. (1986) developed composite membranes in flat sheet as well as hollow fiber form using poly(dimethylsiloxane) as the selective barrier and a suitable module for the separation of organic vapors from waste air streams. They described the parameters determining the selectivity and permeability of a membrane. They measured the permeability of various solvents (like octane, toluene, trichloroethane, acetone) as a function of their vapor pressure and showed 100 - 1,000 times higher permeability of organic solvent over nitrogen. They have also described the recovery of toluene from waste air streams in a painting process and estimated the costs for the process.

Kimmerle et al. (1988) tested acetone/air separation using a thin film composite hollow fiber membrane using poly(dimethylsiloxane) laminated to the inner surface of a polysulfone hollow fiber. Although the actual silicone coating thickness was 1.5 μm, they estimated the theoretical coating thickness to be 12.7 μm due to the low porosity of the polysulfone substrate. They performed stationary and nonstationary experiments to characterize the process parameters. They have also carried out a brief economic evaluation of the recovery cost of the solvent.

Wijmans and Helm (1989) used MTR (Membrane Technology & Research, Menlo Park, CA) multilayer composite membranes assembled into spiral-wound modules for the separation of organic vapors from N_2. They showed that the process was more economic than carbon adsorption process if the organic compound concentration is relatively high and if the air stream to be treated is small. They also estimated the approximate cost of a two-stage system to remove 90% trichloroethane from degreasing bath off-gas.

Behling et al. (1989) used poly(ether imide) as the porous supporting material. They suggested that it has a higher permeability than a polysulfone membrane and has a comparable pore size and it is also much more stable against fuel components like benzene and toluene than polysulfone. Feng et al. (1991) prepared a membrane using a glassy polymeric material alone without any silicone coating. They chose aromatic polyimide material and introduced asymmetricity to the membrane structure to increase the permeation rate. They obtained higher (about 7 times) permselectivity compared to silicone rubber membrane for a couple of organic vapor/N_2 mixtures.

Blume et al. (1991) investigated the sorption and permeation behavior of several organic vapors (ethanol, methylene chloride, chloroform, toluene etc.) in poly(dimethylsiloxane) flat membrane. They measured the solubility and permeability coefficients and observed their strong dependence on the vapor partial pressure. They have also shown that higher sorption does not necessarily lead to a higher permeability value and explained this effect using the concentration dependent diffusion behavior of poly(dimethylsiloxane) film toward these organic vapors.

Although silicone, i.e. poly(dimethylsiloxane), membrane has been used in a number of studies, the resulting membranes or modules used are not highly efficient. For example, the use of a low porosity polysulfone substrate in Kimmerle et al. (1988) led to a very low value of permeability coefficient/membrane thickness; this quantity determines directly the flux of a VOC other conditions remaining constant. Similarly, the MTR-based membranes are flat and supported and are used in the spiral wound form (Baker et al., 1987; Wijmans and Helm, 1989). Therefore the membrane surface packing density in the module is an order of magnitude lower than that possible in a hollow fiber module. This increases the module cost substantially.

Using ultrathin silicone membranes on an appropriate microporous hollow fiber substrate, VOC removal in the highly efficient hollow fiber configuration has been carried out and reported in Chapter 3 of this thesis; this study thereby eliminates the

shortcomings of both Kimmerle et al. (1988) and Baker et al. (1987). The VOCs explored here using VOC/N_2 mixtures permeating through the hollow fibers are toluene and methanol. The concentration levels of these species were varied from 2000 ppmv to 1.4 % for toluene and 500 ppmv to 5 % for methanol.

1.1.3 Microporous Ceramic Membranes

When the VOC concentration is relatively high (2 - 10 %), it is possible to explore the use of microporous/porous membranes for selective separation of vapors from air/N_2. If the pore size of the membrane is relatively small (< 40 Å), the transport mechanism for gases and vapors through this solid membrane can be Knudsen diffusion or surface diffusion or Poiseuille flow. The transport regime is primarily determined by the membrane pore size and pore structure, the nature of the gas and vapors and their chemical interaction with the membrane. If the vapors are highly condensible, there is a possibility of multilayer adsorption and finally pore condensation can occur inside the fine pores of the solid membrane. Since pore condensation will reduce or totally block the passage of the nonadsorbable gas from the feed gas mixture, it is expected that highly enriched condensible vapor species will be obtained in the permeate via a proper driving force. This condition will also yield a high value of separation factor.

Microporous polymeric membranes usually have a pore size distribution. Thus a variety of transport mechanisms may operate simultaneously; the vapor/N_2 selectivity will be affected since pore condensation-based selectivity is much higher than those based on other mechanisms. Ceramic membranes, currently available, however have essentially one pore size (i.e. a very narrow pore size distribution). Therefore they may be ideal for pore-condensation studies of VOC separation.

Carman (1952) investigated the permeability of silica powder and reported that in pore condensation, the capillary pressure difference which is due to the action of surface tension at the curved meniscus in the pores is the main driving force for producing the

condensate flow.

Gilliland et al. (1958) studied the steady state permeability of a number of hydrocarbon vapors using a porous glass in the pressure range including the capillary condensation region. They derived a surface flow equation based on the hydrodynamic flow of the adsorbed film under the influence of its spreading pressure and applied this equation to the experimental permeability and diffusion coefficients.

Tamon et al. (1981) investigated the flow mechanism of an adsorbable gas through the porous adsorbent in the presence of capillary condensation and derived a new transport model taking into account the hopping behavior of adsorbed molecules in the adsorbed phase and the viscous flow of capillary condensate. Using the pore size distribution and the Kelvin equation, portions of surface flow and capillary condensate flow were calculated and the overall permeability of condensed phase was calculated as a summation of surface permeability and condensate permeability.

Rhim and Hwang (1975) proposed a transport model having six regimes; the model included the liquid phase flow and the interfacial resistance at the meniscus of the condensate. Later Lee and Hwang (1986) developed a modified model considering the blocking effect of the adsorbed phase on the basis of a cylindrical pore structure. More recently, Qiu and Hwang (1990) investigated organic vapor separation from N_2 in the range of pore condensation using a porous membrane permeator. Using a porous Vycor glass membrane having an average pore diameter of 40 Å, they changed the feed side pressure from 0 to 20 psig while the permeate side pressure was kept constant at atmospheric pressure. They have also developed a theoretical model to describe the permeator performance and compared the model with the experimental results.

Uhlhorn et al. (1990) described the transport of pure gases through a thin, supported, crack-free layer of γ-alumina membrane. In order to reduce the pore size, they modified the membrane with magnesia and studied the separation of C_3H_6/N_2 mixture using that modified membrane and showed that the transport mechanism is pore

condensation in the resulting small pores.

Many researches have been carried out in the area of vapor transport and capillary condensation through the porous media (Gilliland et al., 1958; Tamon et al., 1981; Lee and Hwang, 1986). The capillary condensation mechanism, which can be expressed as the combination of enhanced condensate flow and the reduction of the noncondensible flow, is one of the strong features of a high performance membrane for the separation of condensible vapors from inert air/N_2. Chapter 4 of this thesis considers experimentally pore condensation based separation of a vapor from N_2 through the γ-alumina ceramic membrane (ALCOA, Warrendale, PA) which has the pore size of 50 Å in a thin surface layer supported by much larger pores in the substrate. The vapors and the vapor mixtures studied in such a system were toluene and p-xylene in nitrogen. Two modes of operation wherein the permeate was either under vacuum or at atmospheric pressure were utilized at different feed pressures (0-30 psig) and at different degrees of permeate side vacuum (absolute pressures of 0.05 cmHg to 50.6 cmHg).

1.2 Objectives

The primary objective of this study is to investigate experimentally the capabilities of membrane modules having different types of membrane for separating water vapor as well as VOCs from N_2 using two different transport mechanisms, namely, permeation and pore condensation. Another objective of this study is to develop a simple model describing the permeator behavior for water vapor removal by incorporating the partial pressure-dependent permeance equation. An associate objective is to develop a comparative perspective on these different membranes and processes for the selective removal of VICs and VOCs from inert gas streams. A hydrophilic polymeric gel membrane was used for the selective permeation removal of water vapor and VOCs like toluene and methanol from a N_2 stream. A thin film composite silicone membrane was used for the selective permeation removal/recovery of VOCs such as toluene and methanol from an inert N_2

stream. For pore condensation-based removal of VOCs such as toluene and xylene from N_2 stream, microporous ceramic membrane having a 50 Å pore in the skin was used.

CHAPTER 2

VAPOR REMOVAL IN A PERMEATOR BY HYDROPHILIC HOLLOW FIBER GEL MEMBRANE (CUPROPHAN)

2.1 Introduction

2.1.1 Background

Humidity control problem in confined spaces is attracting some attention now-a-days. In air conditioning systems not only the temperature of the air in the confined space, but also the humidity needs to be controlled to ensure the comfort of the occupants inside the confined space. Further certain items (damaged easily when the humidity is very high) are not to be exposed to high humidity. Generally there are two kinds of method for removing water vapor from the atmosphere. One method, most widely practiced, involves condensing the moisture contained in the atmosphere by cooling the atmosphere below the dew point. The second method employs hygroscopic agents or salts to remove moisture from the atmosphere. The former method applies well to the reduction of high humidities to reasonable levels, but it requires a large amount of energy to cool the atmosphere and thereby achieve condensation of the moisture. The second method is favored for reduction of lower level of humidities to a relatively dry state. But in this case, the salts must be regenerated or discarded after absorbing quantities of water.

The utilization and application of membrane techniques can allow the removal of condensable vapor in the ambient air, especially water vapor, in a continuous, stable and efficient manner. It may be operated continuously for a long time under conditions of low energy consumption and low operating cost. In addition, since the membrane module is a compact device, the surface area/volume is very high compared to other devices.

There are certain amount of VOCs and VICs present in any atmosphere. This

study is aimed at removing such VICs (like water vapor) and VOCs (like toluene, methanol) using a highly hydrophilic polymeric gel membrane. Due to its high hydrophilicity, Cuprophan membrane becomes a hydrogel by immediately absorbing the ambient water vapor. The separation of water vapor from N_2/air through a permeator built out of Cuprophan hollow fibers has been studied here. The objective is to be able to quantitatively describe the observed permeator behavior and provide a basis for designing such permeators wherein the air humidity can be reduced substantially. Such permeators may serve different goals. For example, in space flights, such a permeator can be used to recover moisture for drinking purposes from humid cabin atmosphere relatively free of pollutants (VOCs) present (see Figure 2.1a). Under terrestrial conditions, such a permeator may be used to recover moisture from spent air being discharged from a building into fresh air entering a building (see Figure 2.1b).

For such applications to be successful, it is necessary that the permeated water vapor have much less of the pollutants present in the air being treated. The extent of removal of VOCs by Cuprophan hollow fiber membrane has therefore been studied here also from an exploratory point of view. The VOC concentrations employed are much higher than normally encountered in ambient atmosphere. Since this is an exploratory study from VOC removal point of view, the objective is to explore VOC removal capabilities of Cuprophan hollow fibers. If it is successful, future studies can explore much lower concentrations of VOCs. Two VOCs, toluene and methanol, were chosen for this study on the permeation of VOC through the hydrogel membrane in the presence of moisture.

2.1.2 Cuprophan Capillary Membrane

Cuprophan is one type of regenerated cellulose prepared by the cuprammonium process. It is manufactured by Akzo Faser of West Germany and is used mainly in the area of hemodialysis. It is one of the cheapest hollow fiber membranes available in the market.

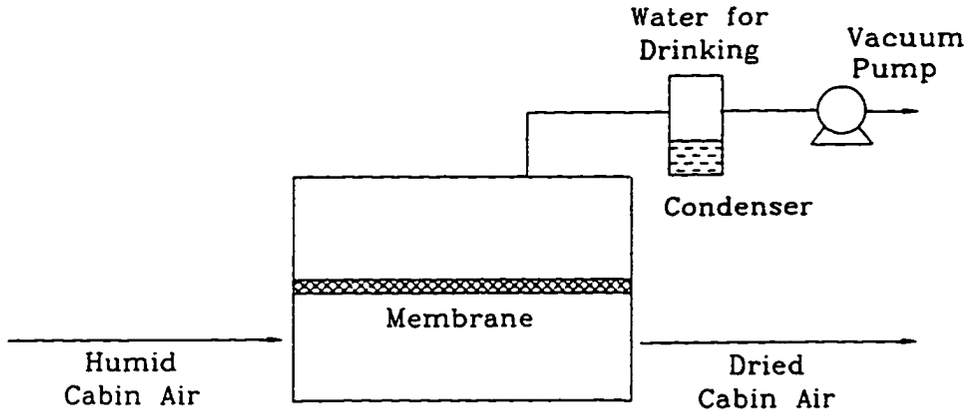

Figure 2.1a Membrane Regeneration of Water from a Humid Cabin Air

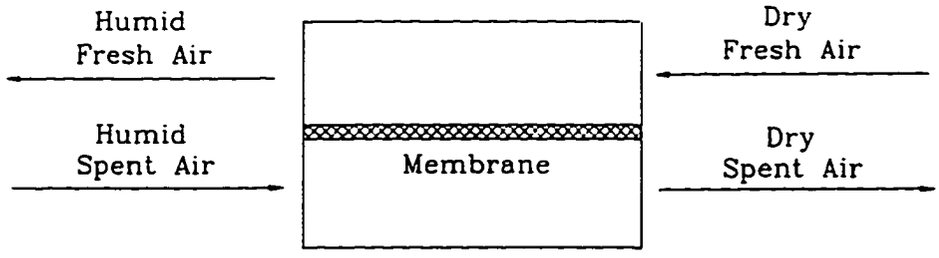

Figure 2.1b Membrane Removal of Moisture from a Humid Spent Air

Cuprammonium process employs a wet spinning method capable of producing a membrane having a very thin wall. The membrane thickness by this process is usually 11 - 16 μm: membrane having only 8 μm thickness has also been commercialized. The wet spinning process for Cuprophan employs a coagulant liquid (isopropylmyristate) acting as a filling material which prevents the hollow fiber from collapsing and enables the preparation of thinner membranes (Kim et al., 1988). The membranes contain some impurities as a result of their manufacturing process. Ward et al. (1985) reported that these impurities may be residual salts, oligomers of cellulose, glycerin and other organic spinning aids such as isopropylmyristate, a pharmaceutical agent, for maintaining the dimensions. These impurities must be removed by proper washing prior to the experiments.

2.2 A Model for Vapor Separation in a Hydrogel Hollow Fiber Permeator

2.2.1 Water Vapor Removal from Inert N_2

Figure 2.2 shows the schematic of the vacuum mode of operation of a hollow fiber permeator with countercurrent flow of feed gas and the permeate stream. Moist nitrogen flows through the fiber bore and vacuum is pulled on the shell-side. Consider water vapor transport to start with. At steady state, the differential equation governing the membrane permeation is obtained from a material balance of the species being transferred over a differential membrane area dS of length dz in the direction opposite to that of feed flow. If the axial coordinate 'l' is positive in the direction of permeate flow, the governing differential equation for permeation of water vapor is given by:

$$\frac{d(L\,x)}{dS} = \frac{Q_w}{\delta_m}\,(P\,x - p\,y) \qquad (2.1)$$

Here,

L : total tube side molar flow rate at any location per fiber, mol/sec/fiber

Q_w : permeability of water vapor, mol.cm/sec.cm^2.cm Hg

Q_w/δ_m : specific permeability or permeance of water vapor, mol/sec.cm^2.cm Hg

P : feed side pressure at any location, cm Hg

p : permeate side pressure at any location, cm Hg

x : mole fraction of water vapor at tube side

y : mole fraction of water vapor at permeate side

δ_m : effective membrane thickness of the hollow fiber, cm

The membrane is a hollow fiber in the gel form having an I.D. of d_i , an O.D. of d_o and

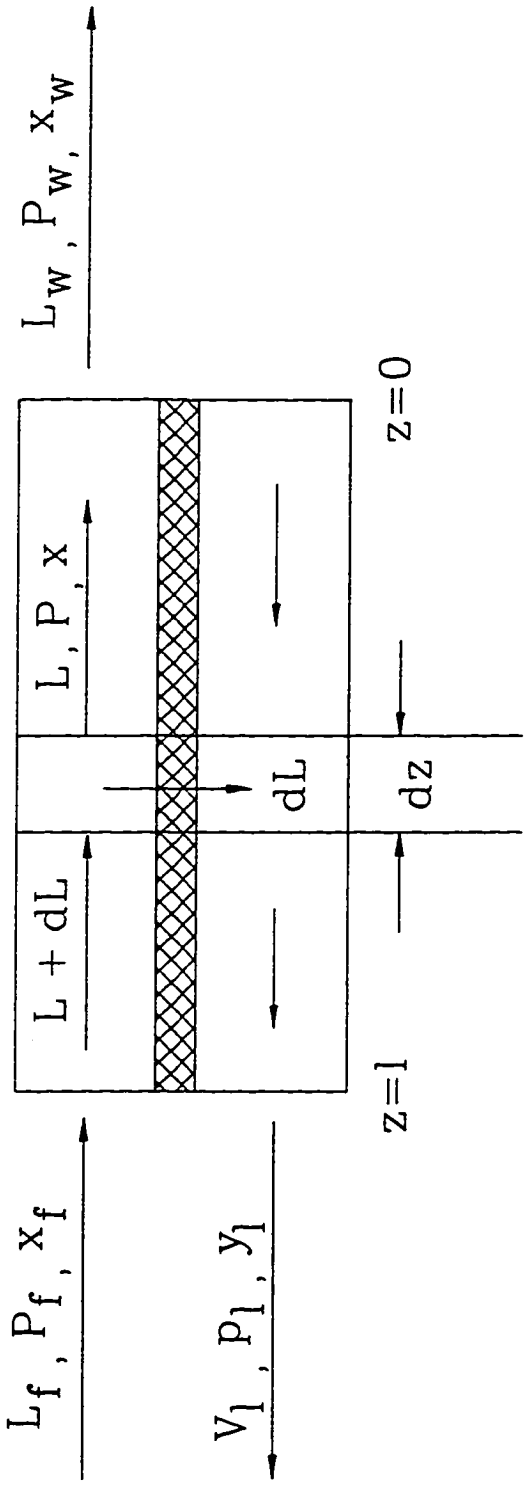

Figure 2.2 Schematic Diagram of a Membrane Permeator in Countercurrent Flow

a logarithmic mean diameter of d_{lm} defined by

$$dS = \pi\, d_{lm}\, dz = \pi\, \frac{d_o - d_i}{\ln \frac{d_o}{d_i}}\, dz \qquad (2.2)$$

By combining equations (2.1) and (2.2), the following equation is obtained:

$$\frac{d(L\,x)}{dz} = \pi\, d_{lm}\, \left(\frac{Q_w}{\delta_m}\right)\, (P\,x - p\,y) \qquad (2.3)$$

In traditional membrane gas permeation, Q_i/δ_m, i.e. the permeance for any species i is usually a constant for most permanent gases and membranes based on rubbery polymers (Stern and Frisch, 1981). For glassy polymers and most gases, the permeance becomes a complex function of the partial pressure of the species due to the presence of Langmuirian sorption of gases in polymer. However this dependence of the permeance on the species partial pressure generally does not appear to change the permeator behavior by more than 20-30% in a hollow fiber permeator (Chern et al., 1985). The situation in the case of vapors is much more complicated and the effect is much greater. Therefore the specific permeability (or permeance) of water vapor through this membrane (Q_w/δ_m) is not considered a constant, rather it is a strong function of the partial pressure (or relative humidity) of water vapor in the feed gas mixture.

Previous studies with cellulosic membranes/films indicate that the permeability of water vapor increases rapidly with increasing relative humidity in the feed gas mixtures (Barrie, 1968). The relationship between the permeance and the relative humidity at any level of relative humidity may be developed from careful experiments by maintaining the

change in the relative humidity level to be as limited as possible along the length of the hollow fiber module. When the change in the mole fraction of water vapor between the feed inlet and outlet of the permeator is very small, the previous equation (2.3) can be written over the whole permeator as follows:

$$L_f x_f - L_w x_w = \pi d_{lm} l \left(\frac{Q_w}{\delta_m}\right)_{\frac{x_f+x_w}{2}} \left[P \left(\frac{x_f+x_w}{2}\right) - p y \right] \quad (2.4a)$$

Here the permeance $(Q_w/\delta_m)_{(xf+xw)/2}$ is an averaged one. If $x_f - x_w$ is relatively small, then this is valid and an averaged x_f defined by $x_{f,avg} = (x_f + x_w) / 2$ can be used:

$$L_f x_f - L_w x_w = \pi d_{lm} l \left(\frac{Q_w}{\delta_m}\right)_{x_{f,avg}} \left[P x_{f,avg} - p y \right] \quad (2.4b)$$

Note that correspondingly y is also an averaged value here. Such a relationship of the specific permeability of water vapor versus partial pressure (or relative humidity) of water vapor can be expressed as a polynomial or in an exponential form. Suppose an exponential form written in equation (2.5) is able to describe the data:

$$\frac{Q_w}{\delta_m} = a \exp (b x) \quad (2.5)$$

where,

Q_w/δ_m : specific permeability (or permeance) of water vapor at a particular relative humidity, mol/sec.cm^2.cm Hg

x : mole fraction of water vapor at tube side

a and b : constants to be determined from experimental data.

Then an analytical solution of equation (2.3) may be developed under certain restrictions. Making additional assumptions given below, equation (2.3) can be simplified further for water vapor removal by a permeator.

1. The partial pressure of water vapor in the permeate side is negligible due to the high vacuum applied (~ 29.9 in Hg by Heise vacuum gauge).
2. Feed side pressure drop is almost negligible at usual experimental gas mixture flow rates.
3. The change in the molar feed gas mixture flow rate, L, along the permeator is small compared to the change in the mole fraction of water vapor. Averaged percent change in mole fraction of water vapor is approximately 30 times greater than the change in the molar flow rate.

By adopting these assumptions, equation (2.3) can be rewritten as follows:

$$L \frac{dx}{dz} + x \frac{dL}{dz} = \pi d_{lm} P \left(\frac{Q_w}{\delta_m}\right) x \cong L \frac{dx}{dz} \qquad (2.6)$$

Here the second term of the left hand side is negligible because the change of L throughout the permeator is very small compared to that of the mole fraction x.

Combining equations (2.5) and (2.6) will give the following equation:

$$\frac{dx}{dz} = \frac{\pi\, d_{lm}\, P\, a}{L}\, x \exp(b\, x) = k\, x \exp(b\, x) \qquad (2.7)$$

where

$$k = \frac{\pi\, d_{lm}\, P\, a}{L}$$

The above equation (2.7) can be solved analytically using the known feed gas flow rate and composition at the feed inlet end. The k value here was assumed constant in the experimental flow rate range (where P is atmospheric). Rearrangement of equation (2.7) leads to

$$k \int dz = \int \frac{dx}{x \exp(b\, x)} \qquad (2.8)$$

The analytical integration of the right hand side of equation (2.8) results in

$$k\, l = \int_{x_o}^{x_f} \frac{dx}{x \exp(b\, x)} = \left[\ln x - \frac{(b\, x)}{1 \cdot 1!} + \frac{(b\, x)^2}{2 \cdot 2!} - \ldots\ldots \right]_{x_o}^{x_f} \qquad (2.9)$$

The mole fraction x of water vapor on the fiber bore side (tube side) was calculated as

a function of permeator length z using the inlet condition. The computer program used to calculate the mole fraction x of water vapor at the feed outlet end is provided in Appendix A. The value of the mole fraction of water vapor at the end of the permeator is obtained by solving the above equation; it may be compared with the experimental feed outlet value of the water vapor mole fraction.

2.3 Experimental

2.3.1 Preparation of Membrane Module

Three membrane modules were prepared using Cuprophan hollow fibers. They are shown in a photograph (Figure 2.3). Modules 1 and 2 had respectively 50 and 150 homogeneous Cuprophan fibers (Enka, West Germany). The I.D./ O.D. of the fibers were 200 / 220 μm and the wall thickness was 11 μm. The effective fiber length was 16.5 cm in both cases. Module 3 had 150 asymmetric Cuprophan D2 fibers (Akzo, Wuppertal, West Germany). The I.D./O.D. of the fibers were 215 / 247 μm, the wall thickness of the fiber was 16 μm, and the effective length of the module was also 16.5 cm. Table 2.1 provides the geometrical specifications of membrane modules used in this study. There are two steps in the preparation of such modules: preparation of fibers and potting of fibers. They are described next.

2.3.1.1 Cuprophan Fiber Exchange Process and Drying

Cuprophan capillary membranes are supplied with a liquid (isopropylmyristate) inside. For the number of fibers needed for a module, the liquid inside the bores as well as the pores of the fibers had to be removed first. One end of the bundle of fibers was tied with a string and was lifted up vertically so that the liquid could flow out downward as much as possible. Then the fiber set was immersed completely in a 500 ml graduated cylinder which contained isopropyl alcohol (the exchanging solution); the exchanging solution was stirred using a magnetic stirring bar. When the stirring bar was turning, the bottom halves of the fibers were spread out almost individually and the exchange performance was enhanced. This process was continued for approximately 20 hours, then the top and bottom portion of the fibers were reversed and the process continued for another 20 hours. The fibers were then taken out, spread individually onto a glass tray and dried in room air overnight (about 16 hours). A completely dried fiber looked transparent; it was

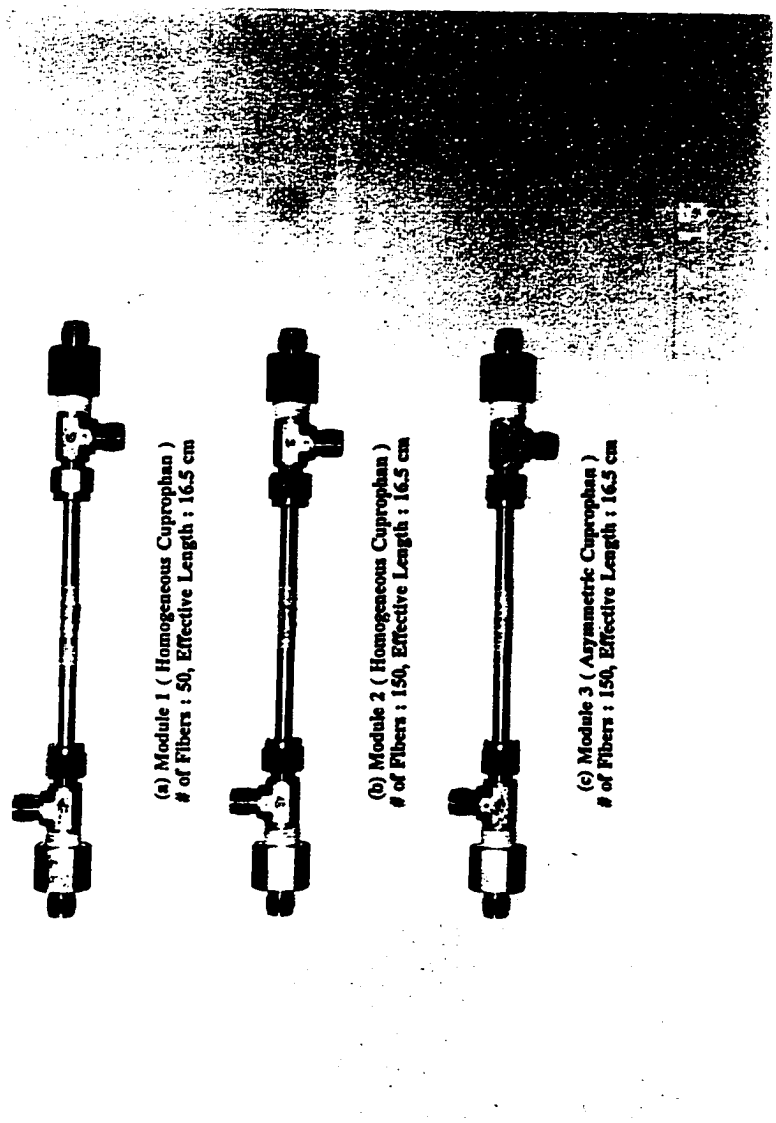

Figure 2.3 Photograph of Three Membrane Modules

Table 2.1 Specifications of Membrane Modules Used

Module	Membrane Type	No. of Fibers	I.D./O.D. of Fibers (μm)	Wall Thickness (μm)	Effective Fiber Length (cm)	Effective Surface Area (cm^2)
1	Cuprophan Homogeneous	50	200 / 220	11	16.5	54.6
2	Cuprophan Homogeneous	150	200 / 220	11	16.5	163.9
3	Cuprophan Asymmetric	150	215 / 247	16	16.5	179.3

observed visually that a few fibers still had a little bit of liquid in the bore of the fibers. Those fibers were discarded when the module was prepared.

2.3.1.2 Potting of Fibers

The selected number of fibers (50 or 150) were taken and introduced into a 1/4" (0.62 cm O.D.) stainless steel tube; then two layers of potting were prepared at each end where a male run tee was connected. The first layer was prepared using a RTV 118 translucent silicone rubber sealant (G.E. Silicone, General Electric Co., Waterford, NY) from the outside end where the fibers were jutting out from the tee end. After 1 day cure, epoxy based on C-4 resin and D activator in the weight ratio of 4/1 (Beacon Chemicals, Mt. Vernon, NY) was applied as a second layer through the shell side opening on the inside. The entrapped air during the mixing of the components of the epoxy were removed in a desiccator using a vacuum pump for 5-10 minutes before potting. The effective surface areas of the three modules prepared were 54.6 cm^2, 163.9 cm^2 , and 179.3 cm^2 respectively.

2.3.2 Materials, Chemicals and Equipment

The following materials, chemicals and equipment were used in the experiments:

Multiple flow controller (Model 8249, Matheson, East Rutherford, NJ)

Mass flow transducer (Model 8141, Matheson, East Rutherford, NJ)

Mass flow controller (Model 8250, Matheson, East Rutherford, NJ)

Cuprophan hollow fibers (homogeneous: Enka, West Germany; asymmetric: Akzo, Wuppertal, West Germany)

Gas chromatograph (Hewlett Packard Model 5890A and Varian Model 3400)

Integrator (Hewlett Packard Model 3392A and Varian Model 4290)

Humidity measurement device (HMI 32, Vaisala, Woburn, MA)

Humidity measurement probe (HMP 32 UT, Vaisala, Woburn, MA)

Humidity Meter Calibrator (HMK 11, Vaisala, Woburn, MA)

Vacuum Pump (Model 1410, Welch Scientific Inc., Skokie, IL)

Cold Trap (Model 8640, Pope Scientific Inc., Menomonee Falls, WI)

Toluene, Methanol (ACS grade, Fisher Scientific, Springfield, NJ)

Nitrogen Extra Dry, Helium Zero and High Purity, Air Zero, Hydrogen Zero, Nitrogen Zero (Matheson, East Rutherford, NJ).

2.3.3 Experimental Apparatus

2.3.3.1 Removal of Water Vapor from an Inert N_2 Stream

The experimental setup schematically shown in figure 2.4 consisted mainly of three sections: feed section, membrane module section, and permeate section. In the feed section, a nitrogen stream from a cylinder was introduced to a bubbler which was almost filled with water. An air diffuser was utilized to make fine bubbles of nitrogen in the water in the bubbler. Another dry nitrogen stream was mixed with the first water vapor-containing nitrogen stream so that the feed nitrogen stream to the membrane module had the required concentrations of water vapor (or relative humidity). In this case, the humidity probes which were connected before and after the membrane module monitored continuously the relative humidity values of the gas streams at room temperature. This incoming gas stream into the membrane module was made to flow through a rotameter which was calibrated beforehand. The exiting gas stream flow rate was measured by a bubble flow meter. All experiments were done at room temperature around 20-23 °C.

In the membrane module section, three different modules described in the previous section were used in different experiments. The feed inlet gas mixture was passed through the tube side (lumen) of the hollow fiber membrane module while vacuum was applied at one end of the shell side. In the permeate section, the necessary partial pressure driving force for gas/vapor permeation was created by a vacuum pump connected to one end of the shell side of the membrane module (the other end was closed). The shell side flow

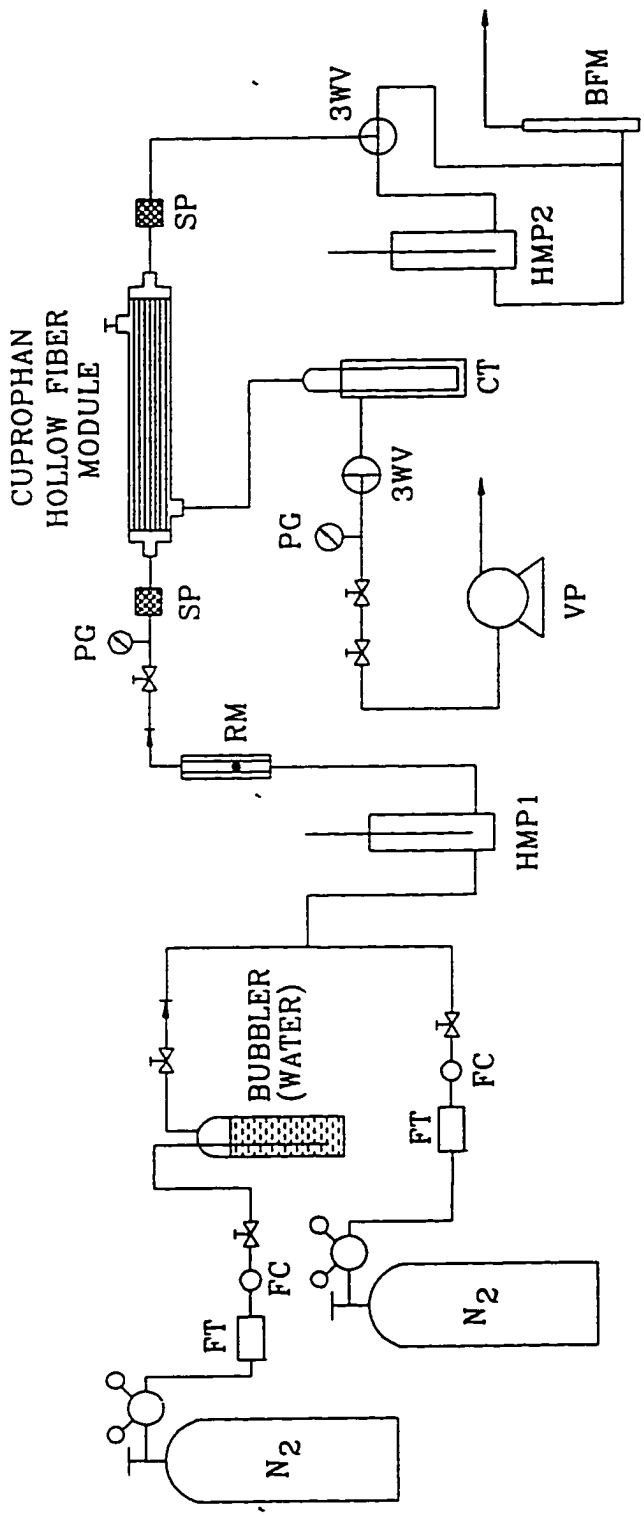

Figure 2.4 Experimental Setup for Removing Water Vapor using a Cuprophan Membrane Module

in the module was countercurrent to that of feed flow. In most cases, a very high vacuum (29.9 in Hg by Heise vacuum gauge) was applied.

2.3.3.2 Removal of Water Vapor and/or VOCs from an Inert N_2 Stream

The experimental arrangement was similar to that for water vapor/N_2 case and is schematically shown in figure 2.5. In the feed section, there was one more bubbler which contained the VOC (toluene or methanol); one nitrogen stream from a cylinder was divided into two streams, one of which was sent through the water-containing bubbler while the other was channelized through the VOC-containing bubbler. The third pure nitrogen stream was mixed with these two lines. Since VOCs can damage the sensor of the humidity probe, the concentrations of water vapor as well as the VOCs were determined using the gas chromatograph (GC) peak areas. A thermal conductivity detector (TCD) and a flame ionization detector (FID) were utilized respectively for the analysis of concentrations of water vapor and VOCs; the corresponding GC columns were Porapak Q (Alltech, Deerfield, IL) and Chromosorb W-HP (Alltech, Deerfield, IL) respectively.

2.3.4 Experimental Procedure

2.3.4.1 Calibration of Humidity Probe and Gas Composition in the GC

The humidity measurement device was calibrated by means of the humidity meter calibrator (Model HMK 11, Vaisala, Woburn, MA) and standard LiCl and K_2SO_4 solutions. Calibration was based on the known equilibrium relative humidity of saturated salt solutions of lithium chloride (LiCl) and potassium sulphate (K_2SO_4). The saturation concentrations of the LiCl and K_2SO_4 solutions were 19.4 gmol/l and 0.66 gmol/l respectively. The solubilities of LiCl and K_2SO_4 in water at room temperature were 82.1 and 11.5 gram per 100 ml of water respectively (Perry and Green, 1984). The relative humidities of saturated LiCl and K_2SO_4 solutions at 25 °C were 12.0 % and 96.7 % respectively. The lithium chloride and potassium sulfate solutions were used for dry

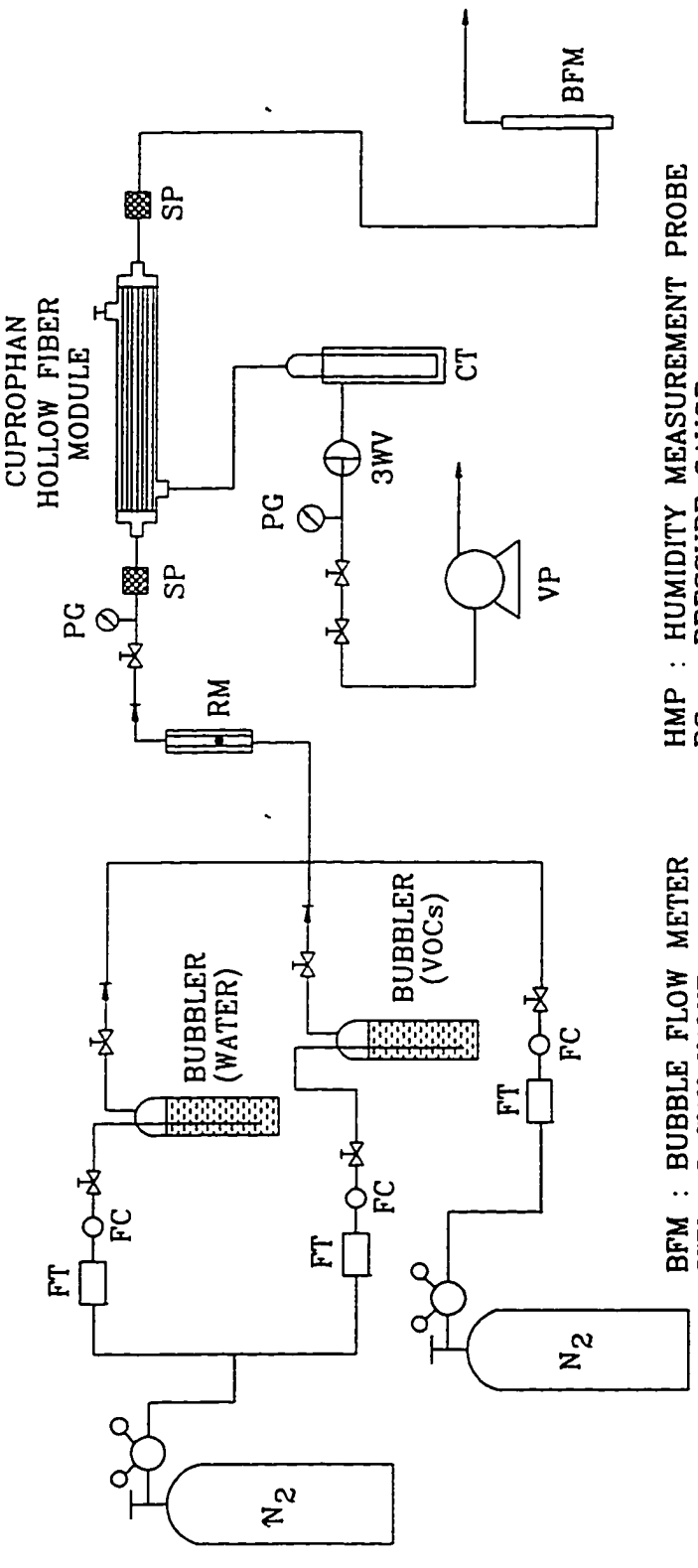

Figure 2.5 Experimental Setup for Removing Water Vapor and VOCs using a Cuprophan Membrane Module

adjustment and wet adjustment, respectively. The probes and the calibrators were kept at least 30 minutes in a room with constant temperature (25 °C), since equilibrium humidity of the calibration solution depends on the temperature.

The humidity probe has a metal sensor inside a Teflon box for the detection of the level of water humidity. If the feed gas mixture having a certain amount of VOCs is flowing through the humidity probe for a sufficiently long time, the sensor may get damaged due to continuous exposure to the VOCs used. The inside sensor has a limited resistance to each VOC employed. In this case, instead of using the humidity probe for the measurement of water vapor concentration, a Porapak Q column and a thermal conductivity detector were used in a GC (Hewlett Packard Model 5890A) for the measurement of the relative humidity values.

Two different gas streams (one was pure nitrogen, the other being water vapor containing nitrogen) were mixed to achieve a certain level of relative humidity. Then 1.0 c.c. of the sample gas mixture was taken and injected into the gas chromatograph. The relative humidity levels were changed from 7.5 to 97.5 % (12 different humidity levels were formed by adjusting the flow rate ratio of the two streams); at each relative humidity level 4-5 samples were taken regularly by a syringe and injected into the GC. The average peak areas obtained by GC were plotted as a function of the relative humidity levels. Figure 2.6 shows the calibration of the relative humidity with respect to peak area.

2.3.4.2 Permeance of Water Vapor as a Function of Relative Humidity

As mentioned earlier, the specific permeability (or permeance) of water vapor through the Cuprophan hollow fiber membrane is a strong function of the partial pressure of water vapor (or relative humidity) in the feed gas mixture. To obtain this relationship, eight different feed gas flow rates having different values of the relative humidity (between 12 % to 91 %) were selected and passed through the tube side of the membrane module whereas changing levels of vacuum were applied to the shell side. It was important to

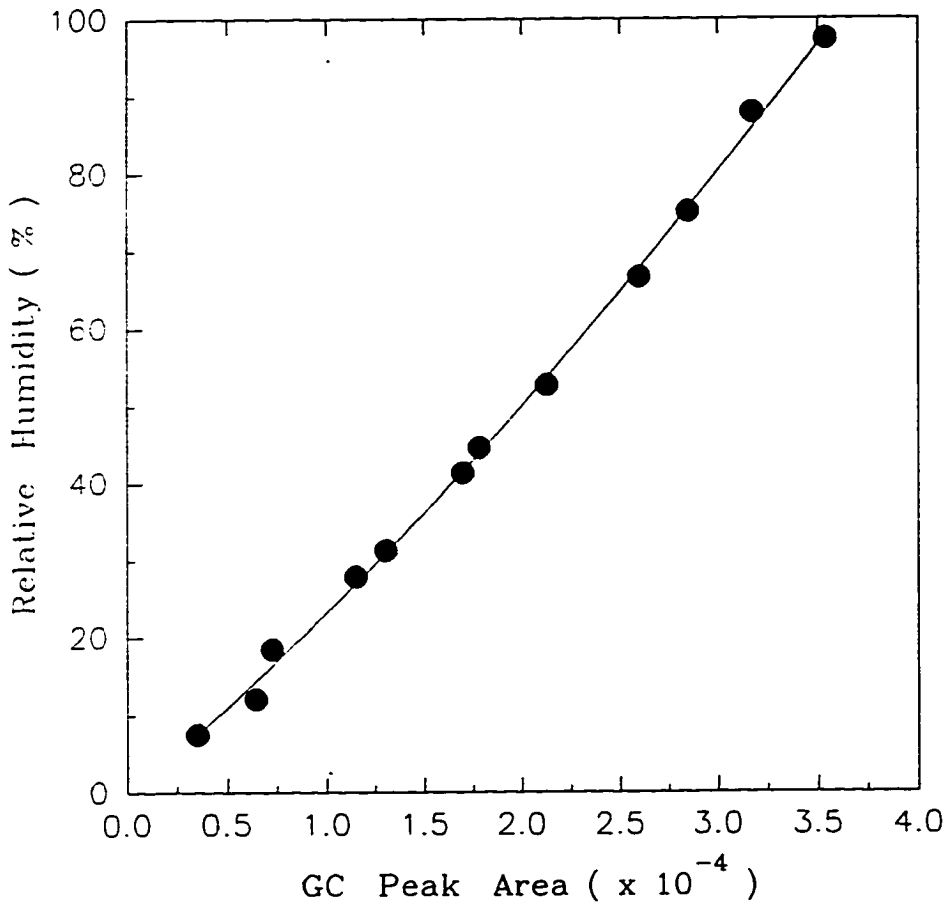

Figure 2.6 Calibration Curve for Relative Humidity vs. GC Peak Area

maintain the relative humidity level as constant as possible throughout the length of the module to obtain the specific permeability data at a certain level of relative humidity. Module number 1 was used for this experiment.

For the low humidity range (less than 50% RH), the feed flow rate did not have to be very high (less than 100 cc/min.) even though the shell side vacuum was close to 29.9 in Hg since the permeation rate of water vapor was not much in these cases. But for high levels of relative humidity (up to 95% RH) water vapor permeation rate was high for the same level of the shell side vacuum. Therefore the feed flow rate had to be maintained at a high level (up to 200 cc/min); otherwise there would be considerable partial pressure drop of water vapor throughout the module. Even though the feed flow rate was maintained high (180 - 200 cc/min), there was still significant permeation of water vapor through the membrane at 50-75% relative humidity range for a vacuum level close to 29.9 in Hg. To avoid having a large partial pressure drop of water vapor along the length of the module, the applied vacuum in the shell side of the module was reduced in this case to 28.3 in Hg. In the case of 90% relative humidity in the incoming gas, the shell side vacuum was lowered even further to 27.3 in Hg.

2.3.4.3 Permeance of Nitrogen as a Function of Relative Humidity

For the analysis of nitrogen permeation through the Cuprophan hollow fiber membrane at a given level of relative humidity, feed gas (N_2 plus water vapor) and sweep gas (He plus water vapor) were allowed to flow countercurrent to each other through the tube and the shell side of the membrane module respectively. The feed and sweep gas flow rates were in the range of 20-25 cc/min. The relative humidity of the feed and sweep gases were maintained as close as possible so that water vapor permeation may be neglected compared to nitrogen permeation. Further the membrane swelling condition would be constant throughout. In addition, the relative humidity would be essentially constant throughout the module. For this experiment, module number 2 was used and experimental

setup is shown in figure 2.7.

The relative humidity levels on both sides of the module were changed from 5% up to 95% (8 different runs were made). The rate of permeation of nitrogen into the shell side was determined using a Varian 3400 gas chromatograph and a Varian 4290 integrator. A thermal conductivity detector (TCD) and a Porapak N column (Alltech, Deerfield, IL) was used for the analysis. From the sweep outlet flowrate and the corresponding nitrogen peak area, the nitrogen permeation rate was calculated at different relative humidity levels.

2.3.4.4 GC Calibration for Toluene and Methanol

Before initiating toluene and methanol calibration, one experimental run (including water vapor and VOC) was performed in the usual fashion. One cm^3 of the gas mixture sample was taken with a syringe and injected into the GC in a preset condition. The peak area obtained in this experiment was used as an indication of the mid range of calibration of toluene and methanol.

For toluene calibration, isopropyl alcohol was used as a diluent. Different volume combinations of toluene and isopropyl alcohol were prepared in small glass bottles and mixed thoroughly (the toluene concentrations were changed). Exactly 1.0 μl of this liquid mixture was taken with a syringe and injected into the HP 5890A GC. The GC settings used in the calibration as well as the experiments were as follows: oven temp. = 150 °C, injector temp.= 150 °C, detector temp. = 150 °C. From one glass bottle (one toluene concentration), 4 to 5 samples were taken and injected into the GC. The known number of moles of toluene in a 1.0 μl sample mixture and the corresponding GC peak areas were obtained and plotted together. The total number of moles of toluene taken in a 1.0 cm^3 syringe when the usual experiments were running could also be calculated by the ideal gas law (PV = nRT). By comparing the total number of moles of toluene with the actual number of moles of toluene in a 1.0 cm^3 sample obtained by the peak area, the mole

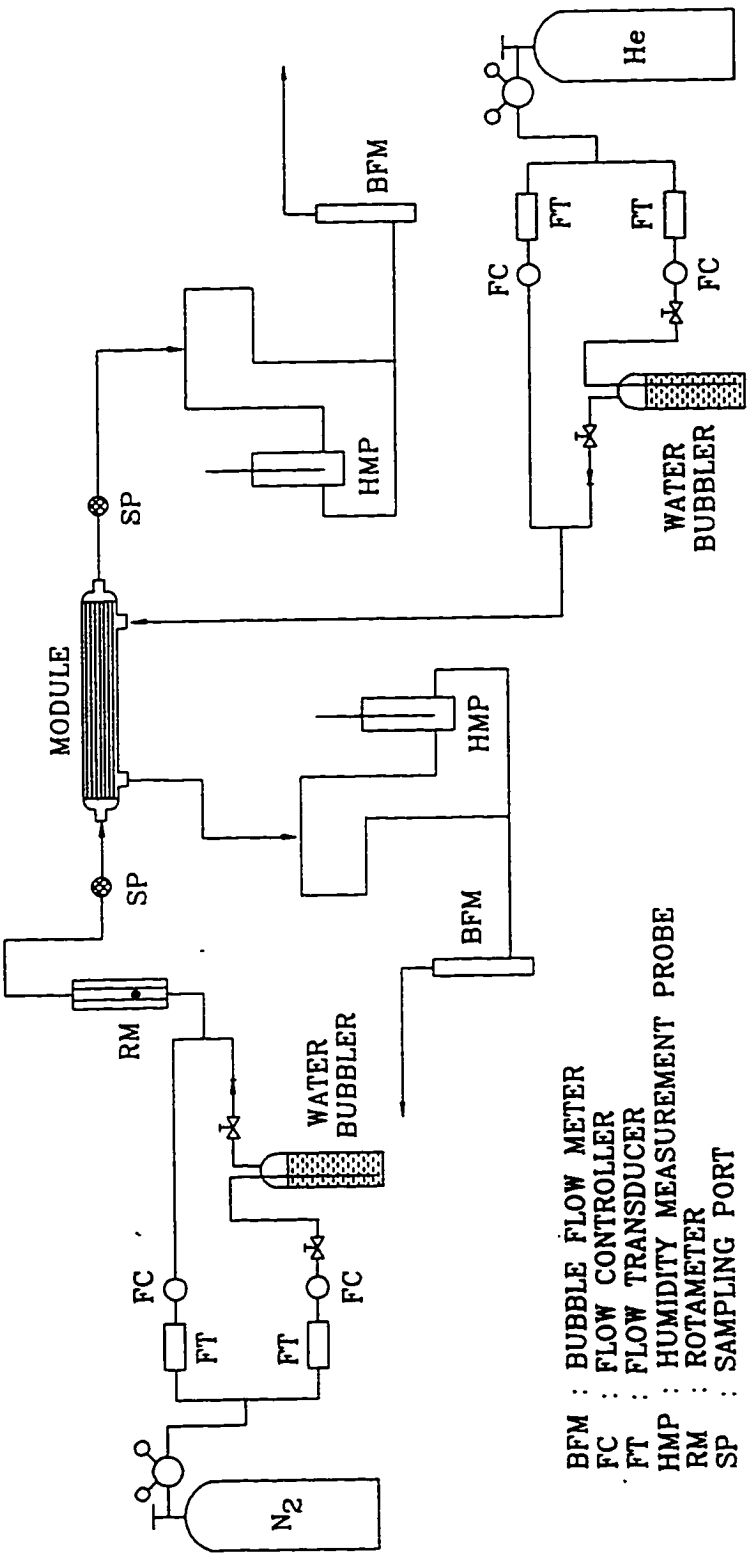

Figure 2.7 Experimental Setup for the Measurement of Permeance of Nitrogen as a Function of Relative Humidity

fraction (or concentration) of toluene could be calculated. In the case of methanol, the same method was used. Figures 2.8 and 2.9 are the calibration curves for toluene and methanol respectively. The retention times for toluene and methanol were 0.85 and 0.35 minutes respectively.

2.3.4.5 Carbon Dioxide Permeation through Cuprophan Membrane

In one set of experiments, a feed gas (extra dry CO_2) and a sweep gas (He) both of which were almost saturated with water vapor were allowed to flow through module 1 countercurrently. The relative humidities of the feed and sweep gases were initially 91.3 % and 95.5 % respectively. Then the feed and sweep gases were bypassed from the water containing bubbler to make the gases dry and these dry gas streams were made to flow through the tube and shell side of the module. Since the two gases are dry, the values of relative humidity will continuously go down. The humidity measurement probes connected to the feed and shell side outlet streams continuously monitored the relative humidity values. The flow rates of feed gas and sweep gas were adjusted to 15-20 cc/min. and the experimental run continued overnight (more than 20 hours). The purpose of this experiment was to check the permeation rate of CO_2 when the membrane was almost in a dry state (very low relative humidity level). A portion of the sweep gas was injected into the GC (Varian model 3400) continuously for the detection of any permeated gas from the feed gas. The peak areas of the permeated gases and the relative humidity values in the feed and permeated side were continuously reported.

In another set of experiments, pure CO_2 (extra dry) gas was passed through the tube side of the module 1 and pure He was passed through the shell side of the module countercurrently to the feed flow. The relative humidity levels in the tube and shell side of the module was maintained almost similar and it was changed from 23 % to 97 %. This experiment was aimed at determining the CO_2 permeation rate through the Cuprophan gel membrane for varying humidity levels. The flow rates of the gases in the

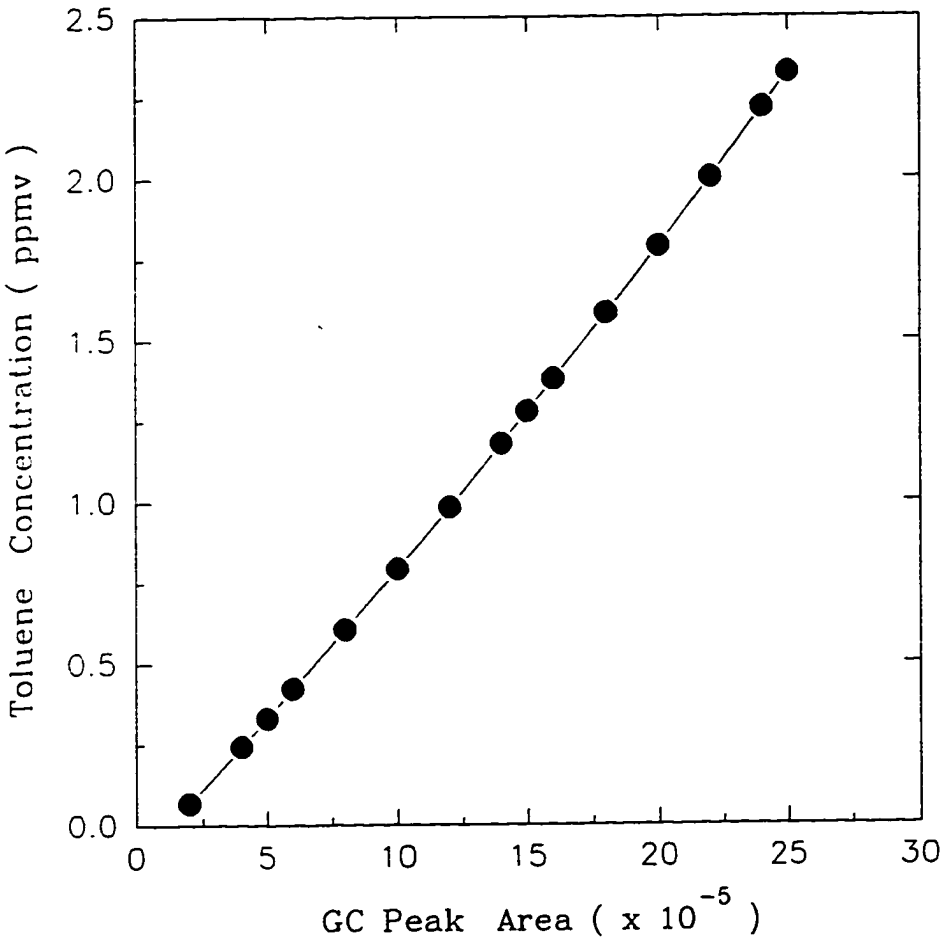

Figure 2.8 Calibration Curve for Toluene Concentration vs. GC Peak Area

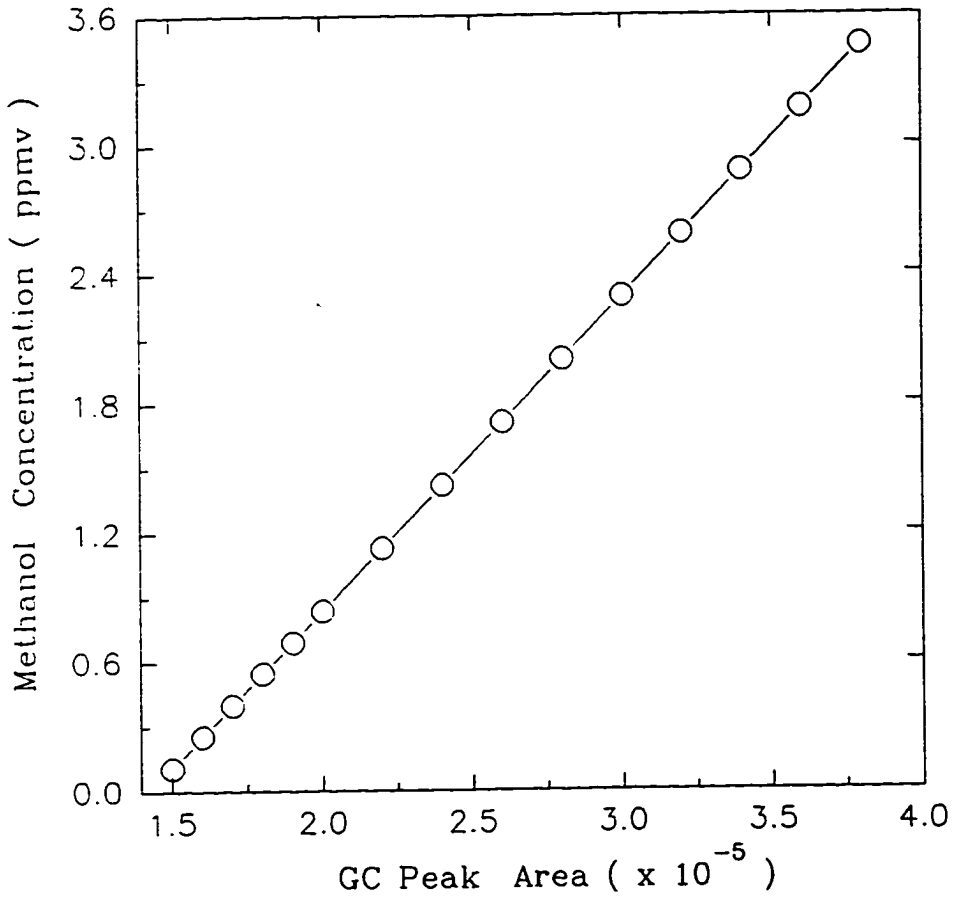

Figure 2.9 Calibration Curve for Methanol Concentration vs. GC Peak Area

tube and shell side were in the range of 10-25 cc/min. When the relative humidity levels were low (20-30 %), the sweep gas flow rate was reduced to around 10 cc/min. so that the CO_2 peak area can be detected by the GC. Gas chromatograph Varian Model 3400 was used to determine the peak areas of the permeated CO_2. Each experimental run continued until a steady peak area was obtained. Usually it took 4 hours to get a steady value.

2.3.4.6 Removal of Water Vapor from an Inert N_2 Stream

For this type of experiment, three modules were used. The total flow rates were changed from 10 to 40 cc/min. in the case of module 1. The relative humidity values were also varied from 15 % to 90 % at a given feed flow rate. The pressure drop through the membrane module was negligible in this case. In the case of modules 2 and 3, the feed flow rate was changed in the range of 30-120 cc/min; at each feed flow rate, the relative humidity values were also changed from 10 % to 90 %. First, using module 1, the feed gas mixture was allowed to flow through the tube (lumen) side of the membrane module. Vacuum was applied at one end of the shell side (other end was closed) so that the shell side flow was countercurrent to that of feed flow. To observe the general water vapor transport behavior through the module, the feed flow rate was changed from 3 to 40 cc/min. maintaining the feed inlet relative humidity level constant (95-96 %). The changing feed outlet relative humidity values with time were measured at each flow rate keeping the shell side vacuum level constant (29.5 in Hg). In another set of experiments, the level of shell side vacuum was changed from 15.0 in Hg to 29.0 in Hg at each constant feed flow rate to observe the effect of shell side vacuum on the flux and the fractional removal of water vapor.

In all cases, one nitrogen stream was sent into an air diffuser immersed in the water bubbler to produce fine nitrogen bubbles rising through the water. Another pure nitrogen stream from a cylinder was blended with the first water vapor containing

nitrogen stream. By changing the ratio of the flow rates of these two nitrogen streams, the desired feed relative humidities were obtained. Feed gas relative humidities were usually changed from 10% up to 90% or above.

The feed gas mixture was passed through a rotameter and into the tube side of the membrane module whereas vacuum (29.9 in Hg) was applied to the shell side. Feed outlet flow rate was measured regularly by a bubble flow meter; feed inlet flow rate was also measured by a bubble flow meter at the end of each run. Inlet and outlet humidities were monitored continuously by the humidity measurement probes connected before and after the membrane module.

2.3.4.7 Removal of Water Vapor and/or VOCs from an Inert N_2 Stream

One nitrogen stream from the cylinder was divided into two lines; one was sent into the water-containing bubbler and the other line was introduced into the VOC-containing bubbler. The third stream of pure nitrogen was blended with these two streams to achieve the desired concentrations of water vapor as well as VOC. As candidate VOCs, toluene and methanol were selected and module 2 was utilized throughout this experiment.

To obtain the desired water vapor and VOC concentrations, the flow rates of three nitrogen lines were adjusted carefully. When the VOC concentration was varied at a constant relative humidity level, the flow rate of the nitrogen stream connected to the water bubbler was maintained constant whereas the flow rates of two other nitrogen streams were varied individually to obtain a certain level of VOC concentration (the total flow rate was constant). The total feed flow rates were changed from 10 to 90 cc/min. and at each flow rate three different relative humidity levels (25 - 75 %) were employed and the VOC concentration was varied between 1,000 to 6,000 ppm at each relative humidity level. The feed gas mixture was passed first through the rotameter and then through the tube side of the membrane module. The vacuum pump was connected at one end of the shell side (the other end kept closed) to create the needed partial pressure

difference between the feed and the permeate streams. Instead of using the humidity measurement probe, a Hewlett Packard 5890A GC was used containing a Porapak Q column and a thermal conductivity detector calibrated beforehand to measure the relative humidity levels of feed inlet and outlet samples. For the VOC concentration measurement, a Chromosorb W-HP column and a flame ionization detector were used in the Hewlett Packard 5890A GC. The retention time for the water vapor, toluene and methanol at the present GC settings were 1.89 min., 0.85 min., and 0.35 min. respectively. When the experiments were going on, the feed inlet and outlet samples (1.0 cm^3 by syringe) were periodically taken and injected into the GC. For each experimental run, 3 to 4 samples were injected into the two different columns separately; it took about 4 hours to finish one experimental run.

2.3.5 Performance of the Membrane Module

The performance of the Cuprophan hollow fiber membrane module was calculated in terms of flux, percent removal and module-averaged permeance of water vapor defined by the following equations:

Flux of water vapor (J_w, gmol/min.cm^2) = $(F_i.x_f - F_o.x_w) / A$ (2.10)

Percent removal of water vapor (% R) = $(1 - F_o.x_w / F_i.x_f) \times 100$ (2.11)

Module-averaged permeance of water vapor (Q_w/δ_m, gmol/sec.cm^2.cm Hg)

$$= [(F_i.x_f - F_o.x_w) / A] / [60 \times (\Delta p)_w] \quad (2.12)$$

where F_i and F_o are feed inlet and outlet molar flow rates and x_f and x_w are mole fractions of water vapor at feed inlet and outlet, respectively; A refers to the membrane surface area, $(\Delta p)_w$ refers to module-averaged partial pressure difference of water vapor across the membrane defined as follows:

$$A = \pi d_{lm} l N \quad (2.13)$$

$$(\Delta p)_w = P [(x_f + x_w) / 2] \quad (2.14)$$

2.4 Results and Discussion

The experimental results for water vapor removal from nitrogen via selective permeation through dried Cuprophan hollow fibers subjected to a vacuum are presented and discussed here. Experimental results of permeance of nitrogen, CO_2 and water vapor as a function of the relative humidity of the feed gas stream are provided. The water vapor removal behavior experimentally observed in the hollow fiber modules has been compared with predictions from the model which employs the experimentally obtained relative humidity-dependent water vapor permeance. Experimental results have also been provided here for cases where toluene/methanol was present as a VOC along with moisture in the feed nitrogen stream.

2.4.1 Permeance of Water Vapor as a Function of Relative Humidity

The dependence of the permeance of water vapor through the Cuprophan hollow fiber membrane as a function of the relative humidity is shown in table 2.2 and plotted in figure 2.10. The feed side relative humidity of water vapor was changed from 12 % to 91 %. In each case, the change of the relative humidity level throughout the module was maintained as small as possible. In the case of a high relative humidity, the water vapor removal was unavoidably quite high even if the tube side flow rate was high enough. In this case the degree of vacuum level applied to the shell side of the module was reduced a little bit so that the permeation of the water vapor would be reduced by the decreased driving force. In all cases, the percent removal of water vapor was in the range of 5 to 12 %. At each relative humidity level (the averaged values from 10 to 85 %), the experimental permeance of water vapor was calculated and plotted. The relationship between the permeance of water vapor and the relative humidity was fit very well by the exponential curve, $Q_w/\delta_m = 4.763E\text{-}10 \exp(161.3\ x)$, where Q_w/δ_m is the permeance of water vapor and x is an averaged feed water mole fraction defined in equations (2.4a) and

Table 2.2 Permeance of Water Vapor for Different Feed Relative Humidity Levels (Module # 1)

Feed Inlet			Feed Outlet			Water Flux ($gmol/min.cm^2$) ($\times 10^8$)	Permeance of Water ($gmol/sec.cm^2.cmHg$) ($\times 10^9$)
Flow rate (cc/min.)	R.H. (%)	Mole Fraction of Water	Flow rate (cc/min.)	R.H. (%)	Mole Fraction of Water		
47.3	12.3	0.00259	46.8	11.3	0.00238	0.81	0.71
58.2	21.0	0.00409	57.5	18.9	0.00368	1.98	1.12
90.0	36.0	0.00905	88.4	34.6	0.00870	3.46	1.26
185	49.0	0.0126	182	47.5	0.0122	8.81	1.71
193	57.2	0.0143	188	54.6	0.0137	14.2	2.49
179	76.4	0.0196	174	69.1	0.0177	31.8	4.64
208	91.4	0.0231	202	82.0	0.0208	47.2	7.11

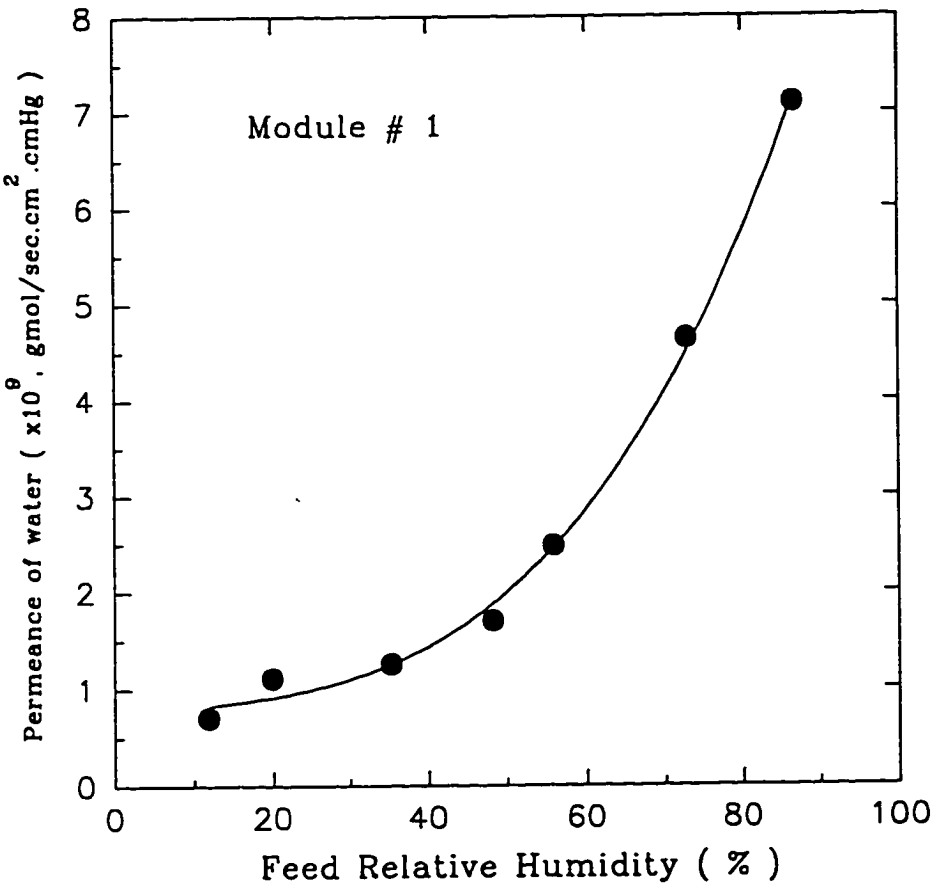

Figure 2.10 Permeance of Water Vapor at Different Feed Relative Humidity Levels

(2.4b). This equation was used in the mathematical model. Exponential increase of the water vapor permeance with respect to the relative humidity levels can be found in some other studies (Stamm, 1956; Barrie, 1968; Krishnamoorthy et al., 1972). The water vapor flux through Cuprophan membrane obtained in this study was of the same order (10^{-7} - 10^{-8} gmol/min.cm^2) as the values obtained using microporous cellulosic membrane (Bonne et al., 1990). The value of highest water vapor permeance with Cuprophan membrane obtained in this study was 0.8 x 10^{-8} gmol/sec.cm^2.cmHg. Cussler et al. (1992) used a composite polyethersulfone membrane for water vapor removal from air; they obtained water vapor permeance (Q_w/δ) values of the order of 10^{-7} gmol/sec.cm^2.cmHg (2.2 x 10^{-7} gmol/sec.cm^2.cmHg). Pan et al. (1978) also obtained a similar value (4.0 x 10^{-7} gmol/sec.cm^2.cmHg) using asymmetric cellulose triacetate hollow fiber membranes. Note that water (from condensation) damages cellulose ester membranes. Further polyethersulfone membranes are quite costly. Too high a permeance is not useful since gas phase resistance takes over (Cussler et al., 1992).

2.4.2 Permeance of Nitrogen as a Function of Relative Humidity

The permeation rate of nitrogen was measured at different relative humidity levels starting from 5 % up to 95 %. The feed side (N_2 plus water vapor) and the shell side (He plus water vapor) humidity levels were maintained almost similar so that the swelling condition on both sides of the hollow fiber membrane would be similar. Table 2.3 shows the experimental conditions and the results. The small flow rate difference between the feed inlet and outlet of the module is due to nitrogen permeation through the membrane to the shell side driven by the partial pressure difference across the membrane. The sweep outlet flow rate was increased a little bit due to the nitrogen permeation from the feed side. The GC peak area of the sweep outlet side was not changed much by the change in the relative humidity. Further since the sweep flow rate was not varied much, it appears that nitrogen permeation is not strongly affected by the relative humidity levels. The

Table 2.3 Nitrogen Permeance as a Function of Relative Humidity (Sweep Run, Module # 2)

Flow Rate (cc/min.)				Relative Humidity (%)		Peak Area	Nitrogen Permeance (x 10^{11}, gmol/sec. cm^2.cmHg)
Feed		Sweep		Feed	Sweep	Sweep Out	
In	Out	In	Out				
20.9	20.8	25.3	25.4	4.4	5.2	132	3.36
20.6	20.4	20.9	21.1	11.3	10.0	137	2.97
20.9	20.7	23.2	23.3	21.1	21.4	128	2.93
20.8	20.7	23.1	23.2	30.9	30.4	132	3.08
21.2	21.0	19.1	19.5	41.8	40.5	139	2.82
23.7	23.5	21.6	21.8	63.0	61.8	123	2.55
22.0	21.8	38.7	38.8	82.3	76.7	72	2.79
21.6	21.5	23.2	23.3	95.6	97.2	122	2.67

permeance of nitrogen was calculated based on the known nitrogen concentration in the sweep outlet side and corresponding feed and sweep side flow rates. The averaged permeance value was 2.8 x 10^{-11} gmol/sec.cm^2.cm Hg. The average permeance of water vapor over changing relative humidity levels was of the order of 10^{-9} gmol/sec.cm^2.cm Hg (see table 2.2). The selectivity of water vapor and nitrogen through the Cuprophan membrane can be calculated by the ratio of the permeance of two species and the value ($\alpha_{H2O/N2}$) was in the range of 20-250 depending on the feed relative humidity levels (higher values at higher relative humidity). Figure 2.11 is a plot for nitrogen permeation rate as a function of feed relative humidity.

2.4.3 Carbon Dioxide Permeation through Cuprophan Membrane

In the first set of experiments, the initial relative humidities of the feed (CO_2) and sweep (He) gases were 91.3 % and 95.5 % respectively. Since dry gases were flowing through the tube and shell side of the module after sometime, the relative humidities of feed and sweep gases dropped continuously. The permeation rate of carbon dioxide through the membrane module decreased continuously as the relative humidity values were decreased. Figure 2.12 illustrates the carbon dioxide peak area and feed side relative humidity levels as a function of time elapsed. In this case, the feed side relative humidity was not the same as the shell side relative humidity. When the feed relative humidity level was very low (~2.1 %, membrane was almost dry), the observed carbon dioxide peak area was very small in the permeate side; this was continued more than 5 hours.

If the gas transport mechanism through the Cuprophan membrane is governed by the pore condensation mechanism, a continuous flow of dry N_2 or CO_2 will eventually dry out the waters in the pores of the membrane and once the pore is open, there will be a lot of N_2 or CO_2 permeating through the openings by leakage. But in this case, there was very little carbon dioxide permeation through the Cuprophan membrane when the membrane was almost in a dry state. In the dry state of the membrane, the polymer

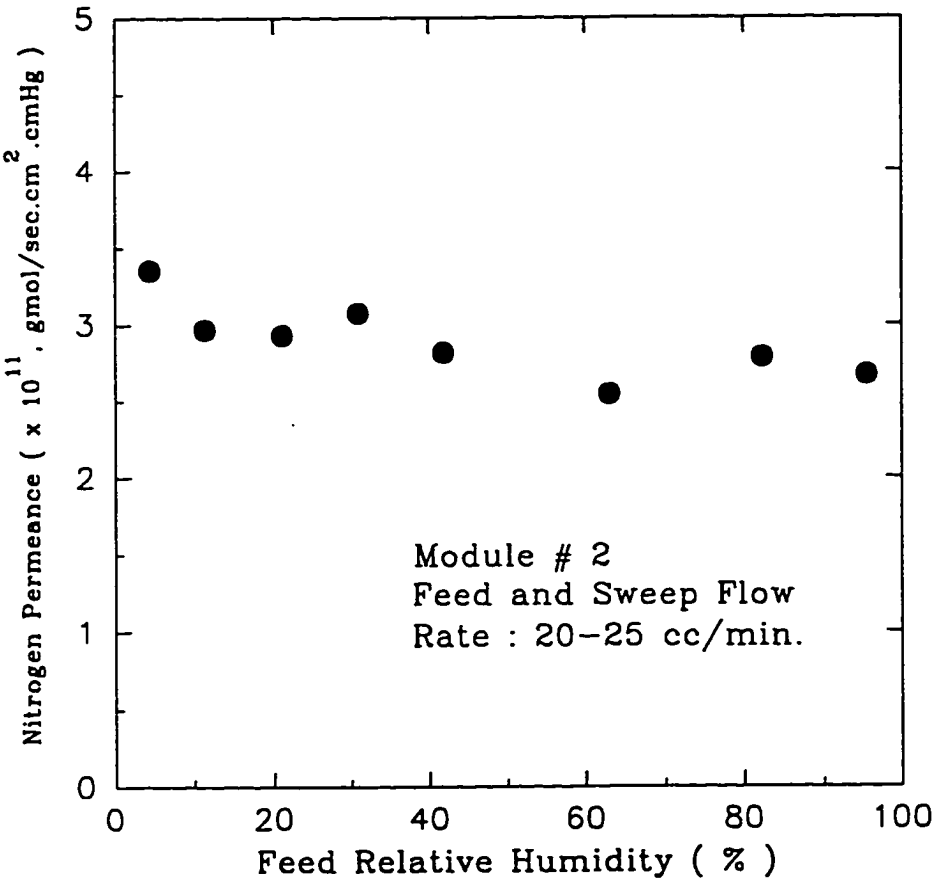

Figure 2.11 Permeance of Nitrogen at Different Feed Relative Humidity Levels

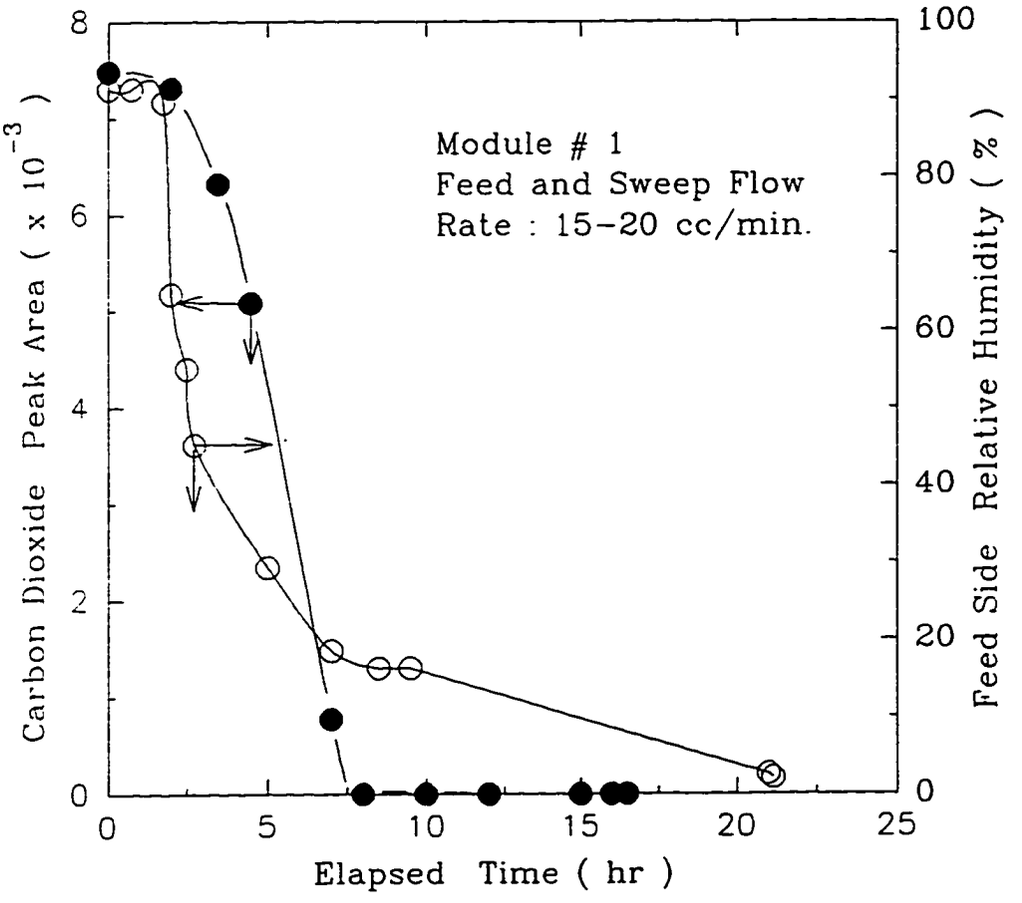

Figure 2.12 Relation between Carbon Dioxide Peak Area and Feed Relative Humidity

matrix was shrunk as much as possible and it appeared that no pore openings were available since the material was like a dense membrane. This is the reason why essentially little carbon dioxide was permeating through the dry Cuprophan membrane.

In the second set of experiments, pure carbon dioxide and helium which had similar humidity levels were passed through the tube and shell side of the module respectively. Six different humidity levels were provided from 23 % to 97 %. Carbon dioxide permeance values were obtained from the sweep outlet peak area (or concentration) and corresponding sweep outlet flow rate (membrane area and partial pressure difference across the membrane were also required). Carbon dioxide permeance was not a constant, but a strong function of the relative humidity levels as shown in table 2.4. It increased almost exponentially with increasing relative humidity levels a behavior not found in the case of nitrogen permeation. The plot is shown in figure 2.13.

The Cuprophan membrane is highly swollen and hydrophilic by nature. It absorbs the moisture from ambient air and forms a hydrogel immediately; mass transport usually occurs through this water swollen gel (Collins, 1985). The openings of the polymer matrix of Cuprophan membrane seems to change according to the levels of relative humidity. When the feed relative humidity level is high (> 80 %), the polymer matrix swells much more and the openings (or pores) of the membrane which are filled with water become larger. The permeation rate of carbon dioxide was much higher in this case. As the relative humidity level was reduced, the permeation rate was also decreased. The solubility of carbon dioxide in water is very high compared to that of nitrogen in water. Pilar (1960) reported that oxygen permeance through regenerated cellulose film was a strong function of relative partial pressure of water vapor and it was extremely sensitive at very high relative pressures (R.H. > 80 %). The permeance of gases which have relatively higher solubility in water through the Cuprophan membrane in the presence of water was strongly dependent on the water vapor partial pressure.

Table 2.4 Carbon Dioxide Permeance as a Function of Relative Humidity (Sweep Run, Module # 1)

Sweep Flow Rate		Relative Humidity (%)		Peak Area	Carbon Dioxide Permeance
Volumetric (cc/min.)	Molar (x 10^3, gmol/min.)	Feed	Sweep	Sweep Out	(x 10^{10}, gmol/sec. cm^2.cmHg)
13.3	0.544	23.0	23.4	-	-
20.6	0.843	33.7	38.6	-	-
12.2	0.499	57.0	55.3	103	0.105
25.2	1.031	64.8	69.7	61	0.129
21.5	0.880	77.7	81.5	1,458	2.59
27.8	1.14	98.9	95.8	4,996	11.48

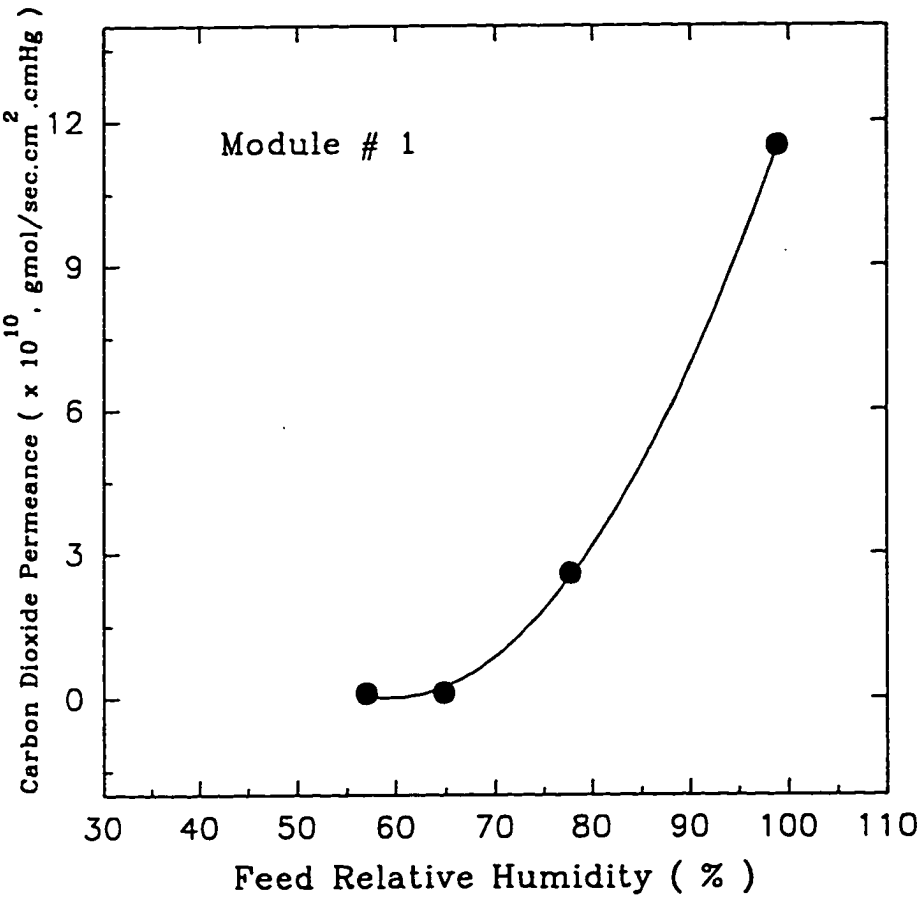

Figure 2.13 Permeance of Carbon Dioxide at Different Feed Relative Humidity Levels

2.4.4 Removal of Water Vapor from an Inert N_2 Stream

Figure 2.14 illustrates the initial time dependence of the feed outlet relative humidity when a feed inlet nitrogen stream having 95 to 96 % relative humidity was flowing through the membrane module # 1. In all cases, the feed outlet relative humidity was continuously reduced and finally reached a certain steady state value. At a very low feed flow rate (2.8 cc/min.), the feed outlet relative humidity came down to 12% within 4-5 hours. The feed outlet relative humidity level stayed higher when the feed inlet flow rate was higher since the percent removal of water vapor was decreasing in these cases.

Figures 2.15 and 2.16 show respectively the steady state water vapor flux and the percent removal of water vapor as a function of the inlet feed gas flow rate. In these experiments, the tube side pressure was maintained atmospheric and the shell side had different degrees of vacuum. The water vapor flux was increased as the feed flow rate was increased. In the case of a very high degree of vacuum (29.5 in Hg) in the shell side, the water vapor flux was 8 to 9 times higher compared to those for a low degree of vacuum (15.0 in Hg) due to the higher driving force when the feed flow rate was approximately 40 cc/min. The percent removal of water vapor was decreased as the feed gas flow rate was increased; as the partial pressure difference between the tube and the shell side was increased by increasing the permeate side vacuum, the water removal rate was also increased.

The feed outlet mole fraction of moisture obtained by solving the model equation (2.7) presented in section 2.2 and the actual experimental data are plotted together in figure 2.17. The model predictions match quite well with the experimental data. The experimental results for water flux and the fractional removal of water vapor as a function of changing feed relative humidity are represented in table 2.5. An increasing feed inlet relative humidity at a specific constant feed flow rate yields increasing values of water vapor flux and fractional removal. When the total feed flow rate was higher, the water vapor flux was also higher but the fractional removal rate of water vapor was reduced.

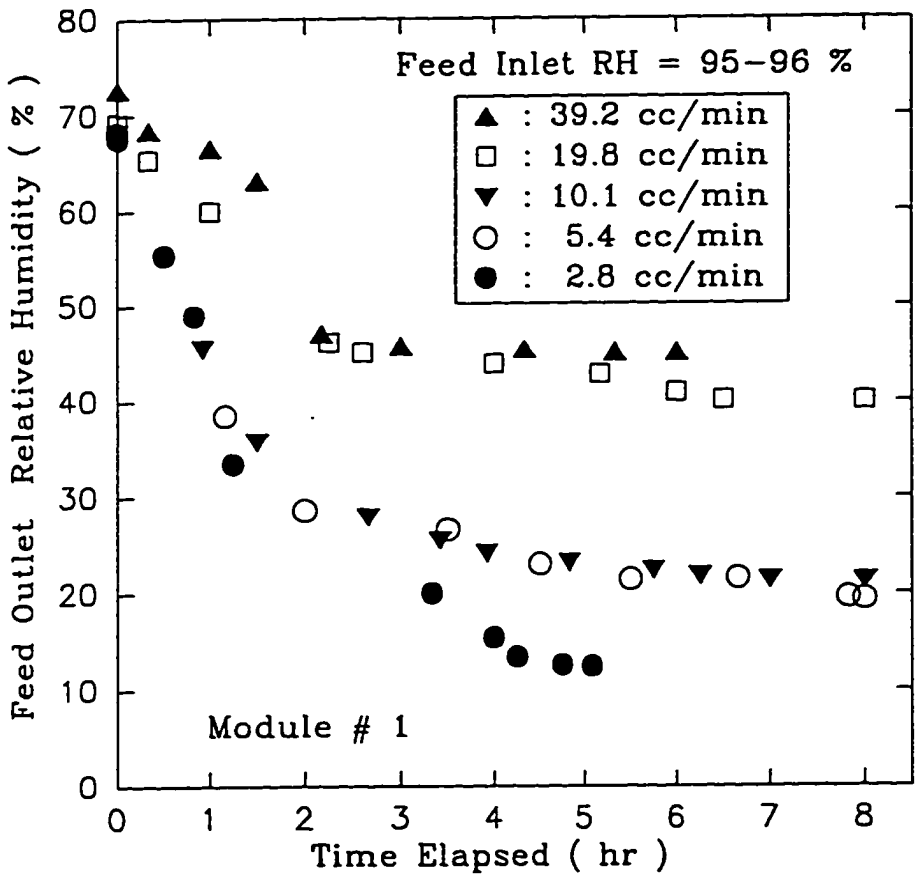

Figure 2.14 Feed Outlet Relative Humidity vs. Elapsed Time at Different Feed Flow Rates

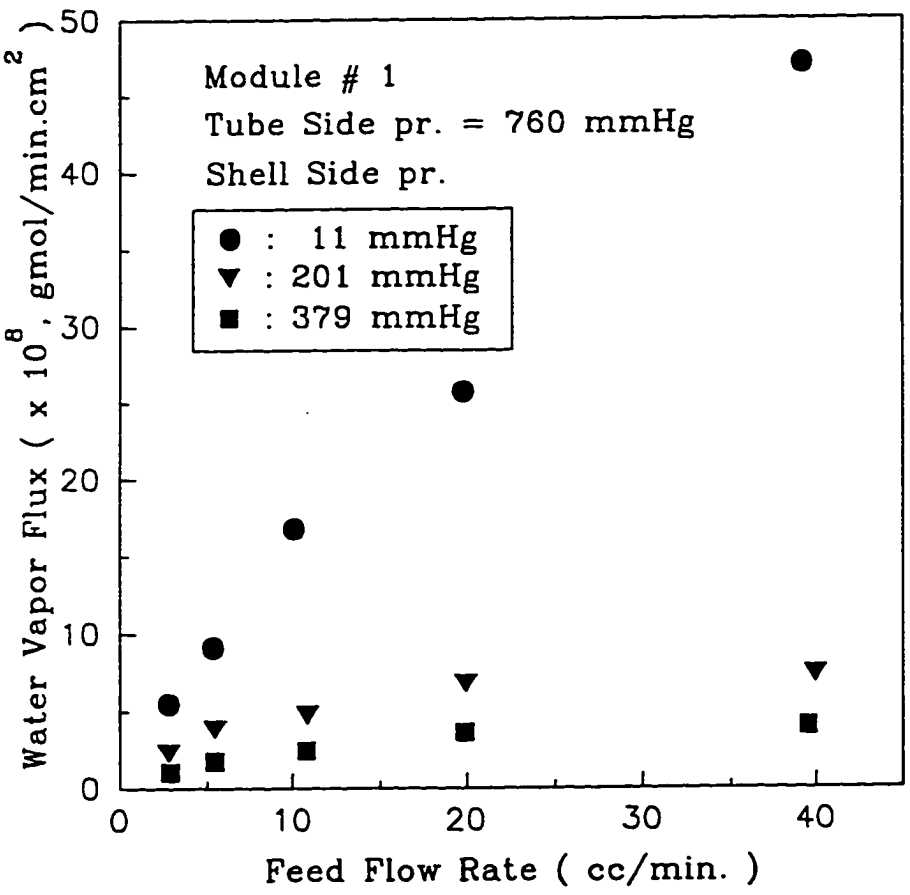

Figure 2.15 Water Vapor Flux vs. Feed Flow Rate at Different Shell Side Pressures

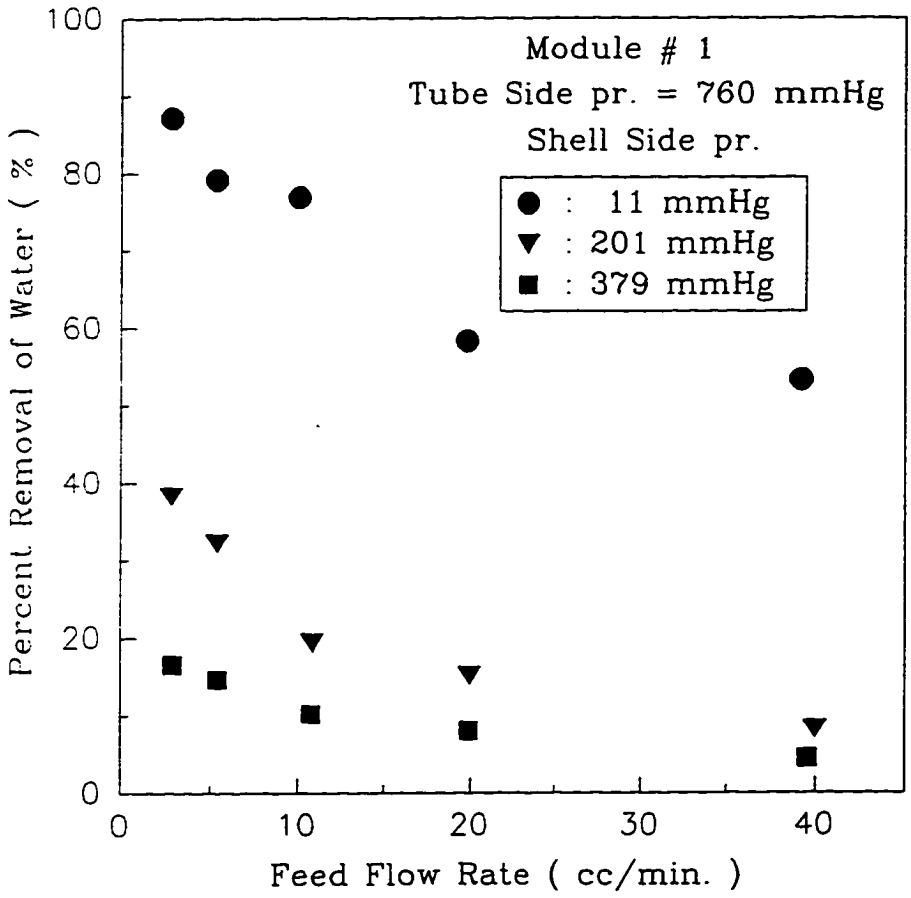

Figure 2.16 Percent Removal of Water Vapor vs. Feed Flow Rate at Different Shell Side Pressures

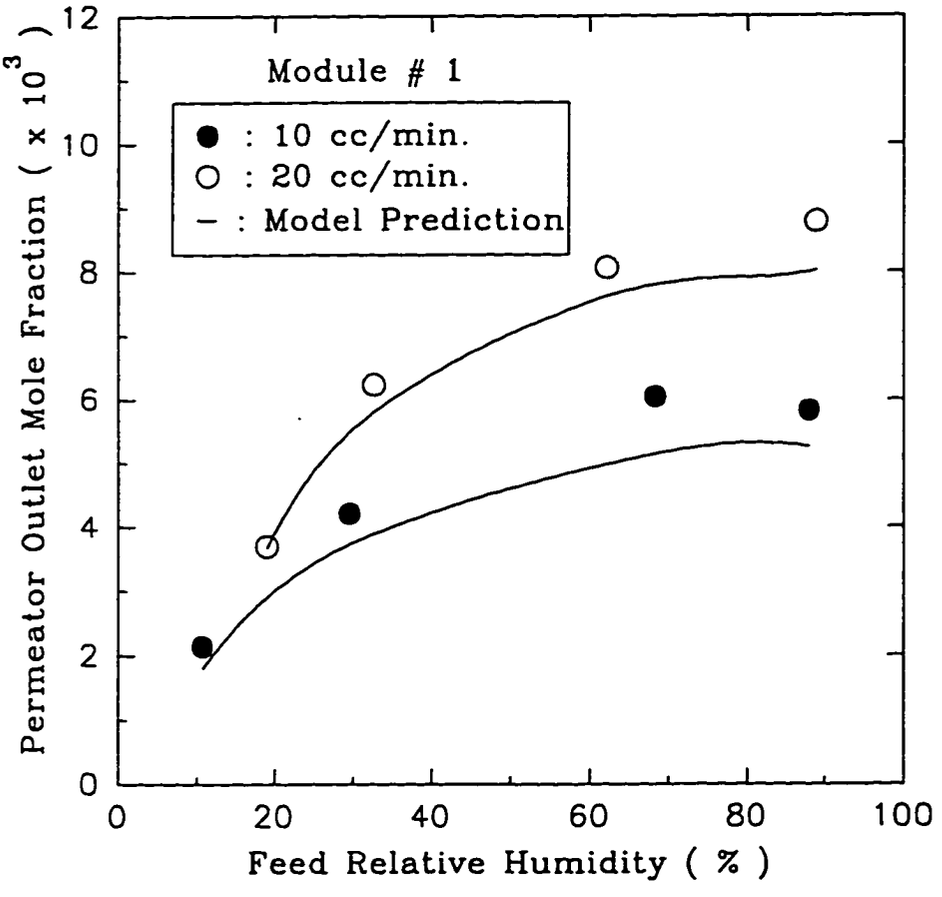

Figure 2.17 Permeator Outlet Mole Fraction vs. Feed Relative Humidity at Different Feed Flow Rates (Module # 1)

Table 2.5 Flux and Percent Removal of Water Vapor vs. Changing Feed Relative Humidity (Module # 1)

Feed Inlet			Feed Outlet			Water Flux ($gmol/min.cm^2$) ($\times 10^8$)	Percent Removal of Water (%)
Flow rate (cc/min.)	R.H. (%)	Mole Fraction of Water	Flowrate (cc/min.)	R.H. (%)	Mole Fraction of Water		
10.2	10.8	0.00267	9.9	8.7	0.00215	0.42	23.7
10.0	29.6	0.00713	9.7	17.5	0.00422	2.29	42.4
10.2	68.3	0.0186	9.9	22.2	0.00604	9.74	68.4
10.3	88.0	0.0223	10.0	23.0	0.00582	12.9	74.5
20.4	19.0	0.0048	20.0	14.6	0.00369	1.83	24.7
21.1	32.7	0.0089	20.5	22.9	0.00623	4.50	31.8
22.7	62.1	0.0152	22.2	33.1	0.00807	12.5	48.0
21.7	80.5	0.0205	21.2	35.5	0.00904	19.2	57.0
21.7	88.9	0.0228	21.2	34.3	0.00879	23.4	62.3
39.9	31.8	0.0079	39.1	27.0	0.00671	4.04	16.9
40.1	40.7	0.00993	39.4	31.6	0.00771	7.16	23.7
39.3	46.6	0.00106	38.8	32.2	0.00734	10.1	31.7
39.5	51.7	0.0122	38.8	29.6	0.00700	16.3	43.8
39.6	68.5	0.0176	38.8	31.6	0.00810	28.9	54.8

Figure 2.18 shows the experimentally obtained and model predicted values of water vapor flux through the Cuprophan fibers as a function of changing relative humidities. The predicted values of water vapor flux were calculated using the model predicted values of mole fraction of water vapor at the end of the permeator by solving the governing equation (2.7) described earlier. The water vapor flux increases as the feed relative humidity increases since the flux is related to the permeance as well as the partial pressure difference of the water vapor. As the tube side relative humidity was increased for a constant shell side vacuum, the permeance as well as the partial pressure difference of the water vapor across the membrane were increased together leading to higher values of the water vapor flux. The amount of water vapor removed (or permeated) per unit time and area was proportional to the feed flow rate and the predicted and experimental values agreed quite well.

The next figure 2.19 represents percent removal of water vapor as a function of the feed relative humidity. The increasing fractional removal of water vapor with increasing feed relative humidity values is due to the increasing flux at higher relative humidity. In the case of the lower feed flow rate (10 cc/min.), the removal range was 20-75 %; as the feed flow rate was increased, the removal rate was decreased to the range of 20-60 %. The module-averaged permeance of water vapor with respect to the feed relative humidity for a given feed flow rate is shown in figure 2.20. One can observe the increasing permeance values at increasing relative humidity. Module 1 was used for the above experiments. Here the values of permeance of water vapor were calculated over the whole permeator length, so this value is an averaged permeance. Actually, as the permeation is going on, the concentration of water vapor is decreasing in the direction of mean gas flow in the permeator. As the feed water vapor concentration is increasing, the concentration difference between the inlet and outlet of the permeator is also increased due to the higher driving force. As the feed flow rate is increasing, the overall permeability value was also increased slightly.

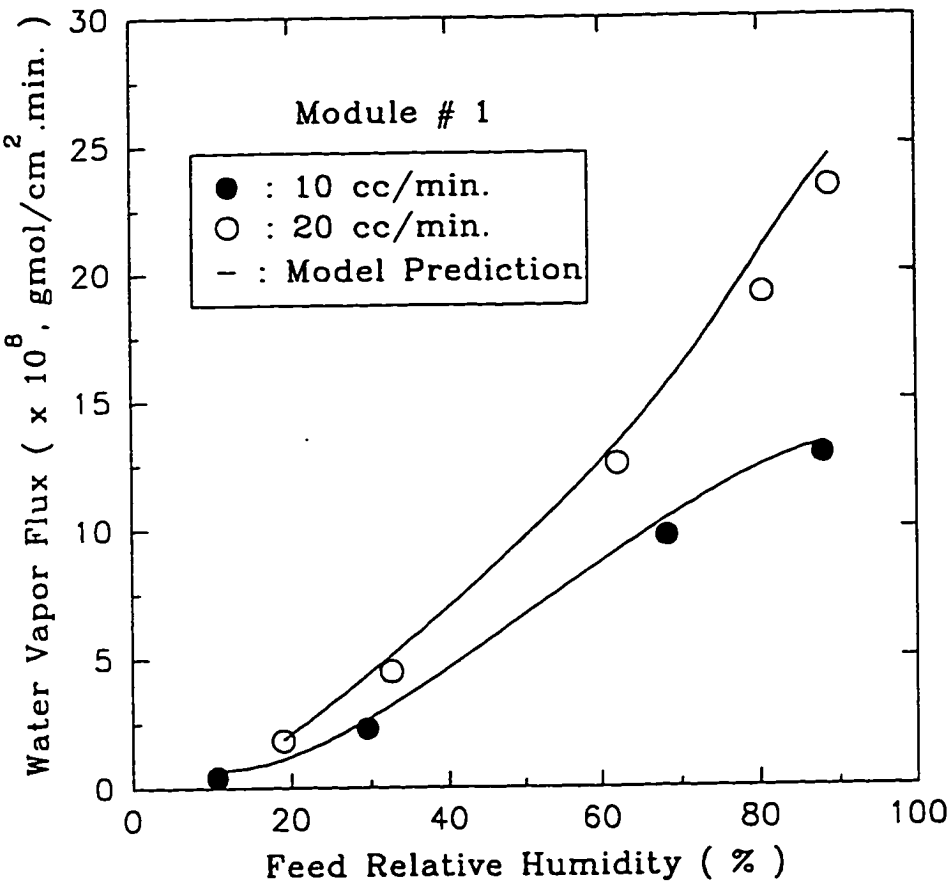

Figure 2.18 Water Vapor Flux vs. Feed Relative Humidity at Different Feed Flow Rates (Module # 1)

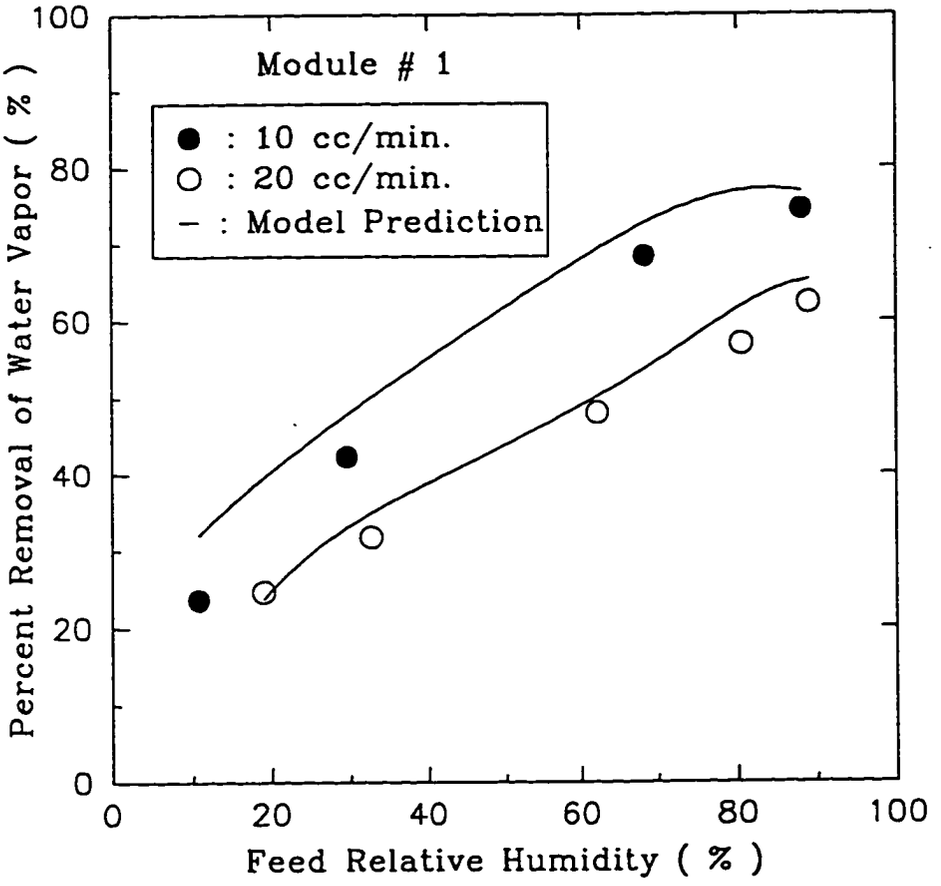

Figure 2.19 Percent Removal of Water Vapor vs. Feed Relative Humidity at Different Feed Flow Rates (Module # 1)

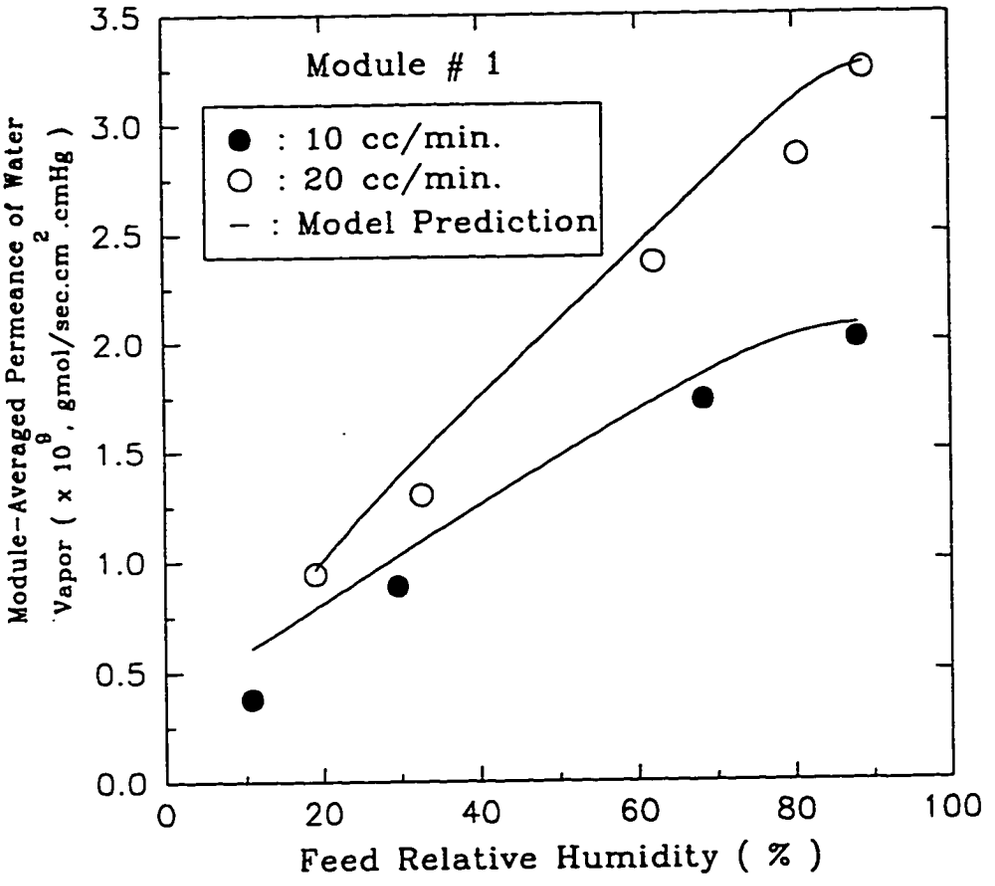

Figure 2.20 Module-Averaged Permeance of Water Vapor vs. Feed Relative Humidity at Different Feed Flow Rates (Module # 1)

The Cuprophan fibers used for module 1 (50 fibers) and module 2 (150 fibers) were similar i.e., homogeneous Cuprophan. The only difference was the number of fibers used in those modules. The equation of the water vapor permeance as a function of feed relative levels developed from module 1 was also used to predict the performance of the module 2. Permeator outlet mole fraction of water vapor was obtained theoretically by solving the model equation (2.7) presented in section 2.2 and plotted in figure 2.21 as a solid curve. Corresponding experimental data at different flow rates are also plotted in the same figure. The model predictions describe the experimental data quite well. Figures 2.22 and 2.23 show the water vapor flux and the percent removal of water vapor as a function of changing feed relative humidity. The experimental data for flux and percent removal of water vapor using this module 2 are described very well by the model based on the experimental data obtained using module 1; note that the feed flow rate per fiber in these modules were identical in both cases. If the feed flow rate is even more reduced in the case of module 2 which has a higher surface area, percent removal of water vapor will be increased even more.

Tables 2.6 and 2.7 show the experimentally measured values of the flux and percent removal of water vapor for modules 2 and 3 respectively. These flux and percent removal values are shown also in figures 2.24 and 2.25 respectively for a very wide range of feed gas flow rates. The experimental conditions used for the module 2 and module 3 were almost identical. It was observed that the feed inlet and outlet flow rate difference was slightly higher in module 2 compared to that in module 3. The values of the water flux at each feed flow rate for similar feed relative humidity levels were higher in module 2 compared to module 3. Generally the flux is inversely proportional to the thickness of a homogeneous membrane whether it is a flat film or a hollow fiber. The wall thickness of the homogeneous Cuprophan fibers contained in the module 2 is slightly less than that of the asymmetric Cuprophan fibers inside the module 3. The water vapor as well as the nitrogen permeation through this homogeneous fibers are more or less greater than those

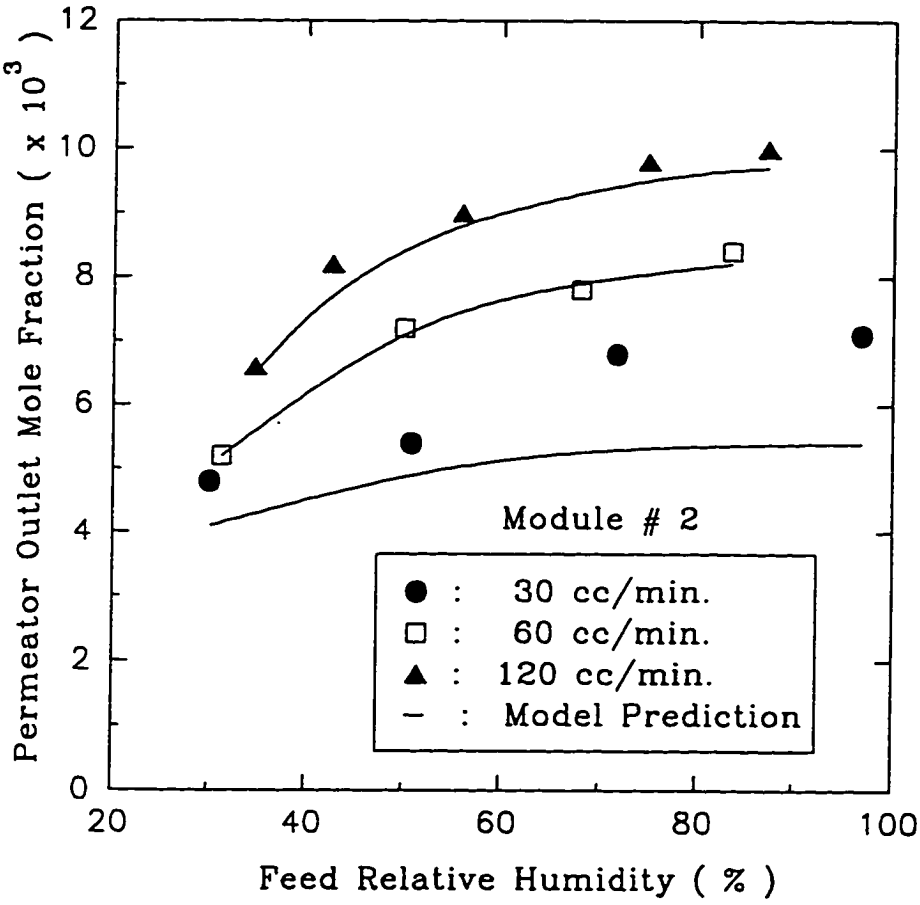

Figure 2.21 Permeator Outlet Mole Fraction vs. Feed Relative Humidity at Different Feed Flow Rates (Module # 2)

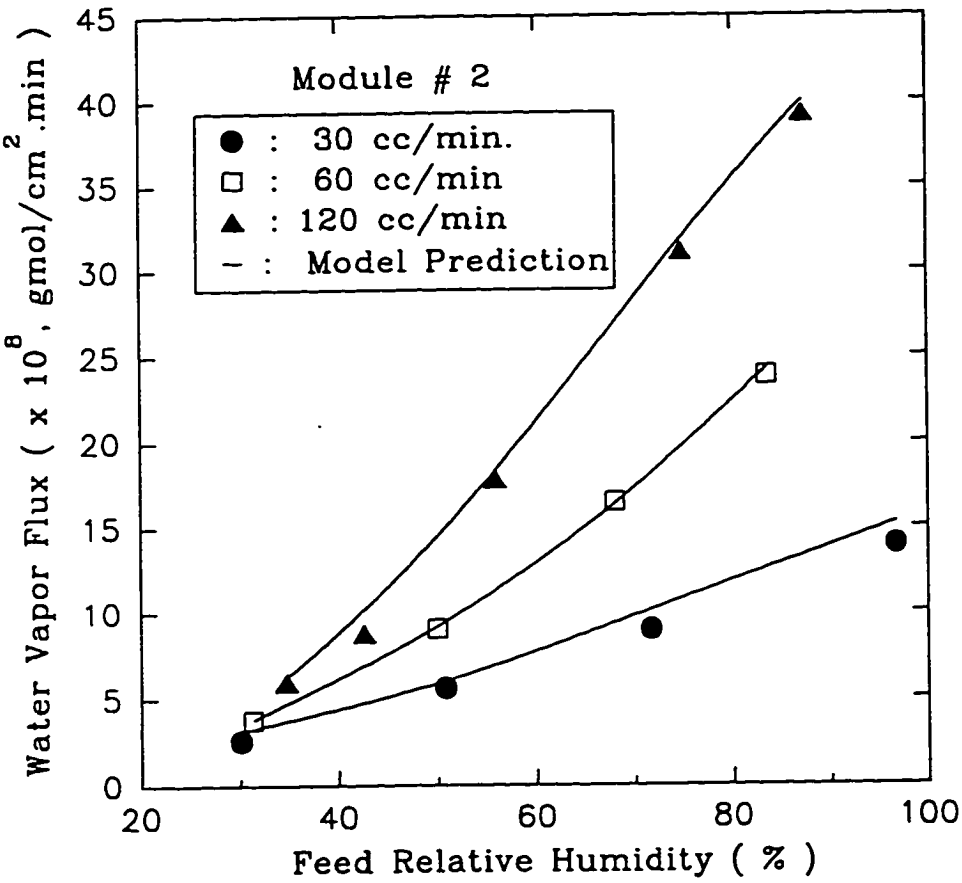

Figure 2.22 Water Vapor Flux vs. Feed Relative Humidity at Different Feed Flow Rates (Module # 2)

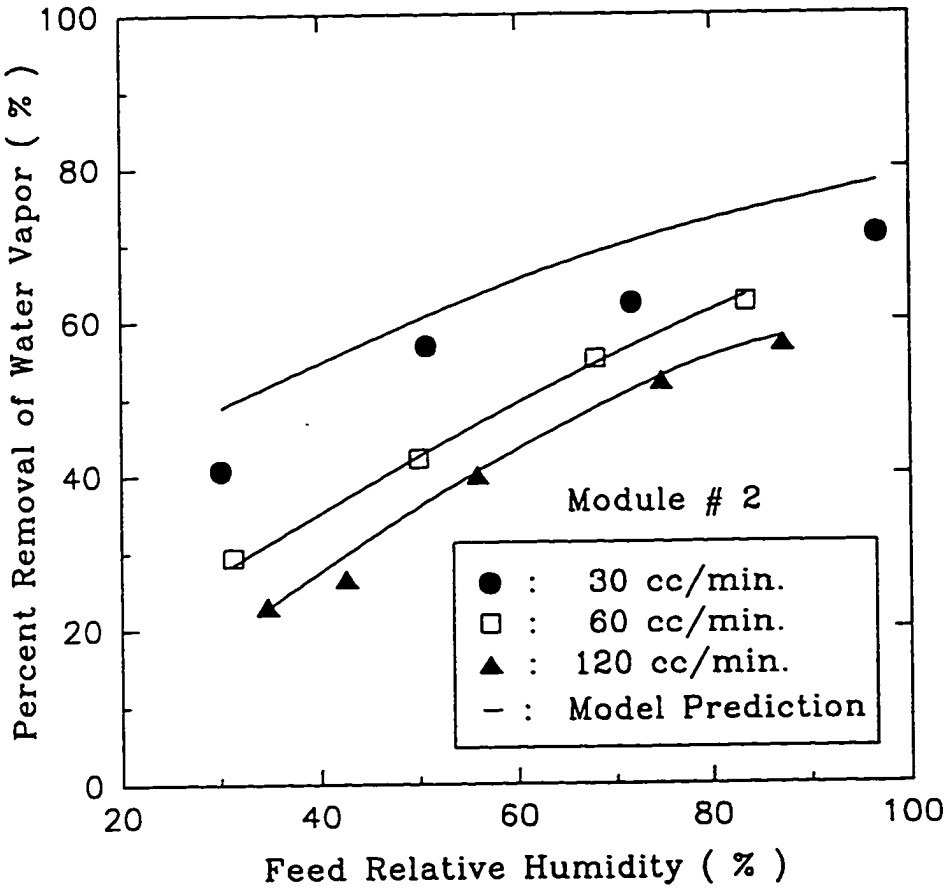

Figure 2.23 Percent Removal of Water Vapor vs. Feed Relative Humidity at Different Feed Flow Rates (Module # 2)

Table 2.6 Flux and Percent Removal of Water Vapor vs. Changing Feed Relative Humidity (Module # 2)

Feed Inlet			Feed Outlet			Water Flux ($gmol/min.cm^2$) ($x\ 10^8$)	Percent Removal of Water (%)
Flow rate (cc/min.)	R.H. (%)	Mole Fraction of Water	Flow rate (cc/min.)	R.H. (%)	Mole Fraction of Water		
31.8	30.1	0.00795	31.1	18.2	0.00481	2.59	40.7
31.7	50.8	0.0123	31.1	22.4	0.00543	5.61	56.8
32.1	71.7	0.0177	31.5	27.5	0.00679	8.97	62.3
31.9	96.8	0.0242	31.3	28.3	0.00707	13.9	71.3
68.9	31.3	0.00731	67.9	22.4	0.00523	3.76	29.4
69.2	50.0	0.0123	68.2	29.3	0.00719	9.06	42.2
68.9	68.0	0.0172	67.9	31.0	0.00784	16.5	55.1
68.8	83.5	0.0221	67.8	31.8	0.00840	23.9	62.4

Table 2.6 Flux and Percent Removal of Water Vapor vs. Changing Feed Relative Humidity (Continued, Module # 2)

Feed Inlet			Feed Outlet			Water Flux (gmol/min.cm^2) (x 10^8)	Percent Removal of Water (%)
Flow rate (cc/min.)	R.H. (%)	Mole Fraction of Water	Flow rate (cc/min.)	R.H. (%)	Mole Fraction of Water		
99.9	37.3	0.00938	98.1	29.9	0.00752	5.05	21.3
99.8	51.2	0.0130	98.0	34.9	0.00889	10.9	33.1
99.7	67.1	0.0172	97.9	34.3	0.00879	21.6	49.8
99.4	83.6	0.0194	97.6	36.2	0.00840	28.1	57.5
122	34.7	0.0084	119	27.2	0.00659	6.0	23.1
120	42.6	0.0109	118	31.9	0.00817	8.8	26.6
119	55.9	0.0148	116	34.0	0.00898	17.8	40.0
118	74.8	0.0200	116	36.5	0.00976	31.1	52.2
119	87.2	0.0228	116	38.2	0.00997	39.2	57.1

Table 2.7 Flux and Percent Removal of Water Vapor vs. Changing Feed Relative Humidity (Module # 3)

Feed Inlet			Feed Outlet			Water Flux ($gmol/min.cm^2$) ($\times 10^8$)	Percent Removal of Water (%)
Flow rate (cc/min.)	R.H. (%)	Mole Fraction of Water	Flow rate (cc/min.)	R.H. (%)	Mole Fraction of Water		
30.0	34.6	0.00784	29.7	21.8	0.00494	2.06	37.6
29.7	51.0	0.0118	29.3	29.1	0.00676	3.57	43.7
29.7	73.1	0.0158	29.3	30.4	0.00655	6.42	59.0
29.6	85.4	0.0201	29.3	30.7	0.00722	8.15	64.4
61.4	32.1	0.00683	61.0	27.0	0.00575	2.10	27.5
61.4	49.4	0.0116	60.9	32.1	0.00755	3.84	34.6
61.0	75.1	0.0169	60.5	33.9	0.00763	7.32	53.8
61.3	92.5	0.0222	60.9	34.1	0.00817	9.40	58.6

Table 2.7 Flux and Percent Removal of Water Vapor vs. Changing Feed Relative Humidity (Continued, Module # 3)

Feed Inlet			Feed Outlet			Water Flux ($gmol/min.cm^2$)	Percent Removal of Water
Flow rate (cc/min.)	R.H. (%)	Mole Fraction of Water	Flow rate (cc/min.)	R.H. (%)	Mole Fraction of Water	($x\ 10^8$)	(%)
91.0	32.2	0.00757	90.3	26.2	0.00616	3.07	25.7
89.3	45.1	0.0111	88.5	30.9	0.00763	7.41	32.2
89.6	56.3	0.0133	88.7	33.7	0.00797	11.2	40.7
89.4	72.4	0.0172	88.5	36.8	0.00876	17.7	49.7
87.5	89.7	0.0216	86.7	37.1	0.00894	21.4	52.4
117	32.9	0.00793	115	25.6	0.00617	4.93	23.1
116	42.2	0.0100	114	30.4	0.00723	7.75	28.9
116	53.0	0.0125	115	36.1	0.00854	11.0	32.6
117	69.7	0.0164	115	39.8	0.00936	19.3	43.7
116	87.4	0.0204	115	42.5	0.00993	28.6	50.2

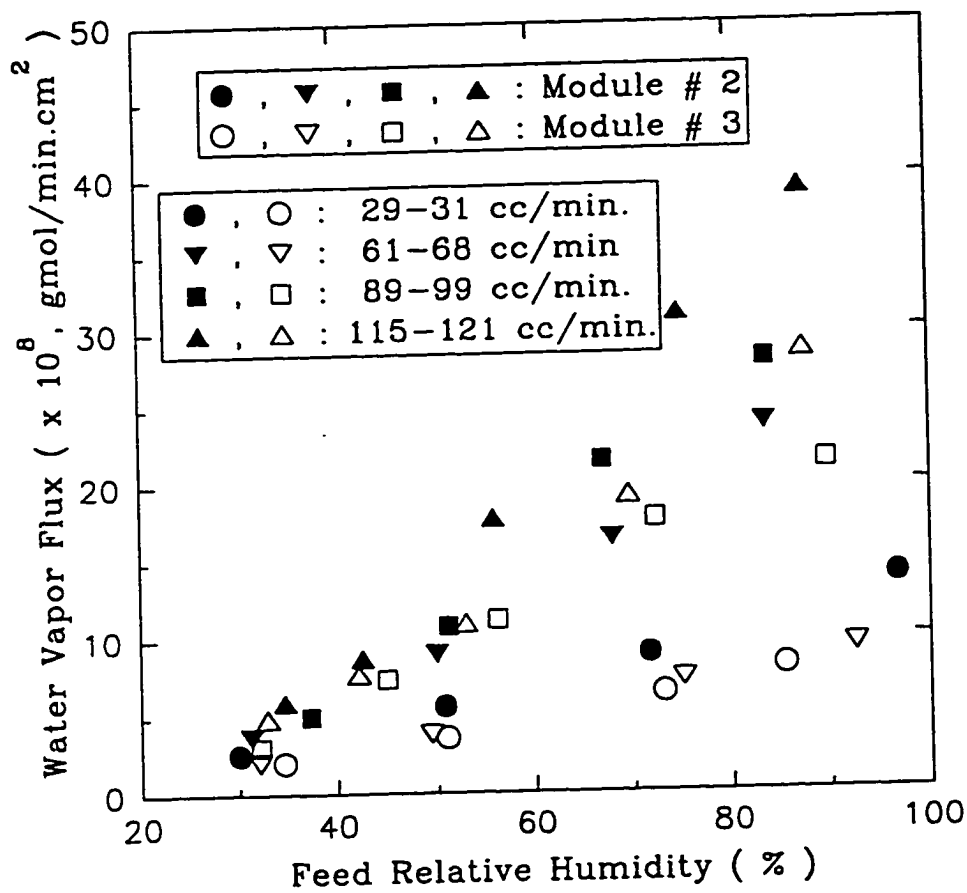

Figure 2.24 Water Vapor Flux vs. Feed Relative Humidity at Different Feed Flow Rates

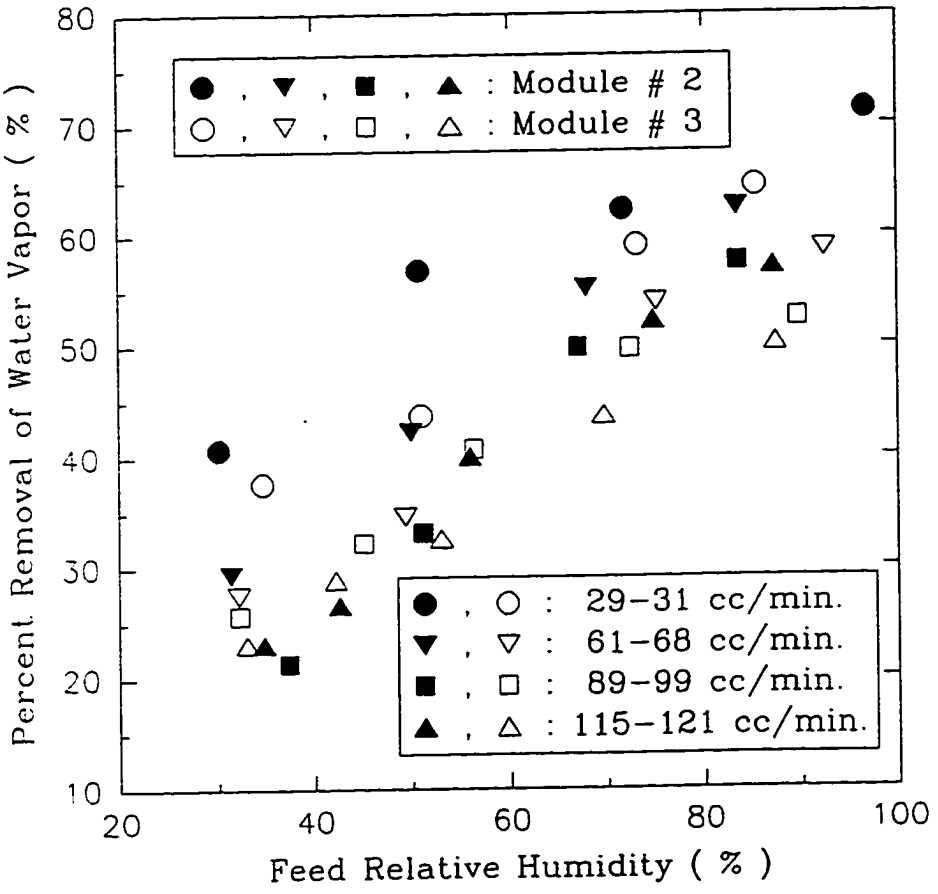

Figure 2.25 Percent Removal of Water Vapor vs. Feed Relative Humidity at Different Feed Flow Rates

through asymmetric Cuprophan fibers. The percent removal was also slightly higher in module 2 for the same reason over the complete flow rate range.

2.4.5 Removal of Water Vapor and/or VOCs from an Inert N_2 Stream

Studies on the transport and permeation of some VOCs through the polymeric hollow fiber gel membrane were also carried out. Among the VOCs, toluene and methanol were chosen. The solubility of methanol in water is very high, but toluene is much less soluble (450 - 500 mg/l). The candidate VOCs can get transported through the hydrogel portion of the membrane as well as through the portion of the cellulosic polymer matrix. Table 2.8 reports the experimental conditions and results. Total gas mixture flow rate (N_2 plus water vapor plus toluene vapor) was maintained around 30 cc/min. and three different relative humidity levels (25-75 %) of water vapor were chosen. At each relative humidity level, toluene concentration was varied from about 1,000 to 6,000 ppm.

The flux of water vapor, as expected, was a function of its relative humidity (or partial pressure) value. As the feed relative humidity level was raised, the flux as well as the percent removal of water vapor was increased. But the water vapor flux at constant relative humidity level was not affected much by changing the feed toluene concentration. It was almost constant irrespective of the feed toluene concentration. The toluene flux, as expected, was directly affected by its concentration level. It was increased almost linearly by the increasing concentration of feed toluene at constant relative humidity level as shown in figure 2.26. The percent removal of water vapor was also higher at higher relative humidity level but at constant relative humidity level it was almost constant with changing feed toluene concentration.

Figure 2.27 illustrates percent removal of water and toluene vapor as a function of the feed toluene concentration. The values of the percent removal of toluene vapor appears to be a constant within the range of 7 to 10 percent irrespective of relative humidity levels as well as feed toluene concentrations. The percent removal of water

Table 2.8 Flux and Percent Removal of Water Vapor and Toluene vs. Water and Toluene Concentrations
(Module # 2, Flow rate : 30 cc/min.)

Feed Inlet				Feed Outlet				Flux (gmol/min.cm^2)		Percent Removal (%)	
Flow rate (cc/m)	R.H. (%)	Mole Fraction		Flow rate (cc/m)	R.H. (%)	Mole Fraction					
		Water	Toluene			Water	Toluene	Water (x10^8)	Toluene (x10^9)	Water	Toluene
31.1	28.4	0.00888	0.00171	29.7	16.1	0.00503	0.00164	3.16	1.10	45.8	8.3
30.6	28.3	0.00885	0.00295	29.1	15.5	0.00485	0.00287	3.24	1.70	47.9	7.6
31.2	28.2	0.00882	0.00333	30.0	18.7	0.00585	0.00324	2.51	1.84	46.6	7.1
30.3	27.8	0.00869	0.00446	28.9	17.5	0.00547	0.00431	2.63	2.65	40.0	7.8
30.4	28.9	0.00903	0.00661	28.9	16.8	0.00525	0.00639	3.05	3.86	45.6	7.7
30.3	61.3	0.0192	0.00169	29.1	19.3	0.00603	0.00163	10.1	1.00	69.8	7.8
30.9	56.2	0.0176	0.00265	29.7	18.0	0.00563	0.00251	9.37	1.82	69.2	8.9
30.6	56.2	0.0176	0.00354	29.4	17.1	0.00535	0.00343	9.50	1.88	70.7	6.9
31.1	55.2	0.0173	0.00436	29.7	15.9	0.00497	0.00420	9.69	2.70	72.4	8.0
31.2	70.8	0.0221	0.00198	30.3	19.2	0.00601	0.00183	12.7	1.55	73.7	10.1
30.8	75.4	0.0236	0.00320	29.9	19.7	0.00616	0.00297	13.5	2.39	74.6	9.7
31.3	75.9	0.0237	0.00447	30.4	20.3	0.00635	0.00412	13.7	3.59	74.0	10.3
31.3	76.0	0.0238	0.00508	30.3	20.1	0.00628	0.00459	13.8	4.95	74.4	12.5

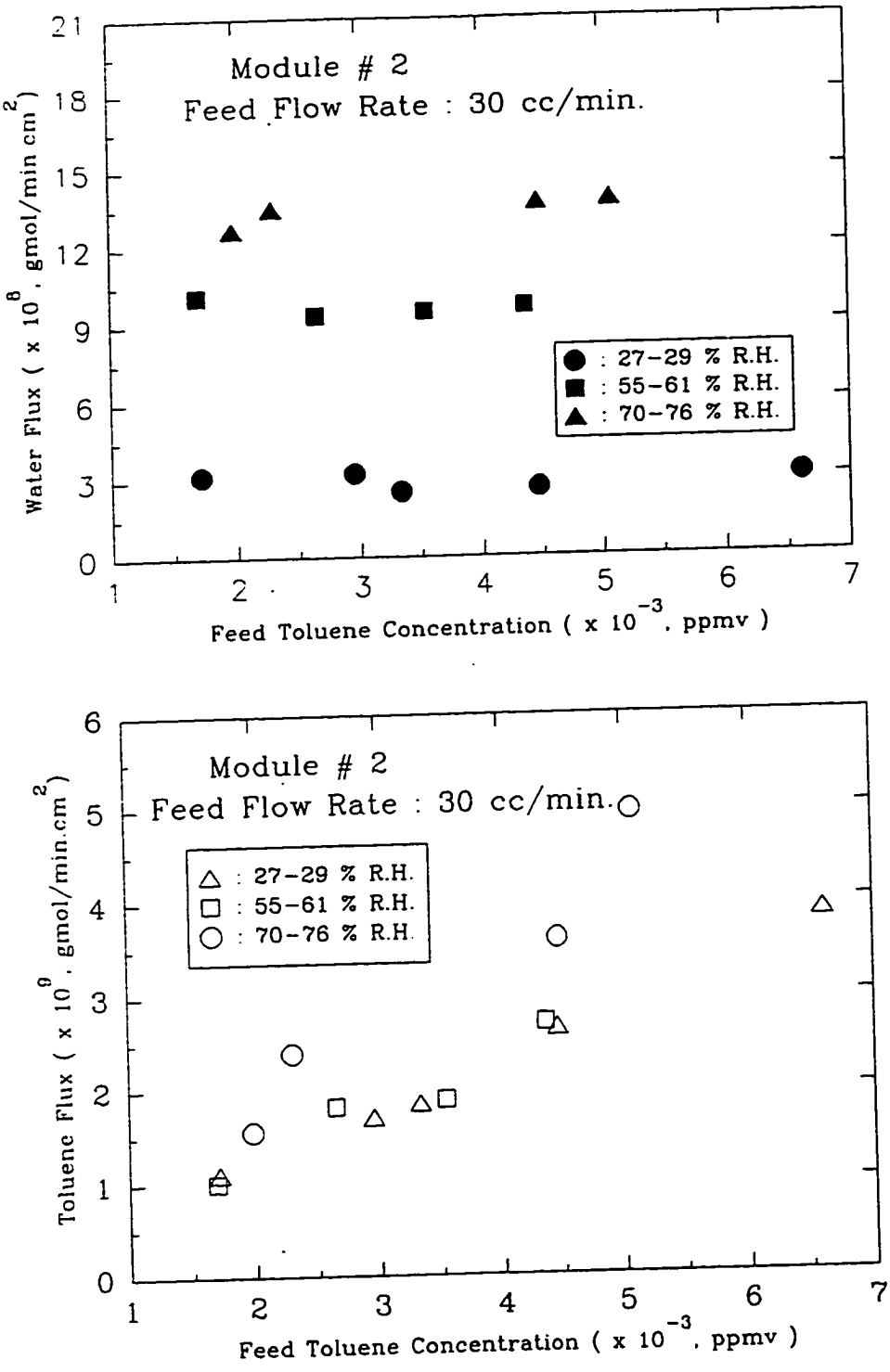

Figure 2.26 Water and Toluene Flux as a Function of Toluene Concentrations at Different Relative Humidity

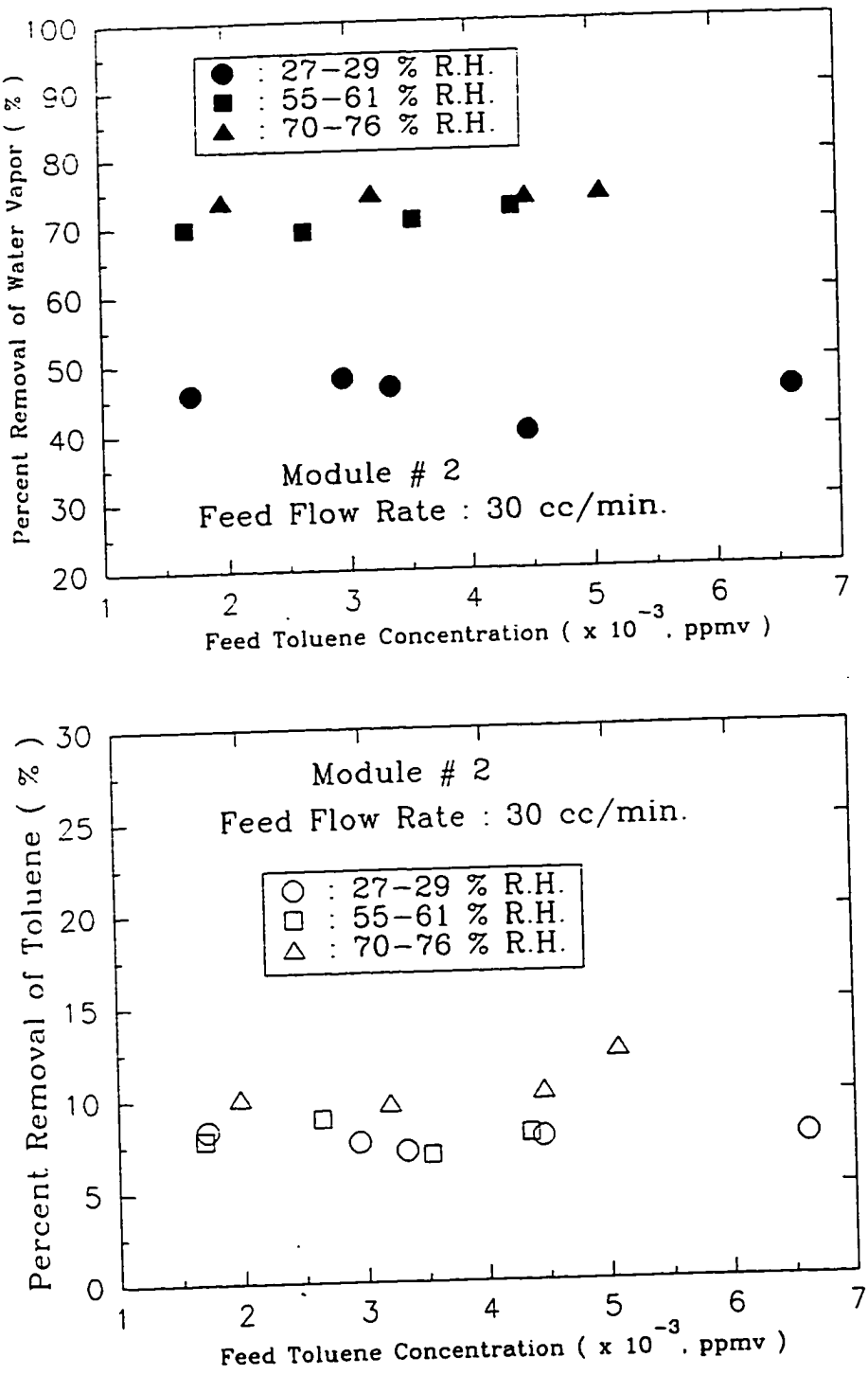

Figure 2.27 Percent Removal of Water and Toluene as a Function of Toluene Concentrations at Different Relative Humidity

vapor changed from 45 to 70 % levels depending on the feed relative humidities; for all experimental conditions employed, it seemed that water vapor removal appeared to be primary compared to the toluene vapor removal. The removal rate of water vapor was 4 to 5 times higher than that of the toluene vapor.

The behavior of the flux and percent removal of water and toluene vapor at constant relative humidity as the toluene concentration is changing and at constant toluene concentration level while the relative humidity of water vapor is changing are shown in table 2.9 and in figure 2.28. At constant humidity levels, the flux of water vapor remained constant but the flux of toluene vapor was increasing as the feed toluene concentration is increased. The percent removal of both vapors was essentially constant for the flow rate used (90 cc/min.) but the values were reduced compared to the low flow rate case (30 cc/min.). If the feed relative humidity was increased keeping the toluene concentration almost constant, the flux and the percent removal of water vapor were increased but the toluene flux and percent removal were not affected.

If toluene vapor is present in the feed with the water vapor and inert nitrogen, one wonders which component is transported faster and also how much of those components are transferred to the permeate side at the given experimental conditions. Cuprophan is a hydrophilic membrane and it becomes a swollen gel in the presence of water vapor. Filho et al. (1992) reported that lumen of Cuprophan pores contains free hydroxyl groups and there is a structuration of water molecules due to hydrogen bonds. This is called the bound state of water and this bound water is very compactly attached to the polymer. Most cellulosic materials hold water by hydrogen bonding of multilayers of water. Water molecules seem to become temporarily immobilized because of its great attractive force for cellulose (Stamm, 1956). When the VOC (toluene or methanol) is present along with the water vapor in the feed nitrogen stream, the membrane absorbs the water vapor instantly and faster than the VOCs and forms a hydrogel immediately.

Since all the openings of the polymer matrix is filled with water depending on the

Table 2.9 Flux and Percent Removal of Water Vapor and Toluene vs. Water and Toluene Concentrations
(Module # 2, Flow rate : 91 cc/min.)

Feed Inlet				Feed Outlet				Flux (gmol/min.cm^2)		Percent Removal (%)	
Flow rate (cc/m)	R.H. (%)	Mole Fraction		Flow rate (cc/m)	R.H. (%)	Mole Fraction					
		Water	Toluene			Water	Toluene	Water (x10^7)	Toluene (x10^9)	Water	Toluene
91.2	49.8	0.0156	0.00229	89.7	20.6	0.00644	0.00222	2.10	2.38	59.3	4.6
91.3	50.0	0.0156	0.00276	89.8	20.8	0.00650	0.00266	2.11	3.41	59.2	5.4
91.2	49.8	0.0156	0.00415	89.7	20.6	0.00644	0.00401	2.10	4.65	59.3	4.9
91.2	49.8	0.0156	0.00620	89.6	20.6	0.00644	0.00600	2.10	6.82	59.4	4.8
91.2	22.1	0.0069	0.00255	89.7	15.8	0.00494	0.00245	0.47	3.35	29.7	5.8
91.4	25.4	0.0079	0.00261	89.9	16.3	0.00510	0.00251	0.67	3.27	36.9	5.5
91.3	50.0	0.0156	0.00276	89.6	20.8	0.00650	0.00266	2.11	3.41	59.2	5.4
91.2	74.3	0.0232	0.00248	89.4	26.3	0.00822	0.00238	3.45	3.32	65.3	5.9

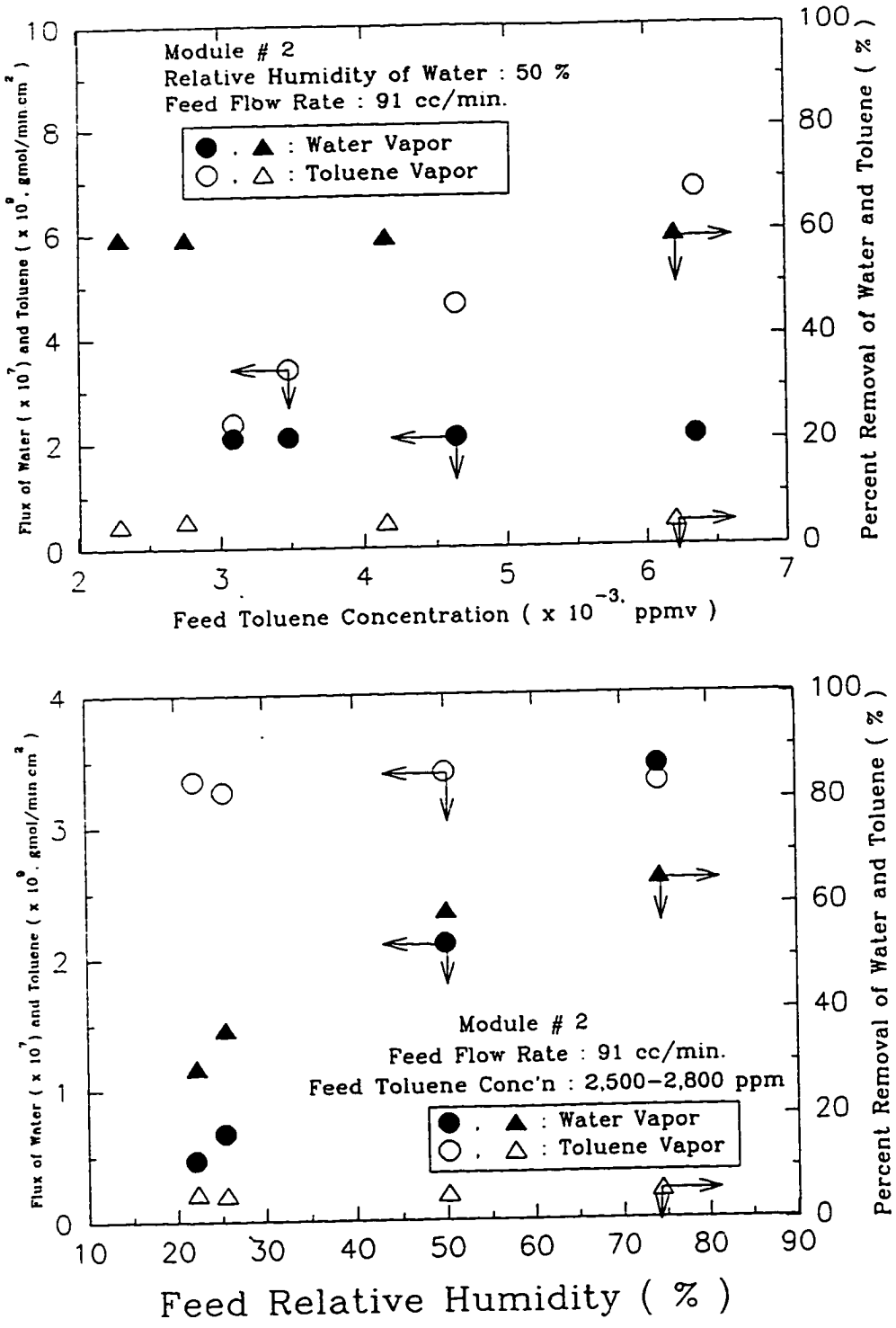

Figure 2.28 Flux and Percent Removal of Water and Toluene as a Function of Toluene Concentrations as well as Feed Relative Humidity

relative humidity level, the transport of toluene can occur through this gel membrane according to their solubility in water. The value of water vapor permeance was of the order of 10^{-9} gmol/sec.cm^2.cmHg and the toluene vapor permeance was generally an order of magnitude lower than that of water vapor (10^{-10} gmol/sec.cm^2.cmHg). The permeance ratio between water vapor and toluene vapor (Q_w/Q_{tol}) was in the range of 6-14 in the employed experimental ranges. The experimental results showed that the removal rate of water vapor was always higher than toluene under all experimental conditions used. The removal rate of water vapor was a strong function of its relative humidity levels but in the case of toluene vapor it was not changed much even though the feed relative humidity level or feed toluene concentration were changed.

When methanol vapor was present with water vapor and inert nitrogen, total gas mixture flow rate was changed from 10 to 90 cc/min. At each flow rate, 2-4 different methanol concentrations were provided between 1,000 ppm and 6,500 ppm. When the total flow rate was maintained constant (30 cc/min.), flux of water vapor was higher as the relative humidity level was higher as was found in the case of toluene vapor (table 2.10). Percent removal of methanol was 4-10 times larger compared to that for toluene (this was mainly due to the solubility difference of methanol and toluene in water) and it was changed according to the concentration of the methanol vapor in the feed. These polar VOCs are not likely to be rejected much by the hydrogel Cuprophan membrane. As the feed methanol concentration is increased at a given relative humidity, fractional removal of methanol was decreased while that of water remained almost constant.

Table 2.10 and figure 2.29 show experimental results and the corresponding plot. Higher percent removal of water vapor was found at higher relative humidity level and it was not affected by the methanol concentrations in the feed. This was also true for toluene vapor. Decreasing fractional removal of methanol vapor for increasing methanol concentrations in the feed was also found in these experiments. The solubility of methanol in water is very high. When methanol vapor is present along with water vapor in the feed,

Table 2.10 Flux and Percent Removal of Water Vapor and Methanol vs. Water and Methanol Concentrations (Module # 2)

Feed Inlet				Feed Outlet				Flux (gmol/min.cm^2)		Percent Removal (%)	
Flow Rate (cc/m)	R.H. (%)	Mole Fraction		Flow Rate (cc/m)	R.H. (%)	Mole Fraction		Water (x10^8)	MeOH (x10^9)	Water	MeOH
		Water	MeOH			Water	MeOH				
32.7	52.4	0.0164	0.00130	31.2	15.8	0.00494	0.00064	10.3	9.5	71.3	53.0
32.7	50.5	0.0158	0.00283	31.1	15.6	0.00488	0.00166	9.86	10.2	70.6	44.1
32.8	47.5	0.0149	0.00420	31.5	14.9	0.00466	0.00301	9.30	10.7	70.0	31.0
32.7	49.9	0.0156	0.00653	31.4	15.4	0.00481	0.00526	9.74	12.1	70.4	22.6
31.1	74.5	0.0233	0.00211	29.7	18.9	0.00591	0.00076	12.1	10.8	75.7	65.7
31.2	72.1	0.0225	0.00268	29.8	18.4	0.00575	0.00167	12.5	10.2	75.6	56.6
31.1	75.0	0.0234	0.00469	29.7	18.7	0.00585	0.00336	12.3	11.5	76.1	31.6
31.1	75.8	0.0237	0.00630	29.8	19.2	0.00600	0.00514	12.2	10.8	75.8	22.0
10.6	31.1	0.0097	0.00278	10.3	5.5	0.00172	0.00196	2.13	2.31	82.9	31.5
10.6	56.6	0.0177	0.00374	10.2	6.4	0.00200	0.00230	4.16	4.02	90.1	40.7
92.6	24.6	0.0077	0.00330	90.8	12.7	0.00397	0.00260	8.79	3.94	49.4	22.8
93.0	67.3	0.0210	0.00317	91.0	21.9	0.00685	0.00238	33.3	19.5	68.2	26.4

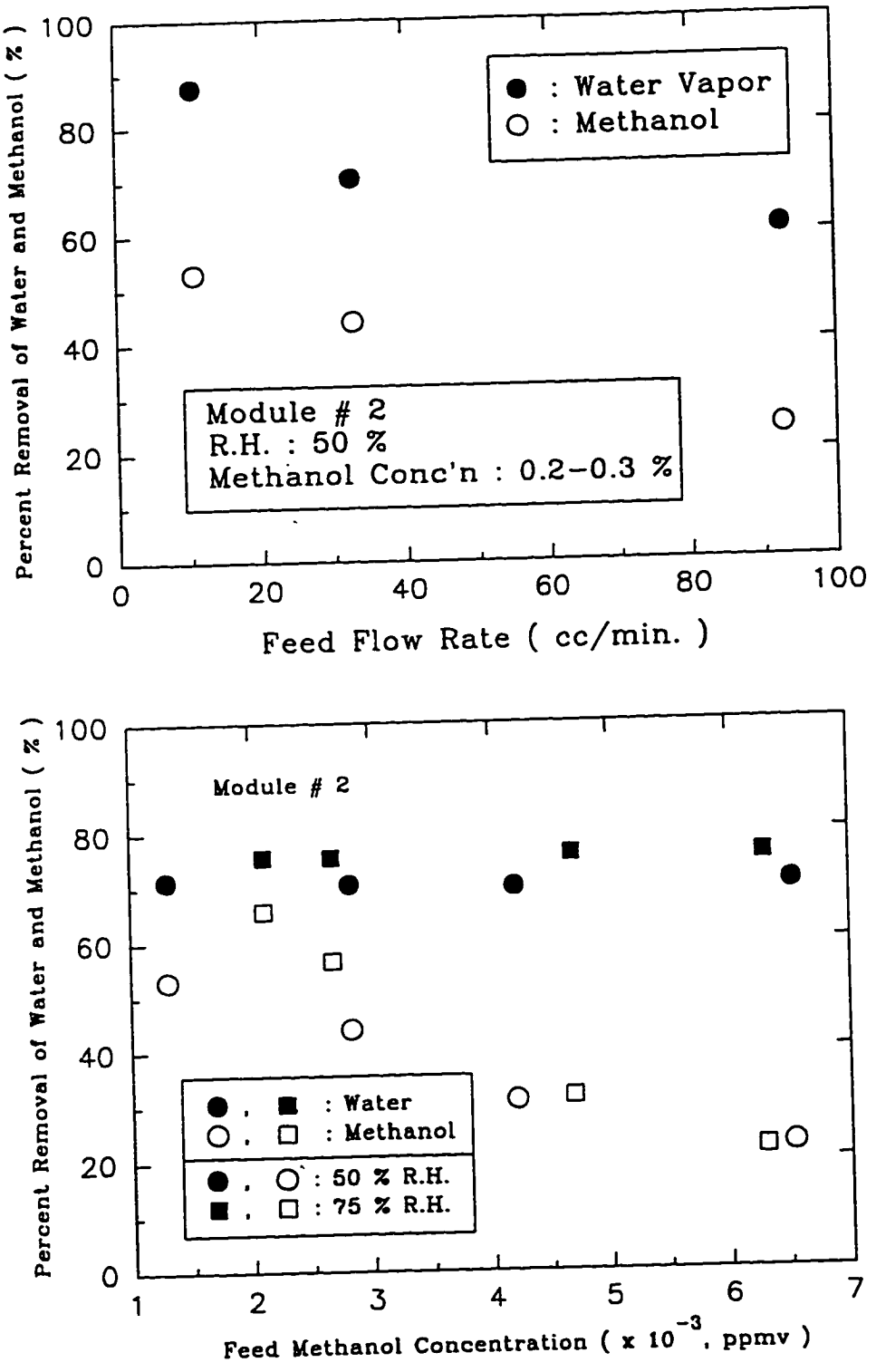

Figure 2.29 Percent Removal of Water and Methanol as a Function of Feed Flow Rate as well as Feed Methanol Concentrations

there may be a strong site competition compared to the toluene vapor case to occupy the pores of the membrane since both components have a possibility of hydrogen bonding with hydroxyl group in the pore. Here we can still assume that water molecules have priority to fill the pores due to the high hydrophilicity of the membrane. Almost constant removal of water vapor at constant relative humidity level even if methanol concentrations are varying will be the basis for such a conclusion. Since VOC transport through Cuprophan gel membrane was done in an exploratory fashion, more systematic study has to be done to find out the whole spectrum of VOC transport behavior. These will include other VOCs, lowering the VOCs concentration levels drastically upto a few ppm, wide concentration changes at different relative humidity levels as well as changing the nature of the hydrogel, etc.

2.5 Conclusions

Water vapor was removed successfully through dried Cuprophan hollow fiber membranes in a multi-fiber module under the vacuum mode of operation. The permeance of water vapor through this hollow fiber membrane is a strong function of its partial pressure (or relative humidity) and this relation was fit well by an exponential curve. A mathematical model-based equation was developed utilizing the observed exponential variation of water vapor permeance with relative humidity. The feed outlet mole fraction of water was calculated by solving the model equation analytically for particular conditions. The performances of Cuprophan membrane modules in terms of the feed outlet mole fraction, flux, percent removal and module-averaged permeance of water vapor were obtained experimentally. The observed values are described well by the model results.

The configuration of this membrane process is such that if the length of a much bigger permeator is equal to that of any permeator used here then the performance of the bigger permeator can be predicted simply on the basis of the feed gas flow rate per fiber in the smaller permeator. If the permeator lengths are different then a numerical calculation has to be carried out based on the equations used here.

Cuprophan membrane is highly hydrophilic by nature and it forms a hydrogel immediately by combining with the water molecules. This hollow fiber membrane seems to expand and shrink according to the ambient relative humidity levels. In the case of high relative humidity levels, the membrane swells more and the water containing openings in the polymer matrix becomes larger and the permeance of water vapor in this case was high. Nitrogen permeation through Cuprophan gel membrane was not affected much by the relative humidity levels of the feed, but carbon dioxide permeation was a function of the relative humidity levels and it showed a behavior similar to that for water vapor.

The selectivity of water vapor with respect to nitrogen through Cuprophan

membrane could be calculated from the ratio of the two species permeances; it was found to be in the range of 20-250 depending on the feed relative humidity levels. Carbon dioxide permeance through the gel membrane was 9-40 times higher than nitrogen permeance especially when the relative humidity levels were over 75 %. When the membrane becomes dry by passing pure carbon dioxide for a sufficiently long time, the membrane swelling is reduced drastically. As a result, the extent of permeation of carbon dioxide through the membrane was also reduced drastically.

When water vapor is present with toluene vapor in N_2, water vapor permeation was dominant compared to permeation of toluene vapor. There seems to be no site competition between water molecules and toluene molecules. Water molecules were primarily filling the openings of the Cuprophan polymer matrix and were also removed primarily by its partial pressure difference across the membrane. The percent removal of toluene vapor was an order of magnitude lower than that of water vapor. Such a process can be applied to the removal/regeneration of water vapor from a humid spent/cabin air. In the case of water vapor and methanol vapor mixture, there seems to be a site competition between the water and methanol molecules to form a hydrogen bond. Still water molecules are likely to be preferred in filling the pores due to the high hydrophilicity of the membrane. Water vapor removal was also primary compared to the methanol vapor as was found in the case of toluene vapor. Fractional removal of methanol vapor was 4-10 times larger than that of toluene vapor at similar relative humidity levels and this was mainly due to the difference in solubilities of methanol and toluene in water.

CHAPTER 3

REMOVAL OF VOCs FROM N_2 BY A RUBBERY MEMBRANE

3.1 Introduction

3.1.1 Transport in Nonporous Membranes

Although research on membrane gas separation processes has been going on for more than 20 years, the research on vapor permeation/separation using membranes has a relatively short history. Membrane vapor permeation is quite similar to pervaporation (Sander and Janssen, 1991). In pervaporation the feed mixture is a liquid and the component to be separated from a liquid feed mixture is permeating through the membrane and evaporated as a vapor at the permeate side of the membrane. In membrane vapor permeation, the feed mixture is in a gas/vapor state and the component to be separated from the feed mixture is just permeating through the permselective, nonporous membrane. The separation of organic vapors by membranes is generally a low-pressure membrane process (essentially atmospheric pressure, Wijmans and Helm, 1989). In this process, the feed gas/vapor mixture is introduced to one side of the membrane module and usually the vapor component preferentially permeates through the membrane by the partial pressure difference on the two sides of the membrane. To create the driving force, a vacuum pump is generally used on the permeate side; the permeated organic vapor is then condensed in the cold trap and collected as an organic liquid.

The permeation of gases/vapors through a nonporous membrane is generally analyzed by the solution diffusion model according to which the gas/vapor molecules get dissolved in the high pressure side of the membrane, diffuse through the membrane and are finally desorbed at the low pressure membrane-gas interface. The rate of permeation is strongly influenced by permeability which is the product of the diffusivity of gas/vapor

through the membrane and its solubility in the membrane. Here diffusivity is a kinetic property and solubility is a thermodynamic property of the permeants. In general, diffusivity of the permeant decreases with increasing permeant diameter. On the other hand, solubility is likely to increase with the permeant diameter.

The permeability is relatively high in most polymer membranes for very small molecules such as He or H_2 due to their high diffusivity through the polymer membrane. Relatively large molecules like CO_2 have also a high permeability due to their high solubility in the membrane. The effects of diffusivity and solubility on the permeability are comparable in the case of simple gases. For vapors, however, the permeabilities are significantly higher than simple gases in most polymers (Baker et al., 1987 & 1988; Feng et al., 1991 & 1993). Because most vapors are highly condensible, the condensibility of the vapors, which is determined by the critical temperature of the vapors, is a measure of the solubility of the species in the polymer.

The permeation of gases/vapors through nonporous polymer membranes depends strongly on whether the membrane is above or below its glass transition temperature, that is whether it is in a rubbery or glassy state. A rubbery polymer such as silicone rubber shows relatively high permeabilities for most gases/vapors since the chain mobility is high but selectivities are generally poor. A glassy or crystalline polymer such as polystyrene shows much lower permeabilities but higher selectivities compared to the rubbery polymers. The permeabilities of simple gases such as He, H_2, O_2, N_2 etc. through a nonporous polymeric membrane are generally not a function of their concentration or partial pressure in the gas phase. For rubbery membranes, the permeabilities of the simple gases are taken as constant (Stern and Frisch, 1981). For glassy membranes, the permeabilities, although generally constant, are considerably lower.

Transport of a vapor through a rubbery polymeric membrane is determined more by its solubility than by its diffusivity. Higher permeability of the vapors is first attributed to the higher solubility of the vapors in the membrane. Further higher sorption at high

organic vapor pressures also leads to plasticization of the membrane; this will increase the diffusivity of organic vapor through the plasticized polymer matrix. Permeabilities of organic vapors are therefore a strong function of their partial vapor pressure in the gas phase; it increases drastically with increasing vapor concentrations.

It is well known that the nonporous silicone rubbery membranes have an extremely high permeabilities for VOCs and comparatively lower permeabilities for nitrogen or oxygen. It is therefore one of the widely used membrane polymers as far as organic vapor separation from air is concerned (Peinemann et al., 1986; Blume et al., 1991). The selective membrane in this study is therefore an ultrathin silicone membrane.

3.1.2 Objective of This Study

The general objective of this study is to develop selective permeation-recovery of VOCs from N_2/air via a novel highly VOC-selective silicone coated hollow fiber membrane. In this system, VOC-laden air/N_2 stream is introduced to the tube side of the hollow fiber membrane module and vacuum is applied to the permeate side. Permeated organic vapors are condensed in the cold trap and purified air stream leaves the module. A schematic of VOC permeation at atmospheric pressure using vacuum mode of operation and a hollow fiber membrane module is illustrated in figure 3.1. This research will explore experimentally the extent of selective removal of VOCs such as toluene and methanol from N_2/air at atmospheric pressure and provide a basis for modeling the separation performance of the hollow fiber permeator.

3.1.3 Membrane Form, Structure and Operational Mode

Membranes in hollow fiber form are self-supporting against any applied pressure difference needed for vapor separation. They are therefore quite distinct from flat membranes which have to be provided additional mechanical support. This fact along with the type of successful module design used for flat membranes, namely, spiral-wound leads

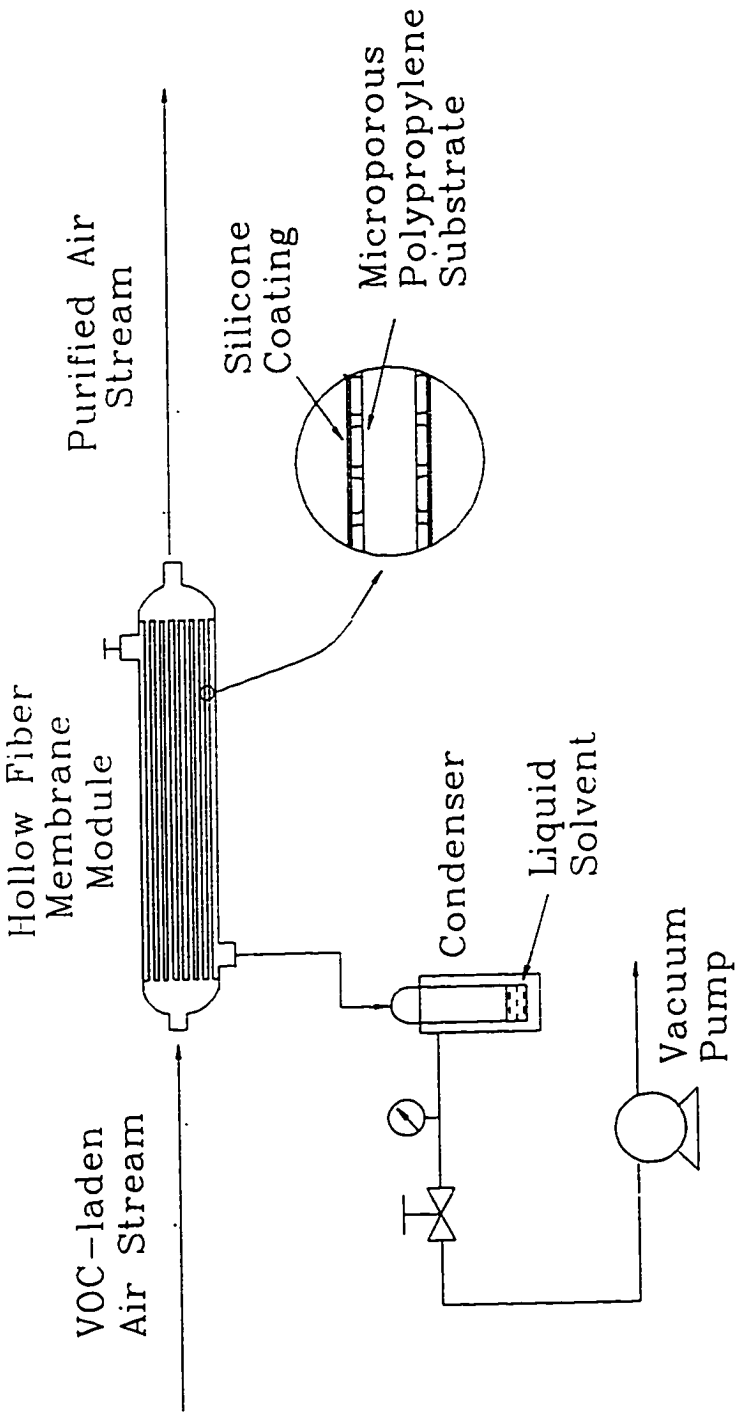

Figure 3.1 Schematic of VOC Separation from Air/N_2 at Atmospheric Pressure by Permeation through a Hollow Fiber Module

to a tremendous advantage in membrane surface packing density for hollow fibers. It is routine for hollow fiber modules to achieve a membrane surface packing density of 40-80 cm^{-1} compared to 5-7 cm^{-1} for spiral wound modules. To increase vapor permeation rate, the membrane has to be ultrathin; thin film composite (TFC) membrane structure is chosen here with the ultrathin membrane being supported on a microporous hollow fiber substrate. To reduce the support resistance, the porosity of the support has to be high.

Ordinarily the flux of a species through a composite membrane consisting of a coating on a microporous substrate will be influenced by the resistances of both layers (Sengupta and Sirkar, 1986). Depending on the nature of the coating, its thickness, the nature of the substrate and its thickness, the species flux through the membrane may be controlled by the substrate or by the coating or by both. Substrate-controlled separation of gas mixture is well known and is illustrated by the PRISM process commercialized by Monsanto (Henis and Tripodi, 1981). The substrate in these membranes had very low porosity.

Celgard x-20 fiber is isotropic and has a porosity of 0.4 which is quite high. The hollow fiber substrate of this study having an ultrathin silicone coating on the outside surface is a Celgard x-20 fiber; thus substrate porosity being high will not reduce the flux through the coating (Matson et al., 1983; Sengupta and Sirkar, 1986).Further the support material should be cheap and have a reasonably high solvent resistance. Polypropylene is quite suitable in this regard since it is cheap compared to polyetherimide (Behling et al.,1989), strong and has considerable solvent resistance compared to polysulfone used by others (Strathmann et al.,1986 & 1988; Kimmerle et al., 1988).

There are additional considerations. Since VOC-containing N_2/air is usually at atmospheric pressure, vacuum is pulled on the other side of the membrane to provide a partial pressure driving force for the VOC. If vacuum is pulled through the porous substrate, there would be considerable pressure drop not only through the substrate but also through the fiber lumen. Therefore it is advantageous to pull the vacuum through the

shell side and have the feed gas flow through the tube side. However this operational mode subjects the silicone coating on the fiber outside diameter to extra stress and possible delamination from the substrate if the silicone coating was applied conventionally where the bond between the coating and substrate is weak. The AMT (Applied Membrane Technology) fibers used in this study have an ultrathin plasma-polymerized silicone layer (~1 μm) which has strong bonds with the substrate and can handle a pressure difference up to 200 psia (Papadopoulos, 1992).

Having the feed gas flow rate through the fiber bore eliminates the possibility of reduced separation by feed bypassing if the feed gas were to flow through the shell-side. Since high VOC removal is desirable in one pass, the gas flow rate through the fiber bore would have to be low; this will reduce the flow pressure drop in feed gas substantially. Thus the membrane form, structure and operational mode chosen for this study are likely to be optimal. Hollow fibers provide high membrane surface packing density. Celgard x-20 substrate is cheap, strong, chemically resistant and has a high porosity. The actual silicone membrane is ultrathin, has a low permeation resistance but is strongly bonded to the highly porous substrate to handle high pressure drops. Feed gas flows through the fiber bore to provide high separation, no feed bypassing and high partial pressure driving force.

When the feed gas-vapor mixture is at a high pressure, it is advisable to pass the feed gas on the shell side. The permeate may be collected from the tube-side under vacuum or as such. This configuration will be better from an improved mechanical stability of the thin film composite membrane although the possibility of shell-side bypassing will be there. A schematic of such a mode of operation is shown in figure 3.2. This configuration has not been studied in this thesis.

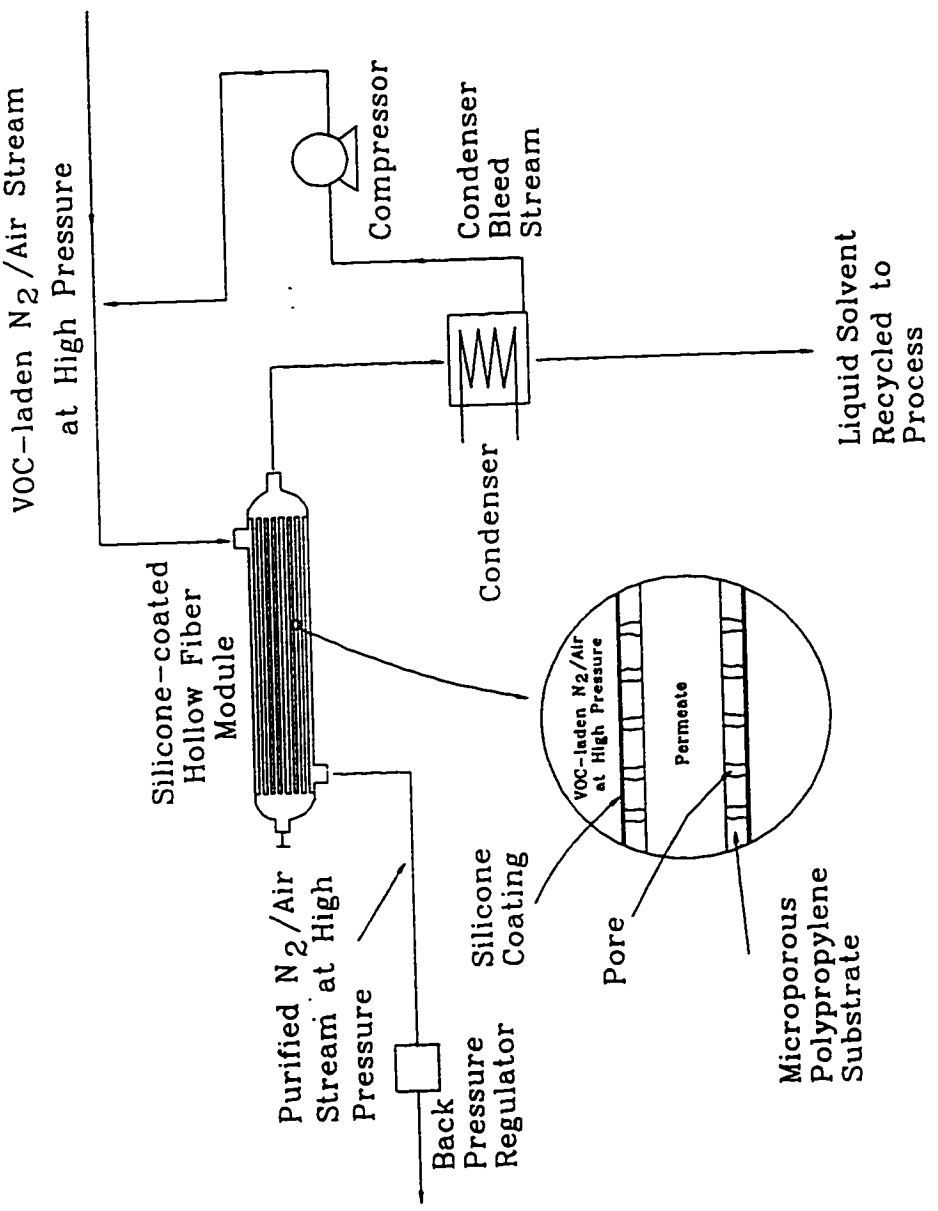

Figure 3.2 Schematic Diagram of VOC Separation-Recycle from Air/N_2 at High Pressure

3.2 Experimental

3.2.1 Materials, Chemicals and Equipments

The materials, chemicals, and equipments used were as follows :

Multiple Flow Controller (Model 8249, Matheson, E. Rutherford, NJ)

Mass Flow Transducer (Model 8141, Matheson, E. Rutherford, NJ)

Mass Flow Controller (Model 8251, Matheson, E. Rutherford, NJ)

Silicone-Coated Hollow Fibers (AMT, Minnetonka, MN)

Gas Chromatograph (GC) (Hewlett Packard Model 5890A)

Automatic 10-port Gas Sampler (Hewlett Packard Model 18900F)

Integrator (Hewlett Packard Model 3392A)

Vacuum Pump (Model 1410, Welch Scientific Inc., Skokie, IL)

Vacuum Gauge (Heise, Newtown, CT)

Cold Trap (Model 8640, Pope Scientific Inc., Menomonee Falls, WI)

Insta-Ice Dry Ice Machine (No.475, Polyfoam Packers Corp, Wheeling, IL)

Constant Temperature Bath

Heater (Haake, Germany)

Bubble Flow Meter (Varian, CA)

Nitrogen Dry, Air Dry, Air Zero, Hydrogen Zero, Helium Zero (Matheson, E. Rutherford, NJ)

Toluene, Methanol (ACS grade, Fisher Scientific, Springfield, NJ).

In HP 5890A gas chromatograph, a 10-port automatic gas sample valve (HP 18900F) which has 0.25 c.c. sampling loop inside the valve was installed for automatic sample analysis.

3.2.2 Hollow Fiber Module Preparation

The fibers used here were supplied by Applied Membrane Technology (AMT, Minnetonka, MN). Fibers were taken from the roll and cut. Required number of fibers of specified length were taken and spread on a vinyl sheet on a table. The fibers spread out were collected and one end was tied with a string. This end was then pulled through the bore of a stainless-steel tubing (I.D. : 0.62 cm) used as the shell for the module.

Three-layer potting was done to prepare a leak-free tube sheet for the module. Figure 3.3 shows the cross-section of one fiber and one module end containing three layers of potting. A two component RTV118 translucent silicone rubber adhesive sealant (GE Silicones, General Electric Co.,Waterford, NY) was applied as the first layer. Since this silicone rubber adhesive is very viscous and its compatibility (or sealing) with the silicone fibers is very good, this material was ideal for potting the first layer. After 1 day cure, another two-component silicone rubber, RTV 615 (GE Silicones, General Electric Co., Waterford, NY), mixed thoroughly using 10 % by weight of the B curing agent with the A silicone compound (entrapped air removed in a desiccator using vacuum pump for approximately 5 min.), was applied as a second layer through the shell side. This compound develops crosslinking via an addition hydrosililation reaction.

The curing time for this silicone rubber depends on the temperature. At a slightly higher temperature (40 - 50 °C) the curing time will be reduced a little bit, but usually it takes over 72 hours. After a 4-day cure, epoxy (C-4: resin, D: deactivator, weight ratio: 4/1; Beacon Chemicals, Mt.Vernon, NY) was applied as a third layer through the shell side (the entrapped air was also removed before potting). Since sealing between the silicone rubber adhesive and the metal part (stainless-steel tubing) may not be very good, epoxy which has also good sealing properties with metal parts was used as a third layer. This epoxy has also a good resistance to the VOCs used in the experiments.

The specifications of the modules are given in table 3.1 and figure 3.4 shows the photograph of the three membrane modules used in this study. The effective surface area

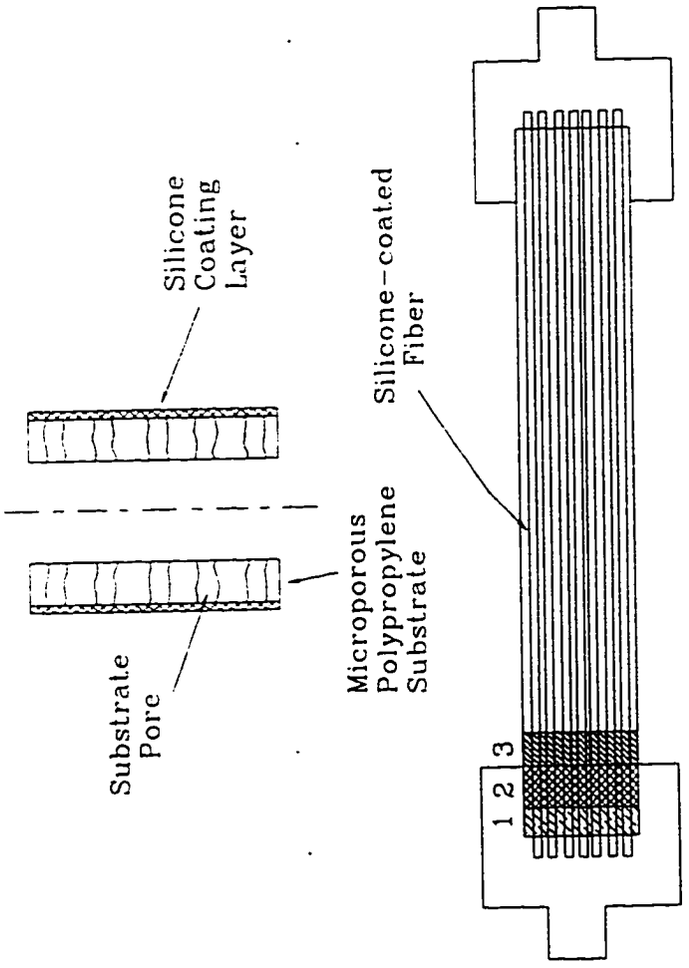

Figure 3.3 Schematics of Silicone-Coated Fiber and Potting

of the module 2 was 103.8 cm^2 (# of fibers : 50, length : 25 cm) and this module was used throughout the experiments. The much smaller module 1 having an effective surface area of 24.9 cm^2 (# of fibers : 30, length : 10 cm) was used for the measurement of permeability of VOCs as well as nitrogen. Module 3, a preexisting module, was used to determine the feasibility of the process.

Table 3.1 Specifications of the Modules Prepared

#	# of Fibers	Effective Fiber Length (cm)	Surface Area of Module (cm^2)	I.D./O.D. of the Fibers (μm)	Coated Layer Thickness (μm)	Average Support Porosity	Avg. Support Pore Size (μm)
1	30	10	24.9	240/290	~1	0.4	0.03
2	50	25	103.8	240/290	~1	0.4	0.03
3	50	12.7	52.7	240/290	~1	0.4	0.03

For testing leakage in a module, distilled water was filled into the shell side of the module. Water pressure was raised to 10-20 psi for about 10 minutes. No water was seen through the tube side; this confirmed that there was no leakage in the module. Pure nitrogen was passed through the tube and shell side of the module for couple of hours to completely dry the fibers prior to experiments.

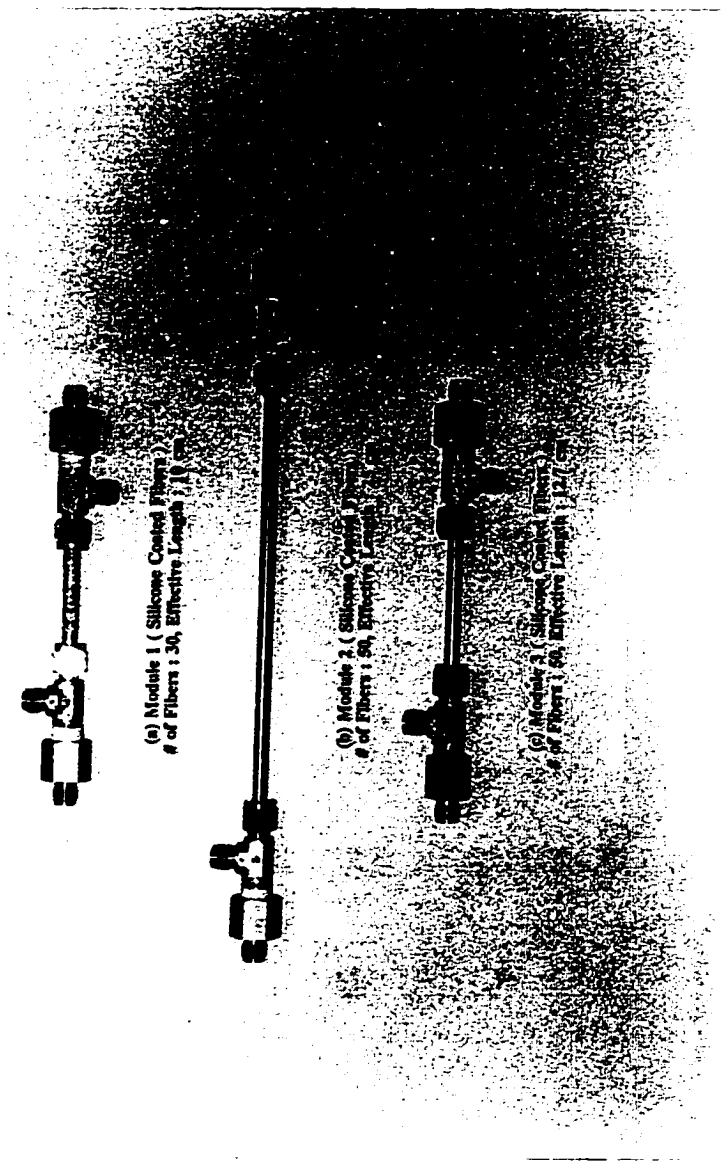

Figure 3.4 Photograph of Three Membrane Modules Used

3.2.3 Experimental Apparatus

The nitrogen stream from a N_2 cylinder was divided into two lines; one was sent into the VOC containing bubbler and the other line was blended with the first VOC containing nitrogen line to form the feed gas/vapor mixture. This feed gas/vapor mixture was also divided into two lines using two different valves. One line which had a very small flow rate (1 cc) of feed gas sample was directly connected to sample loop 1 of the automatic gas sampler and the rest of the feed mixture was sent through the membrane module. The feed outlet flow line was connected to the sample loop 2 of the automatic gas sampler. Using two different valves, only 1 cc of feed outlet sample was injected to the GC and the rest of the flow was vented. In this way, both samples (feed inlet and feed outlet) were analyzed simultaneously during the experimental runs.

The membrane module was immersed in a constant temperature water bath and the water temperature was controlled by an attached heater. For these experiments, the temperature of the water bath was maintained at 30 °C. Coiled brass tubing was used before and after the module to increase the retention time of the gas and thereby help in reaching the desired temperature faster. The vacuum pump which created the pressure difference between feed and permeate streams was connected at one end of the shell side of the module (the other end was closed) so that the flow direction in the shell side was countercurrent to that of the feed side. In the cold trap before the vacuum pump, a mixture of dry ice and acetone was used to condense the VOCs inside the trap. A photograph of the experimental apparatus is shown in figure 3.5. A schematic diagram of the experimental setup is shown in figure 3.6.

3.2.4 GC Calibrations for Toluene and Methanol

For the preparation of the calibration curves of toluene and methanol, different volumes of toluene and methanol were mixed together with the diluent (isopropyl alcohol was used as a diluent). The following GC settings were used throughout the calibration process as

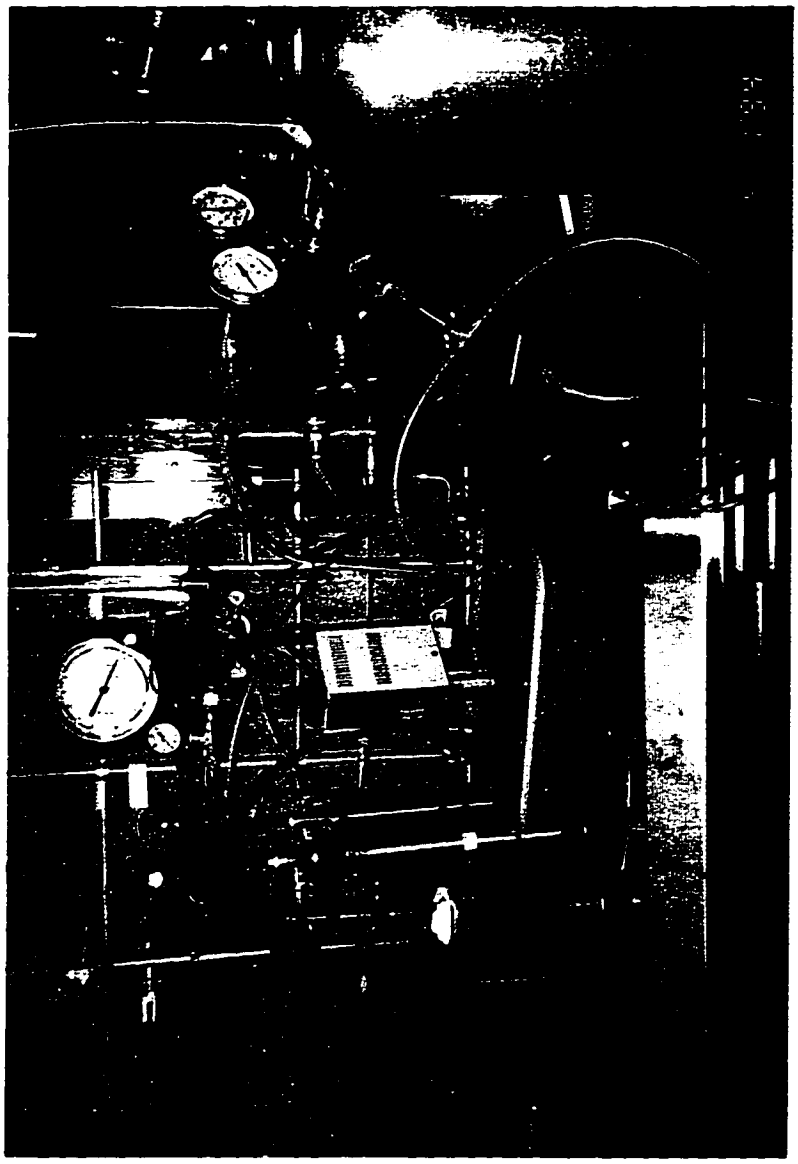

Figure 3.5 Photograph of Experimental Setup

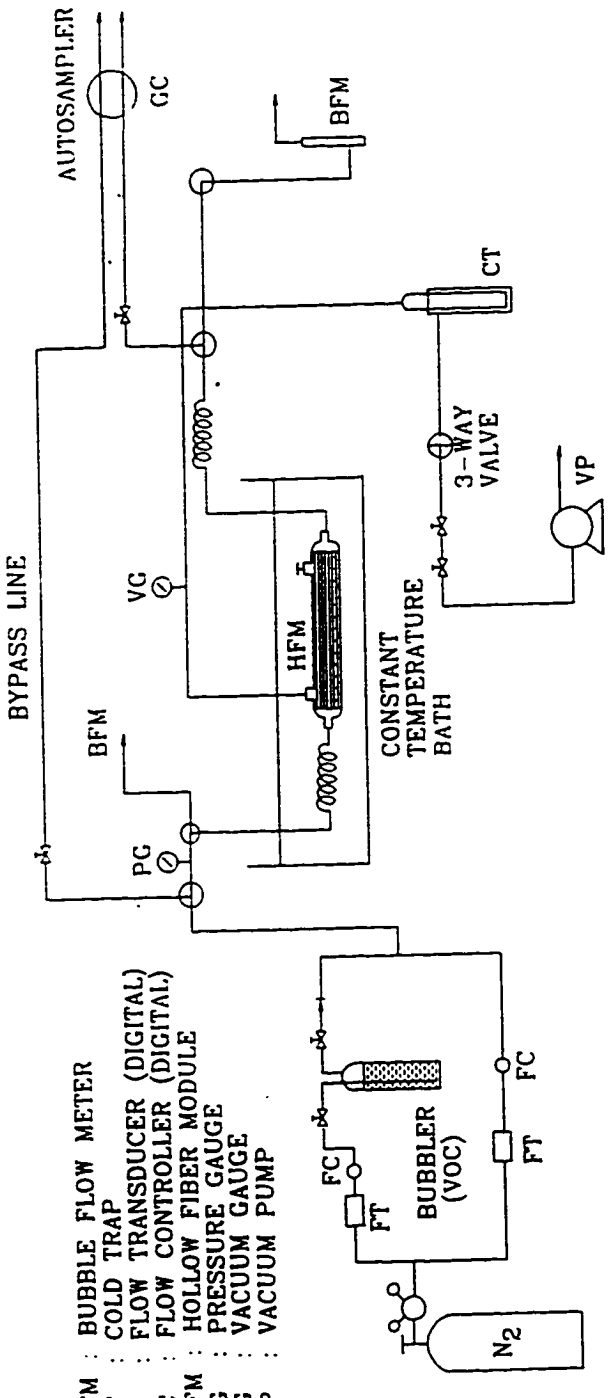

Figure 3.6 Schematic Diagram of Experimental Setup for VOC Permeation from N_2 using Rubbery Membrane

well as experiments : oven temp.= 200 °C, injector temp. = 230 °C, detector temp. = 250 °C. In the case of high concentration range (range = 13), 14 different concentrations of organic solvents mixtures were prepared and in the case of low concentration range (range = 8), 7 different concentrations of toluene and methanol diluted with isopropyl alcohol were prepared.

Due to a significant amount of VOC permeating through the membrane, the concentration difference between feed inlet and outlet was quite large. If the concentration of VOCs in the feed outlet side is too low, it may not be detected in the GC when the range is too high. Low range (range : 8) was employed for the detection of low concentration, since the output peak area in the low range is much more sensitive than that of the high range.

From each sample solution exactly 1.0 μl of sample was taken by a syringe and injected to the HP 5890A GC. Different volumes of organic solvents (toluene, methanol, isopropyl alcohol) and the corresponding GC peak areas (toluene, methanol, 1.0 μl sample was injected to the GC) for the two different ranges are shown in table 3.2 and table 3.3 respectively. The known number of moles of toluene and methanol in 1.0 μl sample and the corresponding GC peak areas were obtained and plotted at high and low concentration ranges respectively.

The total number of moles in the 0.25 cc sample loops of the automatic sampler can also be calculated. The temperature in this case was counted as the injector temperature, which was 230 °C. By comparing the total number of moles and the corresponding number of moles of toluene/methanol obtained by each peak area, the final calibration equations which can directly calculate the concentration (ppm) of feed inlet and outlet samples were obtained in both ranges. Figures 3.7 to figure 3.10 show the calibration lines of toluene and methanol for the two different ranges.

A new carbograph column (8 feet long, s.s., mesh size : 60/80, Alltech, Deerfield, IL) which can separate the VOCs (toluene, methanol) was used in the GC. The retention

Table 3.2 Concentrations of Toluene and Methanol vs. GC Peak Area (Range : 13)

Volume (ml)			Concentration (gmole / μl)		GC Peak Area (Range : 13)	
Toluene	Methanol	Isopropyl alcohol	Toluene (x 10^7)	Methanol (x 10^7)	Toluene	Methanol
0.1	0.1	50.0	0.186	0.489	37,152	9,872
0.2	0.2	50.0	0.371	0.974	58,433	16,211
0.2	0.2	40.0	0.463	1.22	75,256	20,732
0.2	0.2	30.0	0.616	1.62	99,378	27,267
0.5	0.5	30.0	1.51	3.96	217,863	58,237
0.5	0.5	20.0	2.23	5.85	3,380,900	88,469
0.5	1.0	30.0	1.49	7.79	214,570	110,735
1.0	1.0	20.0	4.25	11.2	6,576,900	153,280
1.0	2.0	30.0	2.84	14.9	4,156,100	194,010
0.5	2.0	30.0	1.44	15.1	218,410	205,610
1.0	1.0	10.0	7.80	20.5	1,192,200	248,270
2.0	4.0	30.0	5.20	27.3	789,025	322,370
1.0	1.0	5.0	13.4	35.1	2,241,000	414,220
4.0	8.0	30.0	8.91	46.8	1,170,550	448,040

Table 3.3 Concentrations of Toluene and Methanol vs. GC Peak Area (Range : 8)

Volume (ml)			Concentration (gmole / μl)		GC Peak Area (Range : 8)	
Toluene	Methanol	I.P.A.	Toluene (x 10^9)	Methanol (x 10^8)	Toluene	Methanol
0.1	0.1	210	4.45	1.17	267,020	71,540
0.1	0.1	180	5.19	1.36	315,895	84,322
0.1	0.1	150	6.23	1.63	385,645	102,515
0.1	0.1	120	7.79	2.04	487,565	129,460
0.1	0.1	90	10.4	2.72	643,310	170,955
0.1	0.1	70	13.3	3.50	852,770	228,300
0.1	0.1	50	18.6	4.89	1,184,200	314,280

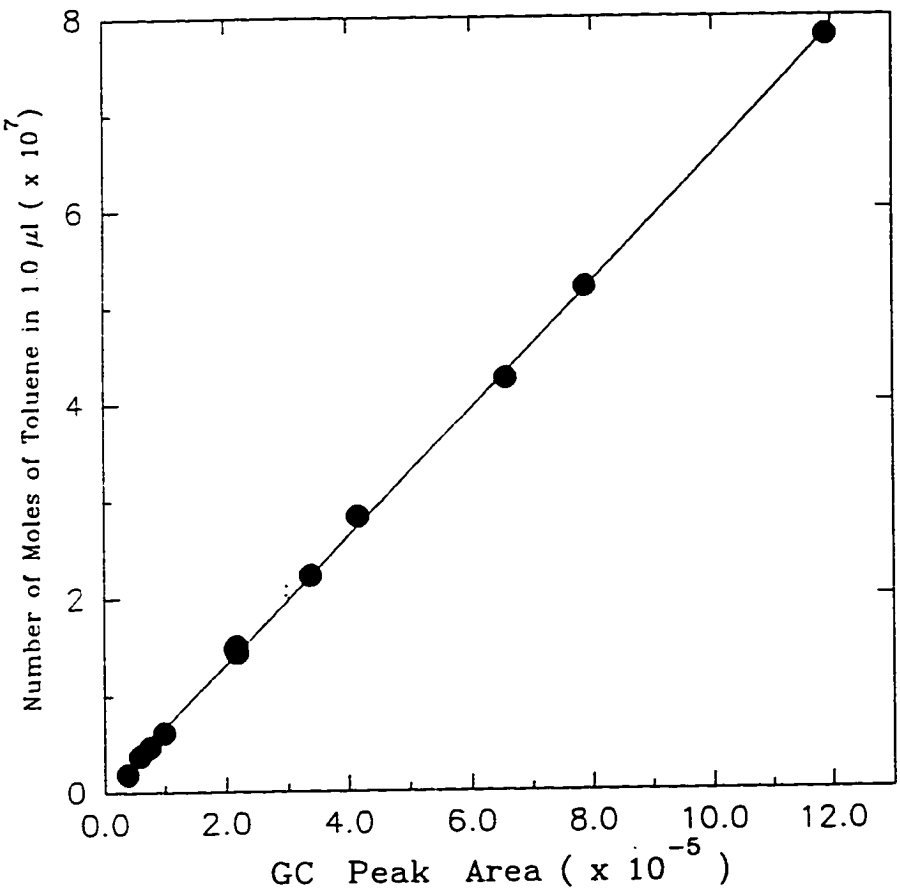

Figure 3.7 Calibration Curve for Toluene (Range : 13)

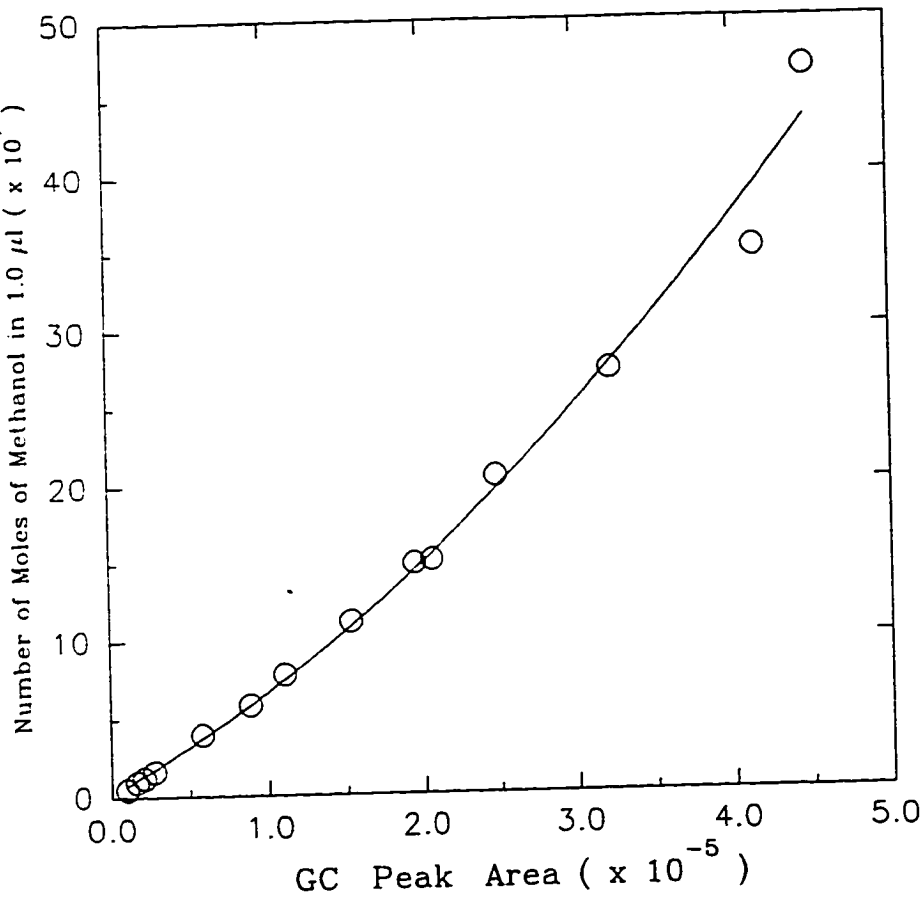

Figure 3.8 Calibration Curve for Methanol (Range : 13)

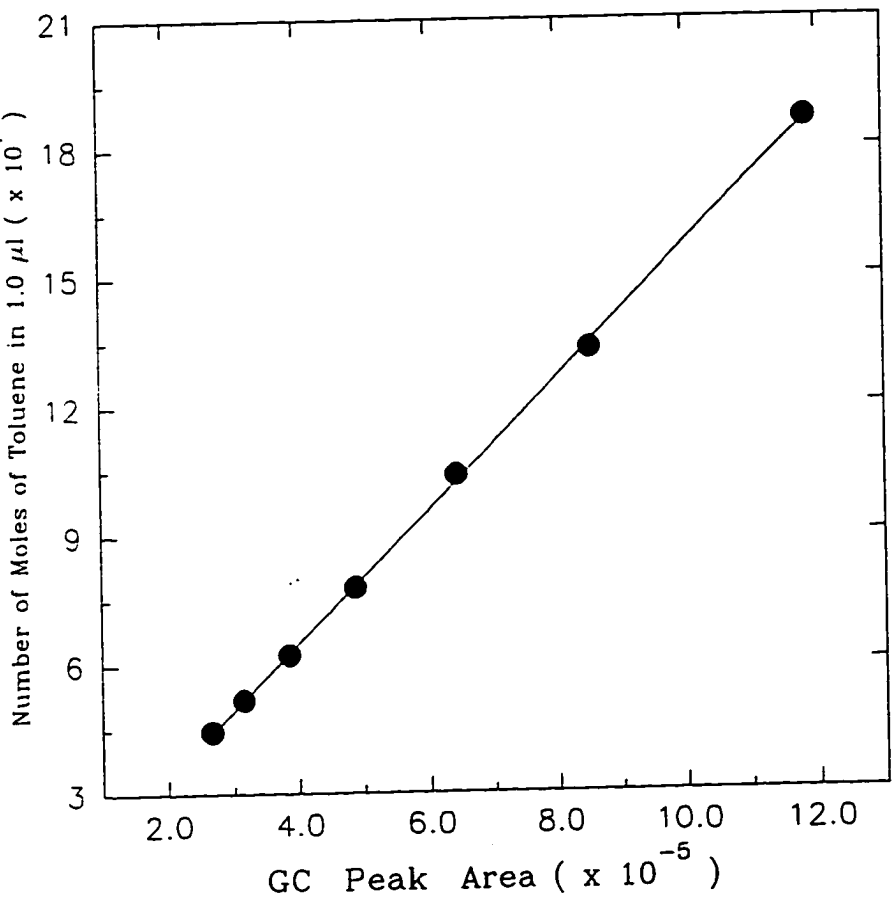

Figure 3.9 Calibration Curve for Toluene (Range : 8)

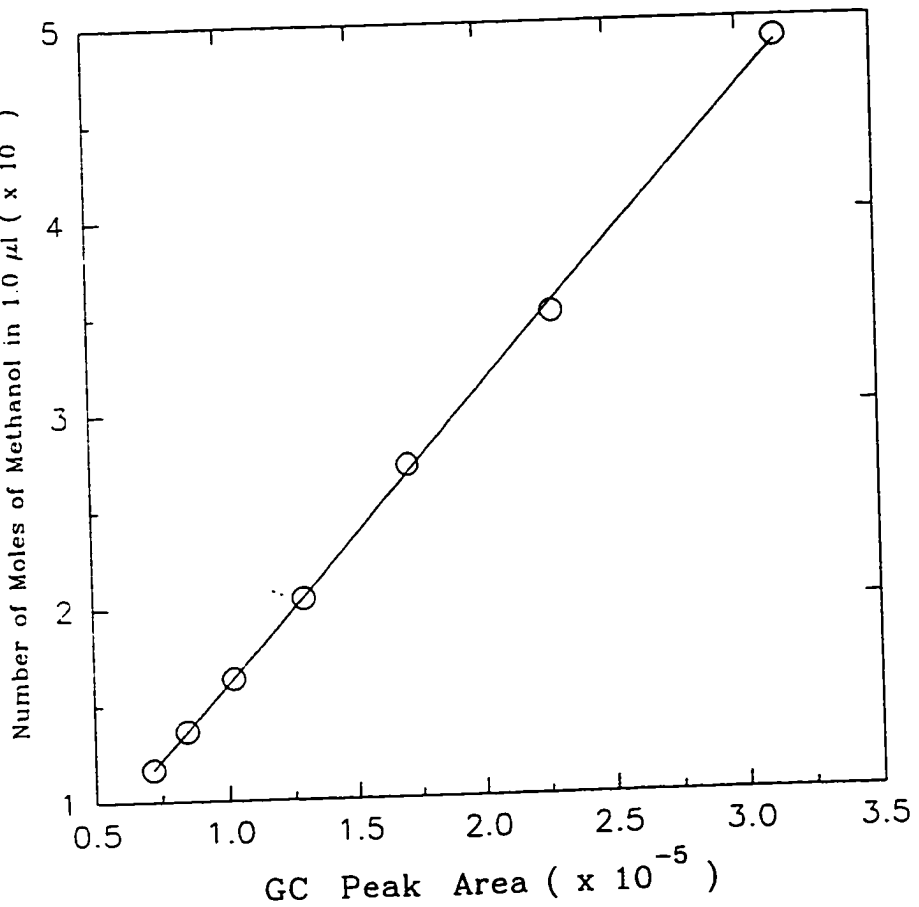

Figure 3.10 Calibration Curve for Methanol (Range : 8)

time of these VOCs were 0.89 min. and 13 min. for methanol and toluene respectively at the employed GC settings. This new column was baked at 200 °C oven temperature with a carrier gas flow rate of 30 cc/min. overnight before using for the experiments.

3.2.5 Experimental Procedure

3.2.5.1 Permeance of VOC as a Function of Concentration

The specific permeability (or permeance) of VOC through the rubbery polymeric membrane is a strong function of its concentration. Module 1, having a much smaller area needed for the measurement of permeability of VOC was used in this experiment. The temperature of water bath was preadjusted to the desired level (30 °C) before starting the experimental runs. The cold trap was filled with dry ice (prepared from Insta-Ice Machine) and acetone. In the case of toluene, the feed inlet concentration was varied from 650 ppm to 26,000 ppm. Eight different concentration levels were formed by adjusting the two nitrogen flow rates. It was important to maintain the feed toluene concentration as constant as possible throughout the module because the purpose of these experiments were to obtain, if possible, the relationship of specific permeability (or permeance) of toluene at given toluene concentration levels. To keep the toluene concentration as constant as possible along the module, the feed flow rates had to be high enough to reduce the fractional removal of toluene vapor as much as possible.

In the case of relatively low feed concentrations (600 ppm to 8,500 ppm), total feed flow rates from 110 cc/min. to 320 cc/min. were employed and at high feed toluene concentrations (12,000 ppm to 26,000 ppm), the feed flow rate ranges were 500 cc/min up to about 800 cc/min. Since the change of toluene vapor composition along the module at high feed concentration range was unavoidable, the level of shell side vacuum was reduced a little bit to lessen the permeation of toluene vapor. The shell side vacuum levels were adjusted to -28.0 in Hg when the feed toluene concentrations were in the ranges of 12,000 ppm to 20,000 ppm, and in the case of 26,000 ppm of feed toluene concentration,

the vacuum was reduced up to -27.0 in Hg.

Two sample lines (feed inlet and outlet) were connected to the automatic sampling valve inside the GC. Approximately 1.0 c.c of feed inlet and outlet samples were continuously taken to the autosampler and analysed during the experimental runs. The samples were analyzed every 20 minutes, and one experimental run usually took 4 hours to show steady peak areas. The analysis of peak area was performed by using range 8 in this case. Feed inlet and outlet flow rates were measured by a bubble flow meter. At the end of the run, pure nitrogen (20 cc/min) was passed through the tube side of the membrane module to prevent the swelling of the fibers due to any toluene that may condense overnight and to clean the module for the next run.

3.2.5.2 Removal of VOCs using a Silicone Coated Membrane

The temperature of water bath was adjusted to the desired level (30°C) before starting the experimental runs. Dry ice was prepared using Insta-Ice Machine (Polyfoam Packers, Inc., Wheeling, IL) and was mixed with acetone for putting into the cold trap. One nitrogen stream was sent into an air distributor which was immersed in a VOC-containing bubbler to produce a nitrogen and organic vapor mixture; the other pure nitrogen stream was blended with the first VOC-containing nitrogen stream.

Module 3 which has 52.7 cm^2 surface area was used in another experiment on gas separation where the pores were filled with some liquid. To use this module in the present study, it had to be cleaned to take out the liquid which may be inside the pores. Isopropyl alcohol was used for this purpose. Using a pressure vessel, pure isopropyl alcohol was passed through the tube and shell side of the membrane module at a very low flow rate (1-2 ml/min.) for at least 5 hours; it was dried with pure nitrogen for about 3 hours at a flow rate of 20 cc/min. before using for the experiments.

Some preliminary experiments were done with this module. A mixture of nitrogen and a VOC (toluene or methanol) was used as a feed in one experiment. In this case, feed

flow rate was changed from 5 to 40 cc/min. Toluene concentration was maintained around 6,000 ppm and methanol concentration was in 4,000 ppm range. In another experiment, nitrogen and VOCs (toluene and methanol together) along with water vapor was employed as a feed mixture. Feed flow rate was approximately 20 and 40 cc/min. in this case. Organic vapor (toluene and methanol) concentrations were analyzed using the flame ionization detector (FID) and for the water vapor concentration analysis, thermal conductivity detector (TCD) was used. Shell side vacuum level was kept constant in this experiment (close to -29.9 in Hg by Heise vacuum gauge).

Most systematic experimental runs were performed with module 2 which has a surface area of 103.8 cm^2. The feed flow rate was varied from 10 to 600 cc/min. At each flow rate, 4-5 different concentrations of organic vapors were used (2,000 - 14,000 ppm for toluene and 400 - 50,000 ppm for methanol). At a given feed flow rate, the desired feed vapor concentration could be obtained by adjusting the flow rate ratio of two nitrogen streams very carefully. As the flow rate of the VOC-containing nitrogen stream was increased (flow rate of pure nitrogen stream was decreased in this case to maintain the total flow rate kept constant), feed vapor concentrations were increased. This feed gas/vapor mixture was introduced to the tube side of the membrane permeator. A feed bypass stream which had a flow rate of approximately 1.0 cc/min. of feed sample was directly connected to the sample loop 1 of the 10-port automatic gas sampler. Feed outlet sample stream was also divided into two lines. One line which had approximately 1.0 cc/min. of flow rate was directly sent to the sample loop 2 of the automatic gas sampler and the rest of the flow was vented. These two samples were analyzed simultaneously and continuously via the automatic gas sampling valve during the experimental runs. The analysis was continued until a steady state was reached; around 4 hours were required to obtain constant peak areas.

In the low feed flow rate ranges (up to 60 cc/min.), there was no pressure drop in the tube side of the membrane module, but in the higher feed flow ranges (150-600

cc/min.), there was pressure drop in the tube side and this was monitored by a pressure gauge. On the shell side, a vacuum pump was applied to provide the necessary driving force for gas/vapor permeation and the permeated organic solvents were condensed and collected in the cold trap immersed in a dry ice/acetone mixture. Vacuum was applied at one end of the permeator so that the flows in the feed and permeate were countercurrent. Most experiments were performed at a very high shell side vacuum level close to -29.9 in Hg; some experiments were also done for different partial vacuum levels (starting from -20.0 in Hg to -27.5 in Hg) at a given feed flow rate and feed vapor concentration. The effective permeation area of the module was 103.8 cm^2 (# of fibers : 50, effective length : 25 cm) and the whole module was immersed into the constant temperature bath during the experimental runs.

Feed inlet and outlet flow rates were measured using a bubble flow meter at the end of each run and after the experimental runs, nitrogen was passed overnight through the bores of the fibers at approximately 20 cc/min. to clean the module.

3.2.6 Performance of the Membrane Module

The quantities flux, percent removal, permeance of VOCs and separation factor were calculated using the equations given below for any membrane module:

Flux of VOC (J_{VOC}, gmol/min.cm^2) = $(F_i.x_f - F_o.x_w) / A$

Percent removal of VOC (% R) = $(1 - F_o.x_w / F_i.x_f) \times 100$

Permeance of VOC (gmol/sec.cm^2.cm Hg) = (Flux of VOC) / [60 x $(\Delta p)_{VOC}$]

Separation factor (α) = $(Q_{VOC} / Q_{N2}) = [(Q_{VOC}/\delta_m) / (Q_{N2}/\delta_m)]$

where Q_{VOC} and Q_{N2} are permeabilities of VOC and N_2, respectively and δ_m is the effective membrane thickness.

3.3 Results and Discussion

The preliminary experimental results obtained using module 3 will be illustrated first. Using a relatively low feed flow rate (20 cc/min.), feed gas/vapor mixture containing nitrogen, water, toluene and methanol vapors was allowed to flow through the tube side of the module and a very high vacuum level close to -29.9 in Hg was applied to the permeate side. This experiment was done at room temperature. Table 3.4 shows the results. Percent removal of water vapor was considerably lower than that of the other organic vapors. Since the silicone rubber selective barrier has hydrophobic properties, it does not allow much water vapor permeation. The permeance of water vapor through this membrane was also very low compared to the organic vapors permeances. In the case of methanol vapor, the permeance was approximately 20 times larger than water vapor permeance. On the other hand, in a polymeric gel membrane like Cuprophan which was discussed in chapter 2 of this thesis, water vapor permeation was much more compared to the organic vapor permeation due to the highly hydrophilicity of such membrane. This is a good example showing that the permeabilities of different species and the selectivities between different species can vary widely depending on the nature of the membrane.

In another preliminary experiment where the feed contained nitrogen and organic vapors (toluene or methanol), four different feed flow rates were used at a given organic vapor concentration. Fractional removals of organic vapors are plotted against changing feed flow rates in figure 3.11. At low feed flow rates less than 10 cc/min., percent removal was above 90 % and it decreased as feed flow rate was increased. In the case of toluene vapor, percent removal was down to 57 % at a feed flow rate of 40 cc/min; but in the case of methanol vapor, the percent removal was above 80 % for all flow rates employed. These results from module 3 showing highly encouraging trends of selective permeation of organic vapors suggested more systematic experiments using the other two fresh modules.

Table 3.4 Permeances of Gas/Vapors through a Silicone Coated Membrane (Module # 3, Total Feed Flow Rate : 20 cc/min.)

Gas or Vapors	Mole Fraction			Partial Pressure Difference (cm Hg)	Percent Removal of Vapors (%)	Permeance of gas/vapors ($x10^{10}$, gmol/sec. cm^2.cm Hg)
	Feed Inlet	Feed Outlet	Permeate			
Nitrogen	0.979	0.987	0.77	74.7	-	2.2
Water	0.00731	0.00685	0.0195	0.54	9.6	5.0
Toluene	0.00834	0.00597	0.0831	0.54	30.0	19.4
Methanol	0.00507	0.0005	0.128	0.21	89.5	118

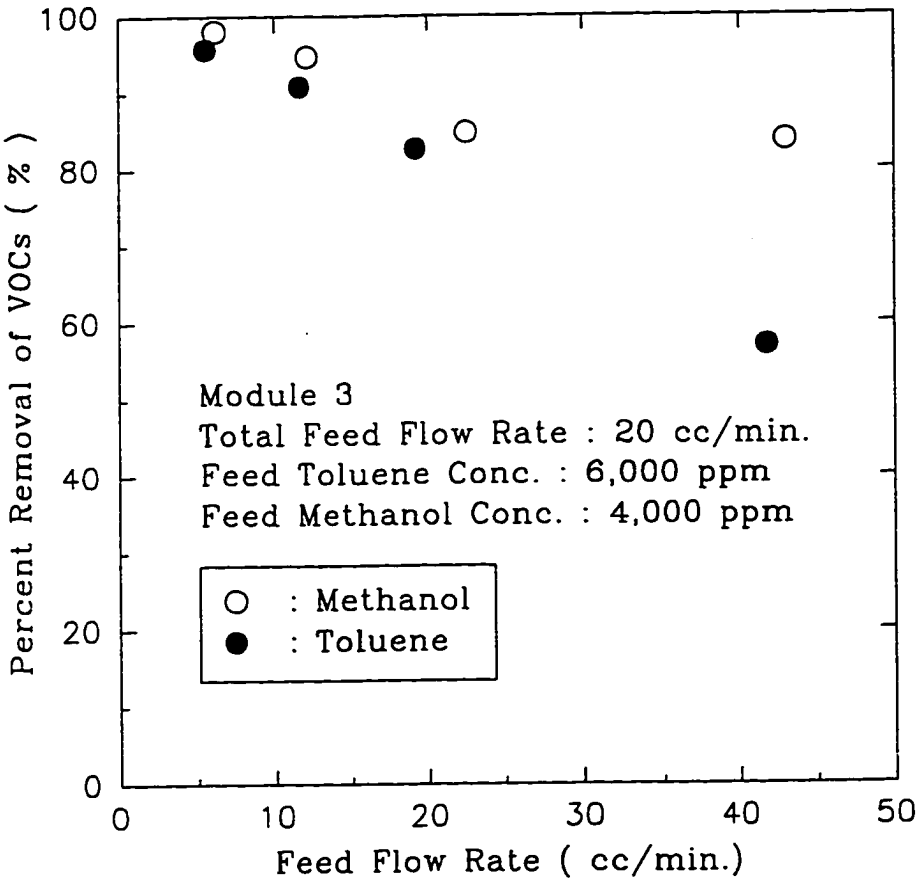

Figure 3.11 Percent Removal of VOCs at Different Feed Flow Rates (Module # 3)

Pure nitrogen permeance value through this membrane is an important quantity. When nitrogen is present with a organic vapor as a feed, nitrogen permeation will greatly affect the selectivity. Module 2, prior to being used with a feed gas/vapor mixture, was used for pure nitrogen permeation experiment along with another module which was being used in other project in our laboratory (surface area of this module was 579.6 cm^2). Different feed pressures were used on the tube side of each module and the permeation rate was measured from the shell side. The steady state permeation rate obtained from module 2 was compared to that from this other module and it had a similar value of 4-5 cc/min. Based on these experimental data, nitrogen permeance was calculated to be 3.9 x 10^{-10} gmol/cm^2.sec.cmHg.

Experiments to determine the permeance of toluene vapor as a function of its concentration were carried out using module 1 which has a surface area of 24.9 cm^2. To maintain the toluene vapor concentration level as constant as possible along the permeator, very high feed flow rates were employed. In the lower toluene concentration levels, the concentration change from inlet to outlet was not considerable; in the high levels of toluene concentration, significant changes were encountered even at high feed flow rate. This suggests exploration of better strategies in future studies.

The feed toluene concentrations were 0.12, 0.20, 0.34, and 0.57 % and pressure levels in the permeate side were 4.88, 6.15, 3.10, and 3.61 cm Hg, respectively. The calculated permeance of toluene vapor plotted as a function of the average feed side concentration is shown in figure 3.12. The relation between Q_i/δ_m and partial pressure of toluene vapor can be best described by an exponential equation, $Q_i = a * \exp(b*Px)$. The regression results for a and b were 2.33 x 10^{-9} gmol/sec.cm^2.cmHg and 12.1 $cmHg^{-1}$, respectively. Such a behavior may provide the framework needed for future modeling of VOC separation in such membrane modules. However, the higher partial pressure of toluene in the permeate side suggests that Q_i should be a function of py as well; or conditions must be such that py must be very small compared to Px (see equation 2.1).

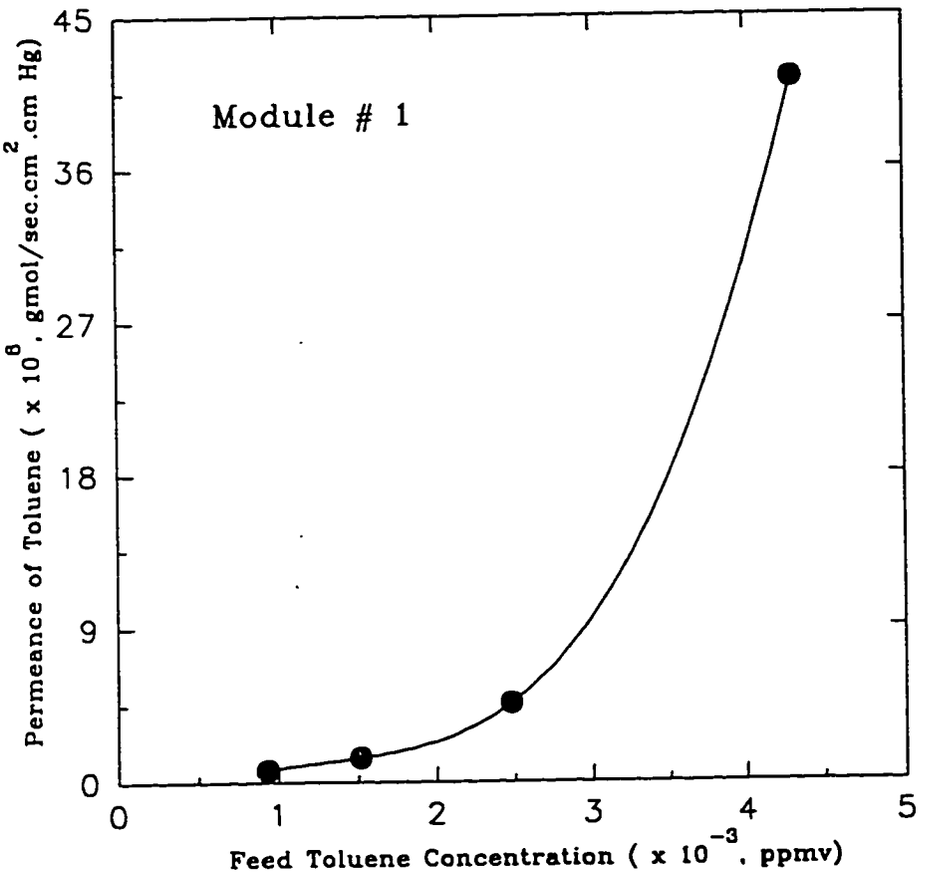

Figure 3.12 Permeance of Toluene Vapor as a Function of Feed Toluene Concentration

Further attention has to be paid to any possible boundary layer effects on the observed toluene permeance since it is so high.

Tables 3.5 and 3.6 show the flux and percent removal of toluene vapor for changing feed flow rates as well as changing toluene concentrations in module 2. Six different flow rates (from 10 to 600 cc/min.) were employed and at a given feed flow rate, toluene vapor concentration was changed from 2,000 ppmv to 14,000 ppmv. Permeate side vacuum level was kept constant close to -29.9 in Hg throughout these experiments. In the low feed flow rate range up to 60 cc/min., there was no pressure drop in the tube side. Toluene vapor mole fraction change between feed inlet and outlet was increased as the feed inlet toluene vapor concentration was increased since the permeation of toluene vapor increases strongly with an increase in the partial vapor pressure difference across the membrane. Calculated values of permeate side mole fraction of toluene vapor were found to increase with the increase of the feed inlet toluene vapor concentrations (figure 3.13).

Feed outlet toluene vapor concentrations are plotted in figure 3.14 as a function of feed inlet toluene vapor concentration. Feed outlet toluene vapor concentrations appear to be increasing as the feed inlet toluene vapor concentrations were increasing at a particular feed flow rate; the differences were increased at higher concentration levels due to greater permeation of toluene vapor. In the low feed flow rate range (below 60 cc/min.), the feed outlet toluene vapor concentration was less than 200 ppmv irrespective of the feed inlet toluene vapor concentration levels; this leads to very high percent removal of toluene vapor for this silicone coated membrane.

Figure 3.15 shows the effect of feed toluene vapor concentration on the permeate toluene vapor flux. Toluene vapor permeation flux increased with an increase in the feed toluene vapor concentrations at a given feed flow rate. The toluene vapor flux for a given driving force is expected to be quite high due to the ultrathin nature of the silicone coating layer since species flux through such a membrane is inversely proportional to the

Table 3.5 Flux and Percent Removal of Toluene at Different Flow Rates (10-60 cc/min.) and Toluene Concentrations (Module # 2)

Feed Inlet			Feed Outlet			Toluene Flux (x 10^8, gmol/min.cm^2)	Percent Removal of Toluene (%)
Flow Rate (cc/min.)	Pr. (cm Hg)	Toluene Mole Fraction	Flow Rate (cc/min.)	Pr. (cm Hg)	Toluene Mole Fraction		
11.3	76	0.00224	6.7	76	0.000096	0.96	97.5
11.5	76	0.00537	6.8	76	0.000076	2.36	99.1
11.4	76	0.00853	6.8	76	0.000091	3.75	99.4
11.2	76	0.0122	6.6	76	0.000066	5.31	99.7
27.3	76	0.0025	22.4	76	0.000097	2.56	96.8
27.2	76	0.00631	22.4	76	0.000103	6.56	98.7
27.0	76	0.00991	22.1	76	0.000095	10.3	99.2
26.7	76	0.0141	21.7	76	0.000185	14.4	98.9
58.6	76	0.00249	54.0	76	0.000105	5.43	96.1
59.1	76	0.00661	54.5	76	0.000151	14.8	97.9
58.9	76	0.0108	54.2	76	0.000455	23.7	96.2

Table 3.6 Flux and Percent Removal of Toluene at Different Flow Rates (150-600 cc/min.) and Toluene Concentrations (Module # 2)

Feed Inlet			Feed Outlet			Toluene Flux (x 10^7, gmol/min.cm^2)	Percent Removal of Toluene (%)
Flow Rate (cc/min.)	Pr. (cm Hg)	Toluene Mole Fraction	Flow Rate (cc/min.)	Pr. (cm Hg)	Toluene Mole Fraction		
156	81.2	0.00301	151	76	0.00072	1.39	76.8
148	81.2	0.00608	144	76	0.00116	2.85	81.5
159	81.2	0.00973	154	76	0.00198	4.82	81.3
148	81.2	0.0138	143	76	0.00252	6.54	82.4
305	86.3	0.00402	297	76	0.00161	2.90	61.0
281	86.3	0.0140	273	76	0.00424	10.8	70.6
660	94.1	0.00207	647	76	0.00127	2.11	39.8
591	94.1	0.0124	577	76	0.00569	15.6	55.1

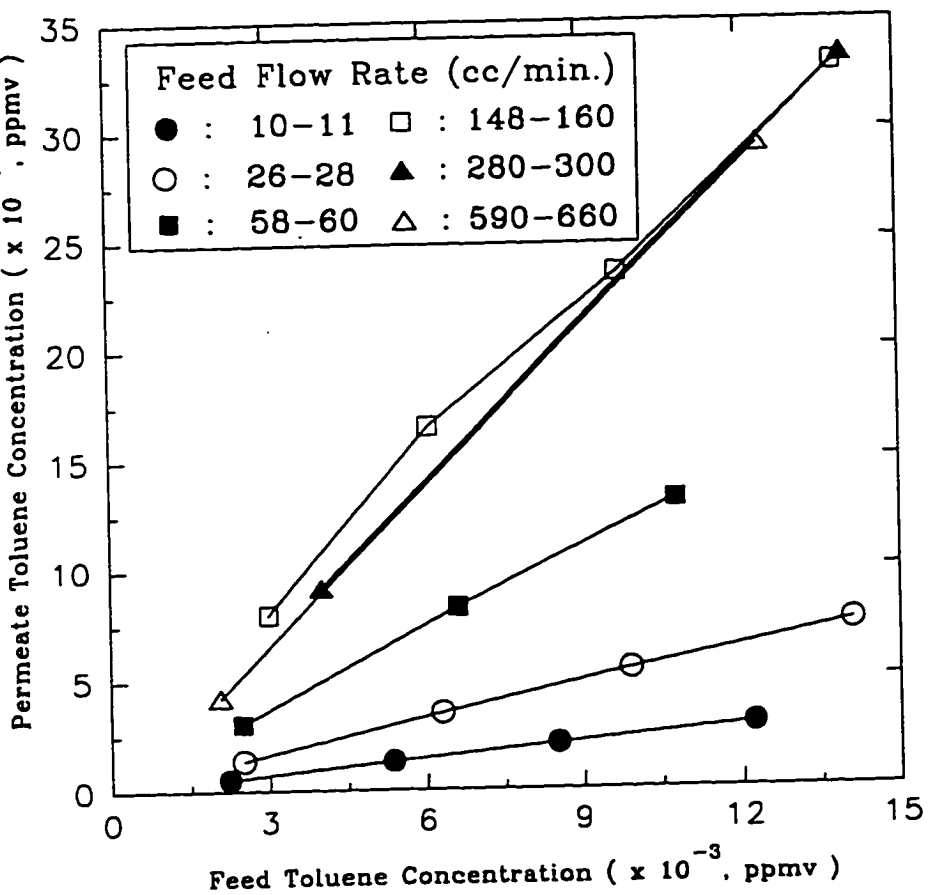

Figure 3.13 Permeate Toluene Concentration vs. Feed Toluene Concentration at Different Feed Flow Rates

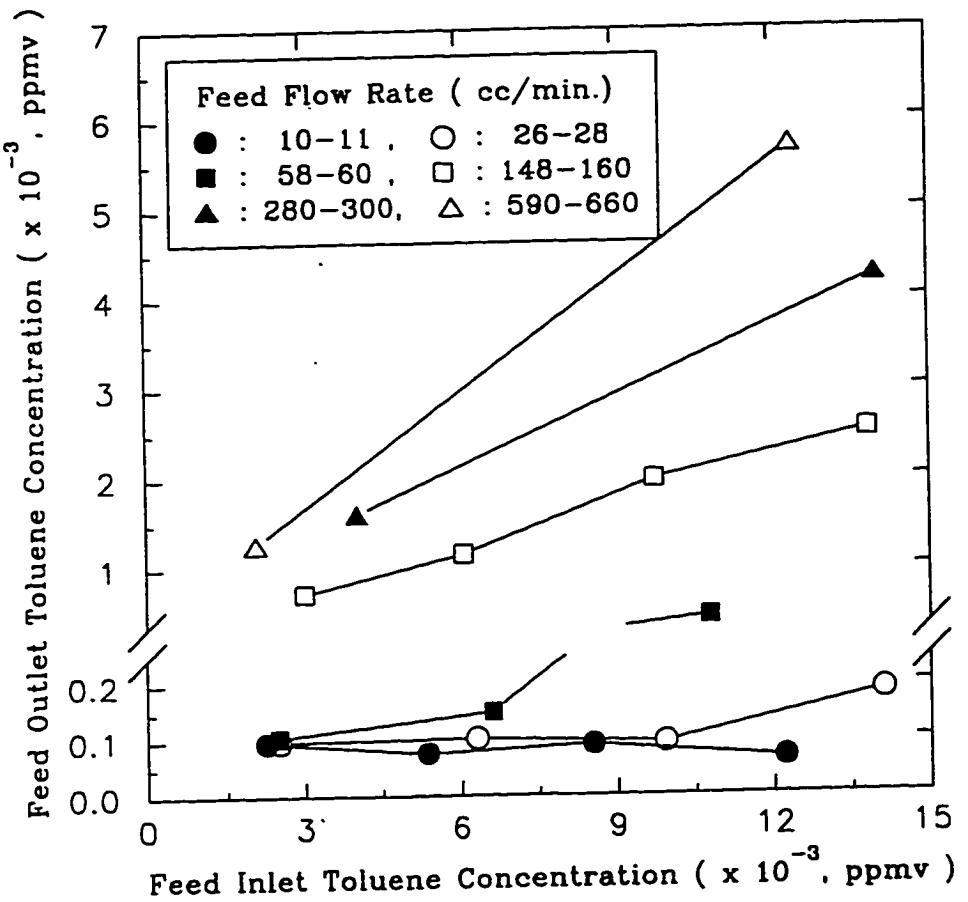

Figure 3.14 Feed Outlet Toluene Concentration vs. Feed Inlet Toluene Concentration at Different Feed Flow Rates

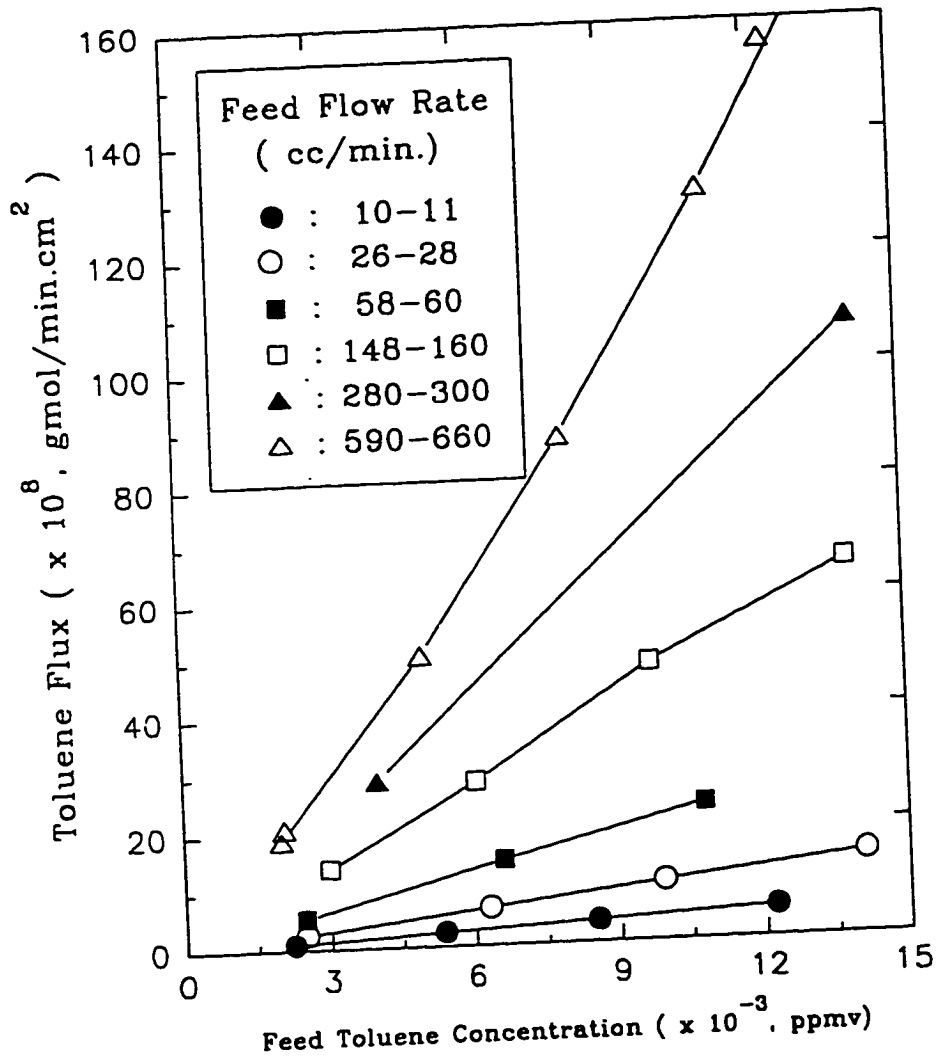

Figure 3.15 Toluene Vapor Flux vs. Feed Toluene Concentration at Different Feed Flow Rates

thickness of the selective barrier (or coating layer). The microporous polypropylene hollow fiber substrate has a high porosity (~0.4); therefore this substrate will not reduce the intrinsically high permeation rate through the silicone rubber skin. Experimental toluene vapor flux data using a dry asymmetric poly (ether imide) membrane was found to be 1.8-3.0 x 10^{-7} gmol/min.cm^2 (Feng et al., 1991) which was similarly obtained with a silicone coated membrane. In higher feed toluene concentration ranges at relatively higher feed flow rate, the permeated toluene flux was higher in the silicone coated membrane compared to the poly (ether imide) membrane.

Nitrogen permeation, on the other hand, was not affected much by feed toluene vapor concentration levels in the low feed flow rate ranges. Nitrogen permeation rate was found to be in the range of 4.5-5.0 cc/min. when there was no pressure drop which is very similar to that obtained in pure nitrogen permeation experiment. Permeate side toluene vapor mole fraction was also increased as the feed flow rate was increased at a similar feed toluene vapor concentration level. This is attributed to the similar nitrogen permeation rate irrespective of the feed flow rates. At higher feed flow rate ranges (larger than 150 cc/min.), there was a small pressure drop in the tube side. When the feed flow rate was around 150 cc/min., tube side pressure drop was about 1.0 psi and when it was increased to 600 cc/min., the pressure drop was about 3.5 psi. Nitrogen permeation was found to be increased a little bit as the feed flow rate was increased due to this pressure drop.

The permeance of nitrogen was found to be 3.8 x 10^{-10} gmol/sec.cm^2.cmHg and it was almost independent of the concentration (or partial pressure) of toluene vapor in the low feed flow rate ranges (below 60 cc/min.). Figure 3.16 shows the nitrogen flux as a function of feed toluene concentration. These appears to be a very slow decrease in nitrogen permeance with increasing toluene concentration.

Percent removal of toluene is plotted in figure 3.17 for changing feed toluene concentrations. For feed flow rates below 60 cc/min., 96-99 % removal of toluene vapor

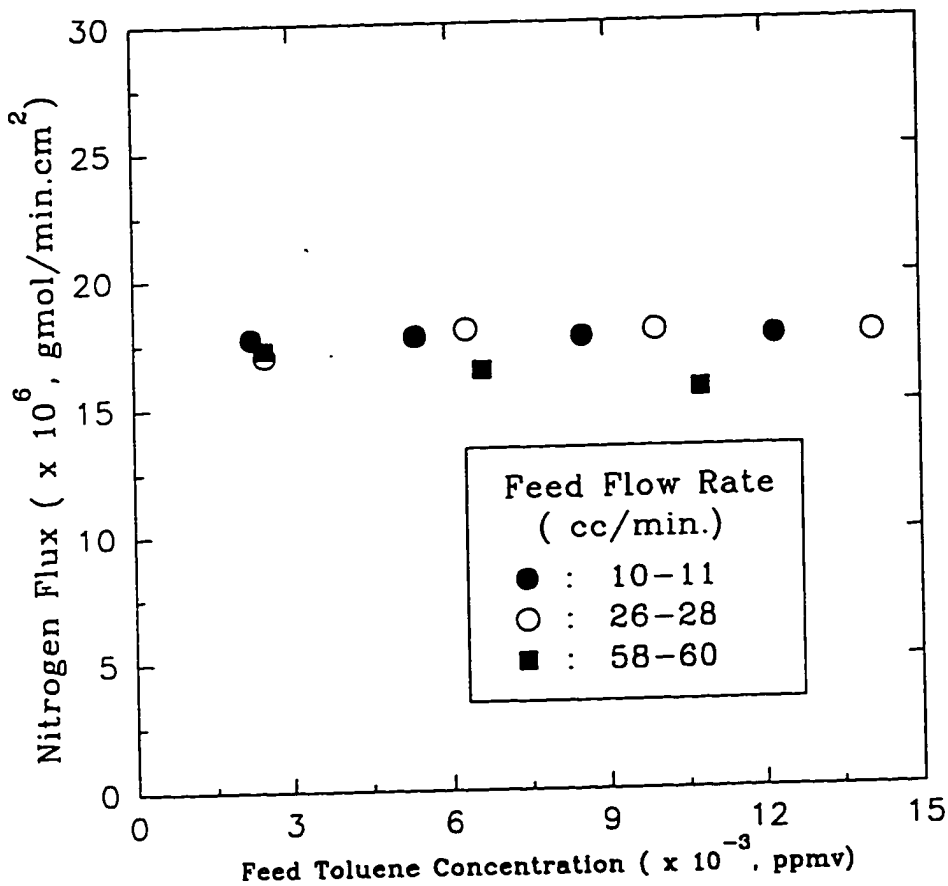

Figure 3.16 Nitrogen Flux vs. Feed Toluene Concentration at Different Feed Flow Rates

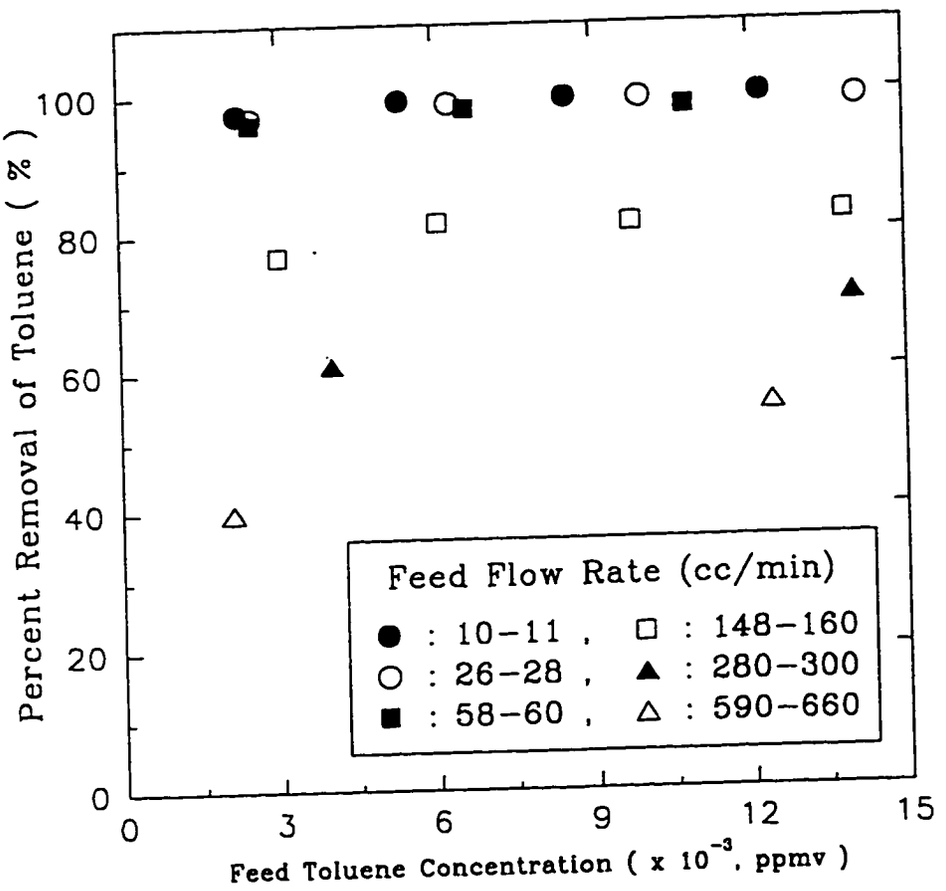

Figure 3.17 Percent Removal of Toluene Vapor vs. Feed Toluene Concentration at Different Feed Flow Rates

was achieved over the whole feed concentration range; this corresponds to 1.2 cc/min. per fiber feed flow rate for a fiber length of 25 cm. For feed toluene concentration above 5,000 ppmv and a flow rate of 30 cc/min, more than 98 % removal of toluene vapor was achieved. The feed outlet toluene concentration was reduced to below 200 ppmv for the whole concentration range in this low feed flow rate range (see figure 3.14). The percent removal of toluene vapor was reduced at higher feed flow rates, however, the percent removal was still considerable. For example, around 80 % of toluene in the feed stream was removed at 150 cc/min. of feed flow rate. The percent removal at a given feed flow rate increases with increasing feed inlet toluene vapor concentration.

The separation factor, which is defined as the ratio of permeances of toluene vapor and nitrogen, has been plotted in figure 3.18 as a function of feed toluene concentration. Separation factor increases slightly with increasing feed toluene concentration at a given feed flow rate. The calculated permeances of toluene vapor and nitrogen used here was based on the whole permeator (module-averaged). Since toluene vapor concentration change along the permeator is very large, the calculated permeance of toluene vapor does not have a specific meaning. The nitrogen flux was similar in the low feed flow rate range; the toluene vapor flux was increasing with increasing feed flow rate. The calculated permeance of toluene vapor was accordingly increased as the feed flow rate increased which resulted in a higher separation factor at higher feed flow rates.

The experimental results showing the flux and percent removal of methanol under different experimental conditions are shown in tables 3.7 and 3.8. In the case of methanol vapor separation from N_2, 5 different feed flow rates (from 30 to 600 cc/min.) were used. The feed methanol vapor concentration was varied from 400 ppmv to 50,000 ppmv for each feed flow rate. The experimental results for methanol vapor are generally quite similar to those for toluene vapor.

Feed outlet methanol vapor concentrations are plotted in figure 3.19 with changing feed inlet methanol vapor concentration. At feed flow rates below 60 cc/min., feed outlet

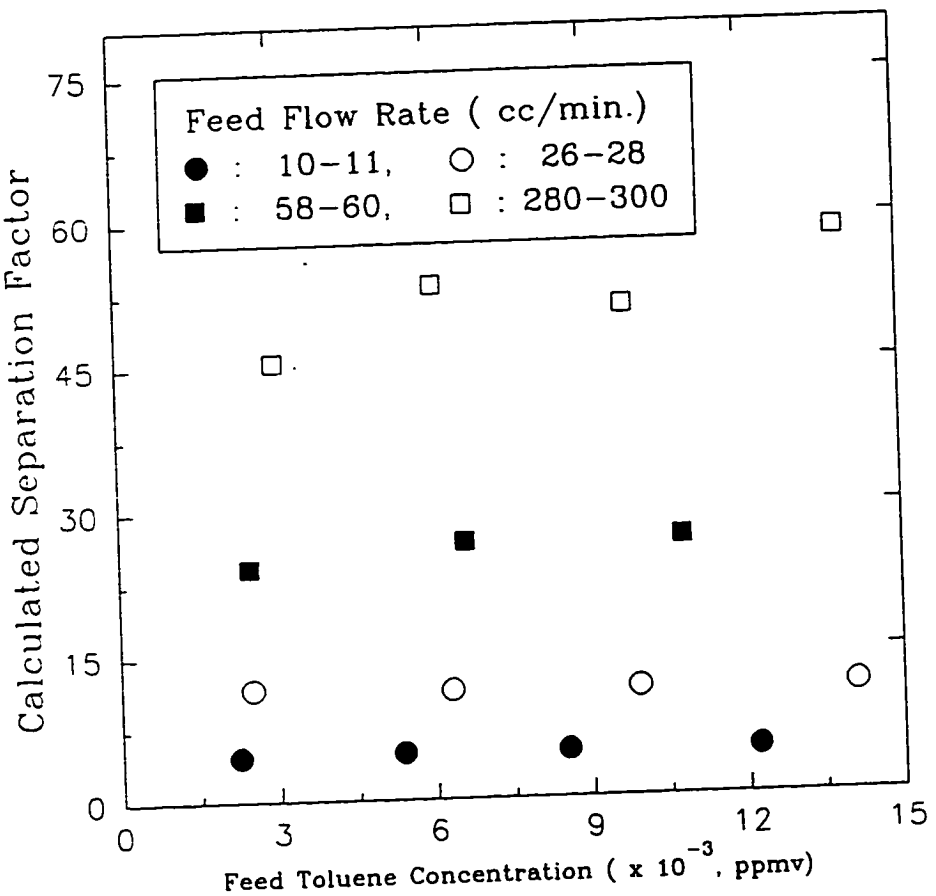

Figure 3.18 Separation Factor vs. Feed Toluene Concentration at Different Feed Flow Rates

Table 3.7 Flux and Percent Removal of Methanol at Different Flow Rates (30-60 cc/min.) and Methanol Concentrations (Module # 2)

Feed Inlet			Feed Outlet			Methanol Flux (x 10^7, gmol/min.cm^2)	Percent Removal of Methanol (%)
Flow Rate (cc/min.)	Pr. (cm Hg)	Methanol Mole Fraction	Flow Rate (cc/min.)	Pr. (cm Hg)	Methanol Mole Fraction		
31.2	76	0.00045	26.8	76	0.000019	0.05	96.4
30.5	76	0.00483	26.1	76	0.000025	0.57	99.6
30.6	76	0.0137	26.1	76	0.000100	1.62	99.5
31.0	76	0.0300	26.5	76	0.000147	3.59	99.6
30.7	76	0.0450	26.1	76	0.000130	5.54	99.8
62.5	76	0.00073	58.0	76	0.000127	0.15	83.8
62.8	76	0.00394	58.3	76	0.000151	0.93	96.4
61.9	76	0.0158	57.1	76	0.000218	3.74	98.7
62.2	76	0.0305	57.4	76	0.000280	7.30	99.2
61.5	76	0.0502	56.6	76	0.000373	11.9	99.3

Table 3.8 Flux and Percent Removal of Methanol at Different Flow Rates (150-600 cc/min.) and Methanol Concentrations (Module # 2)

Feed Inlet			Feed Outlet			Methanol Flux (x 10^7, gmol/min.cm^2)	Percent Removal of Methanol (%)
Flow Rate (cc/min.)	Pr. (cm Hg)	Methanol Mole Fraction	Flow Rate (cc/min.)	Pr. (cm Hg)	Methanol Mole Fraction		
166	81.2	0.00043	161	76	0.000177	0.17	60.3
159	81.2	0.00537	154	76	0.000968	2.73	68.5
149	81.2	0.0177	144	76	0.00493	7.48	73.1
147	81.2	0.0258	140	76	0.00552	11.7	79.5
149	81.2	0.0414	143	76	0.00710	20.0	83.6
336	86.3	0.00356	329	76	0.00143	2.81	60.6
319	86.3	0.0157	311	76	0.00543	12.9	66.4
328	86.3	0.0401	318	76	0.0142	33.5	65.7
594	94.1	0.00706	581	76	0.00366	8.0	49.2
574	94.1	0.0185	561	76	0.00917	21.3	51.6
558	94.1	0.0396	543	76	0.0200	43.3	50.6

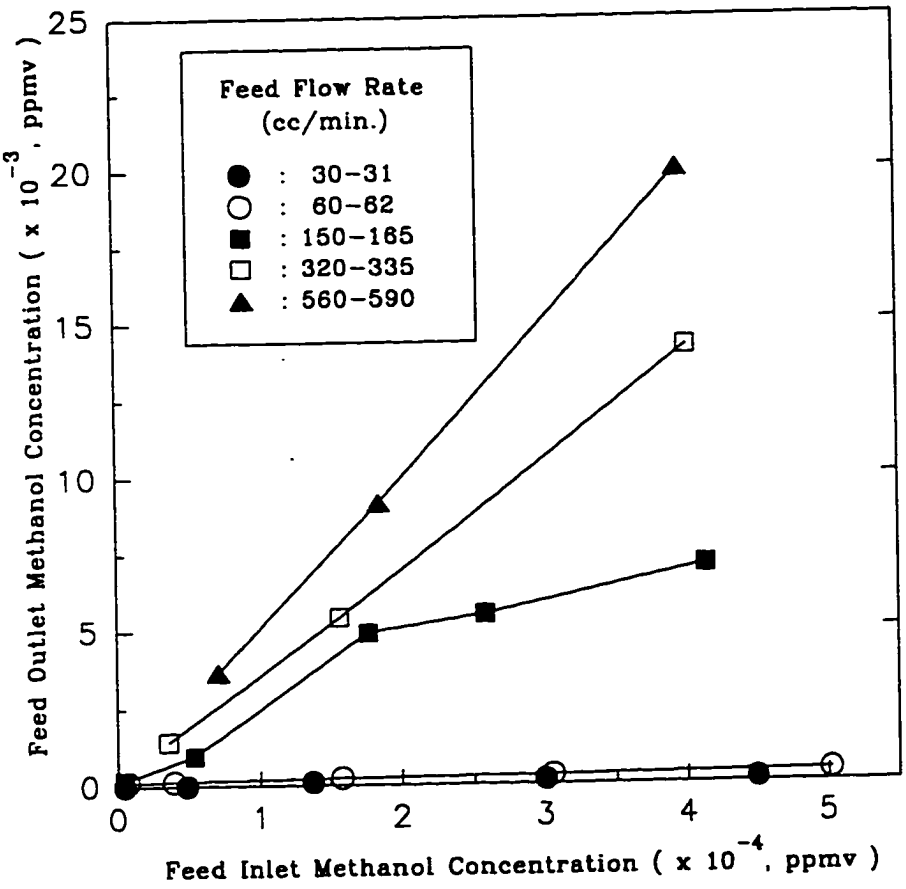

Figure 3.19 Feed Outlet Methanol Concentration vs. Feed Inlet Methanol Concentration at Different Feed Flow Rates

methanol vapor concentration levels were only 100-400 ppmv; it was increased as feed inlet methanol vapor concentration was increased at a given feed flow rate. Since permeation of methanol vapor is proportional to the feed vapor concentration, the concentration difference between feed inlet and outlet was increased with increasing feed inlet methanol vapor concentration. In figure 3.20, permeate methanol vapor concentration is plotted as a function of feed methanol concentration. At feed methanol vapor concentrations below 1 % (10,000 ppmv), the enriched methanol vapor concentration in the permeate was less than 20 %; in the case of high feed methanol vapor concentration (around 50,000 ppmv) at a relatively high feed flow rate, methanol vapor concentration in the permeate side was as high 800,000 ppmv.

Permeation fluxes of methanol vapor and nitrogen are shown in figures 3.21 and 3.22, respectively. Methanol vapor flux through the membrane increased with the increasing feed methanol vapor concentration as was observed for toluene vapor. The interaction of the vapor species with the silicone membrane causes the swelling of the polymer which strongly influences the sorption and diffusion behavior of the permeating species. The increase of vapor species flux with increasing feed vapor concentration becomes even higher for the more selective membrane.

It was interesting to observe that the nitrogen flux was decreasing at the same feed flow rate as the feed methanol concentration was increased. A similar phenomenon was also observed for toluene; but the decrease of nitrogen flux was much less compared to that for methanol. This phenomenon may be explained in terms of substrate pore condensation which will reduce nitrogen flux considerably by pore blocking effect. This explanation will be valid especially for high concentrations of feed methanol vapor as well as substrate pore sizes reduced by penetration of the selective coating layer during plasma polymerization. More systematic experiments with other VOCs is needed to confirm this phenomenon.

Percent removal of methanol vapor as a function of feed methanol concentration

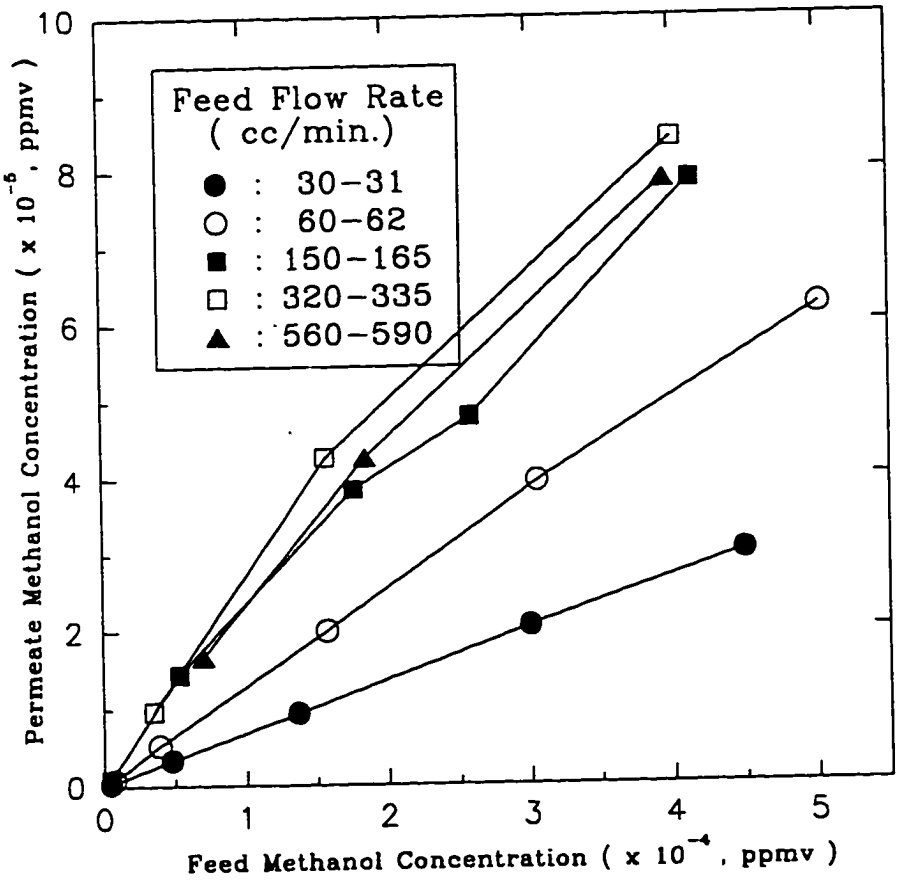

Figure 3.20 Permeate Methanol Concentration vs. Feed Methanol Concentration at Different Feed Flow Rates

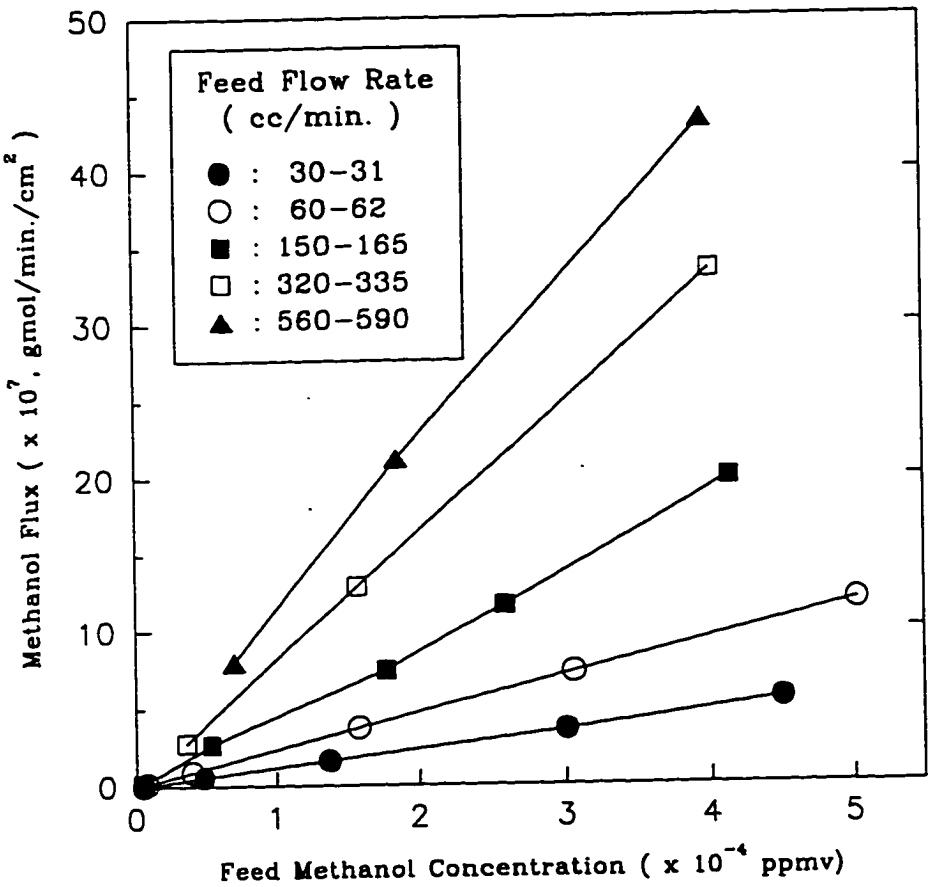

Figure 3.21 Methanol Vapor Flux vs. Feed Methanol Concentration at Different Feed Flow Rates

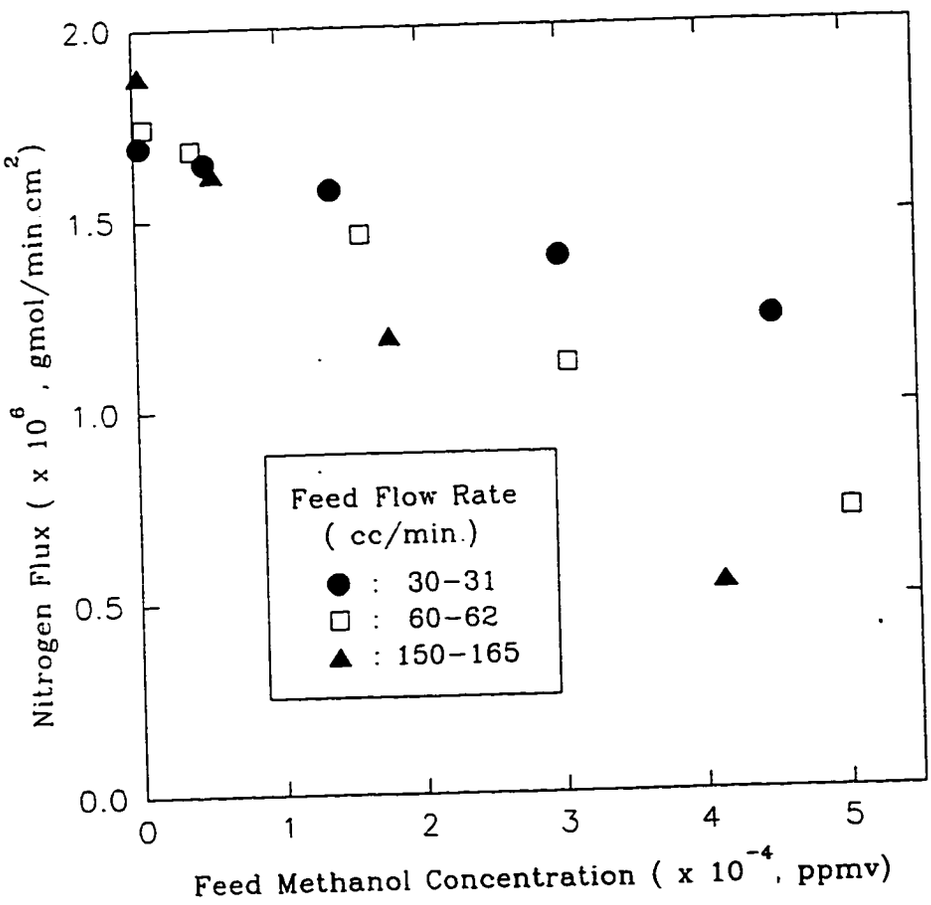

Figure 3.22 Nitrogen Flux vs. Feed Methanol Concentration at Different Feed Flow Rates

is illustrated in figure 3.23. More than 96 % of methanol vapor was removed for feed flow rates below 60 cc/min. (1.2 cc/min/fiber). When methanol vapor concentration was above 1,000 ppmv for a feed flow rate of 30 cc/min., more than 98 % of methanol vapor removal was achieved. Generally the percent removal of methanol vapor was increased with increasing feed methanol concentration; but at very high flow rates (above 300 cc/min.) it remained almost constant. As feed flow rate was increased, percent removal of methanol vapor decreased.

Separation factor of methanol over nitrogen is plotted in figure 3.24 for changing feed methanol vapor concentration. Separation factor was generally higher at higher feed flow rates. In the low ranges of methanol vapor concentration where the nitrogen flux does not change much with the methanol concentration, separation factor remained similar at a given feed flow rate. In the higher methanol vapor concentrations at high feed flow rate, increasing methanol vapor flux combined with decreasing nitrogen flux was yielding a separation factor as high as 150.

Some experiments were carried out with changing permeate side pressure at different toluene vapor concentrations. Experimental results are given in table 3.9. The effect of permeate pressure on the toluene vapor permeation flux is shown in figure 3.25. Feed toluene vapor concentration levels were varied from 2,500 ppm to 13,500 ppm and permeate pressures were changed from 0.5 to 25.0 cm Hg absolute. The toluene vapor permeation flux decreased with an increase in the permeate pressure irrespective of the feed toluene vapor concentrations. At a low feed toluene vapor concentration (2,500 ppm), toluene vapor permeation flux was very small at a high permeate pressure (20 cm Hg) since the toluene partial vapor pressure difference which is the actual driving force for the toluene vapor permeation is very small. As the feed toluene vapor concentration increased, toluene partial vapor pressure difference across the membrane was also increasing at a particular permeate pressure level which leads to a higher vapor permeation flux. The vapor permeation flux is believed to be a nonlinear function of

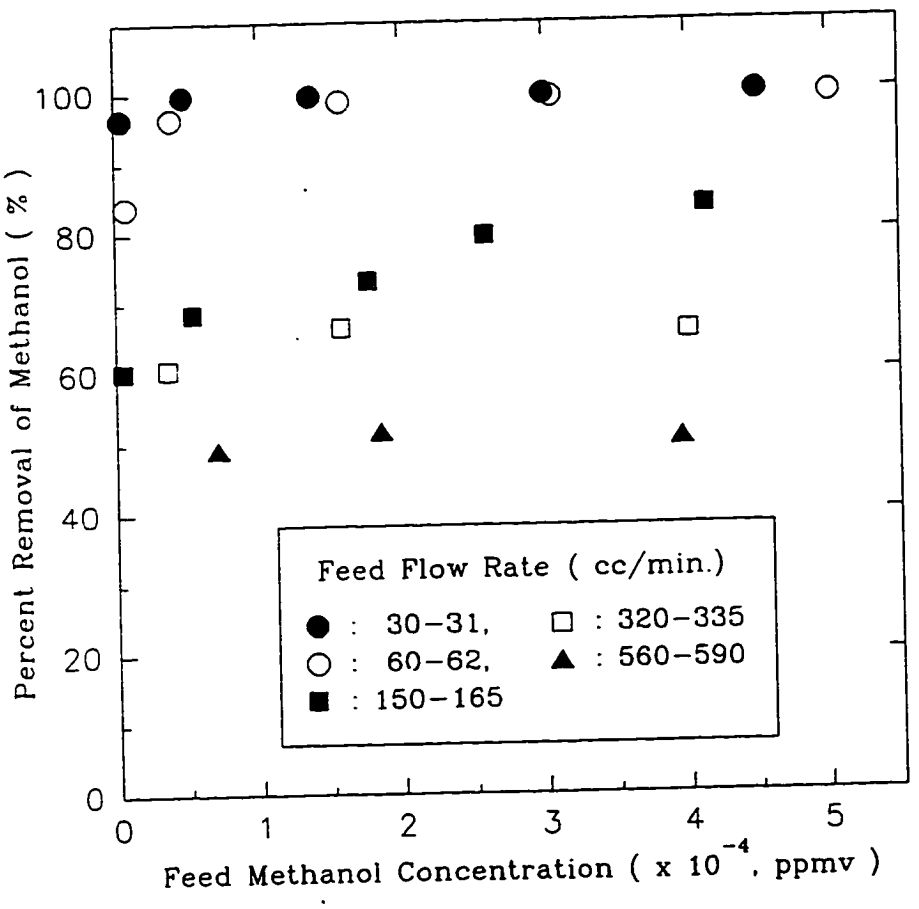

Figure 3.23 Percent Removal of Methanol vs. Feed Methanol Concentration at Different Feed Flow Rates

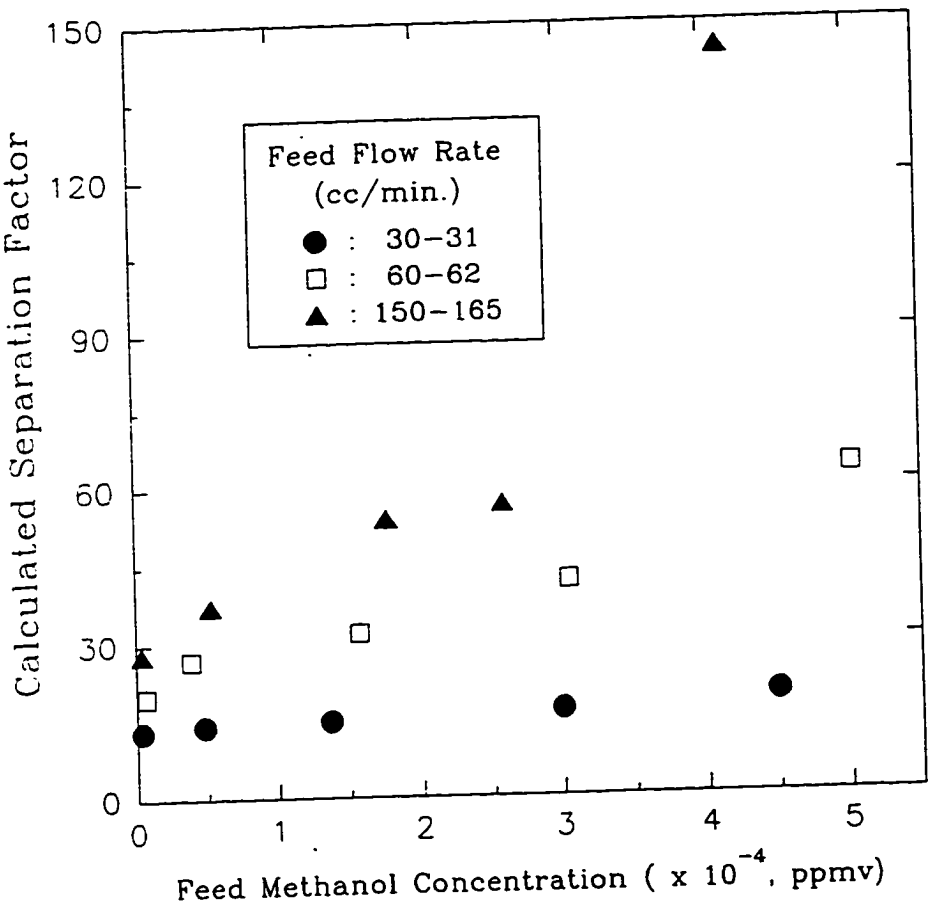

Figure 3.24 Separation Factor vs. Feed Methanol Concentration at Different Feed Flow Rates

Table 3.9 Flux and Percent Removal of Toluene at Different Toluene Concentrations and Different Shell Side Vacuum Levels (Module # 2, Flow Rate : 60 cc/min.)

Feed Inlet		Feed Outlet		Permeate Side Absolute Pressure (cm Hg)	Toluene Flux (x 10^8, gmol/min.cm^2)	Percent Removal of Toluene (%)
Flow Rate (cc/min.)	Toluene Mole Fraction	Flow Rate (cc/min.)	Toluene Mole Fraction			
60.2	0.00249	55.8	0.00189	20.1	1.72	29.6
60.0	0.00242	55.5	0.00139	11.2	2.62	46.6
60.0	0.00280	55.4	0.00093	6.2	4.50	69.3
64.1	0.00974	59.6	0.00766	26.5	6.49	26.8
63.2	0.00944	58.7	0.00589	17.6	9.76	42.1
63.1	0.00920	58.5	0.00218	6.2	17.6	78.1
61.5	0.0133	57.0	0.0100	25.2	9.45	29.9
61.4	0.0140	56.9	0.00707	15.0	17.7	53.2
60.2	0.0137	55.6	0.00246	6.2	26.6	83.4
59.9	0.0135	55.3	0.00064	0.1	30.7	98.2

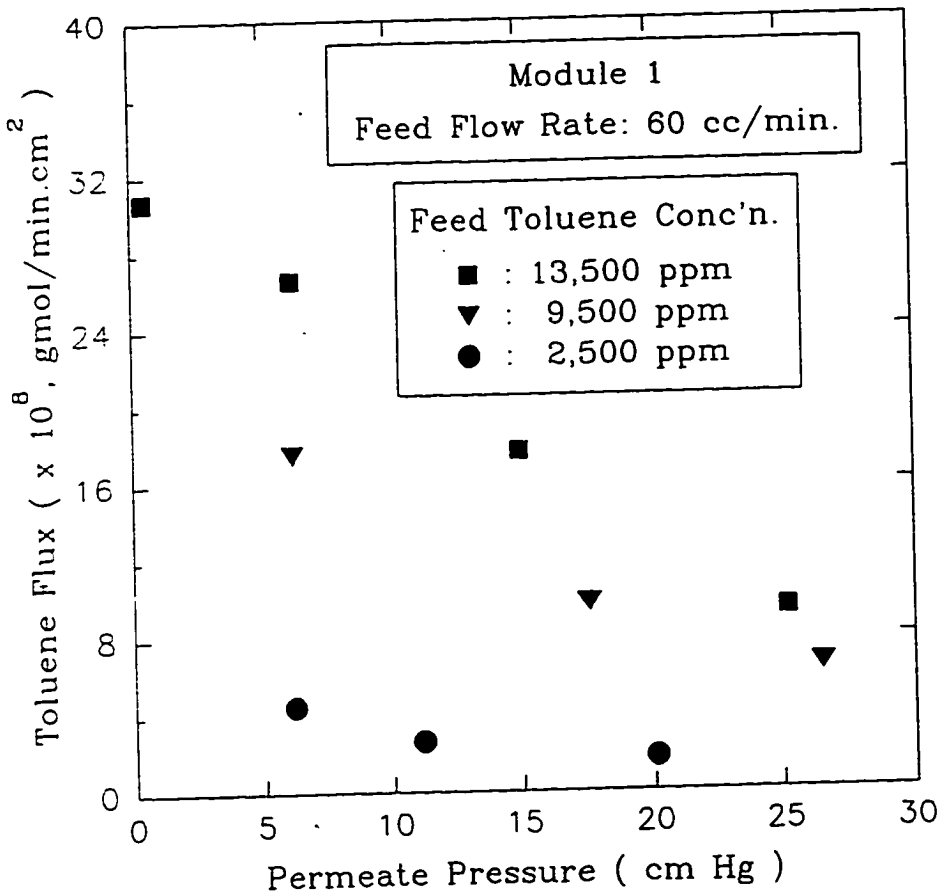

Figure 3.25 Toluene Vapor Flux vs. Permeate Pressure at Different Feed Toluene Concentration

permeate pressure. It was decreased a lot with a little bit of increase in the permeate pressure. If the permeate pressure becomes relatively high, (e.g. permeate side vacuum level > -10.0 in Hg), the flux of toluene vapor will be very small and its dependence on the feed toluene vapor concentration will be reduced.

Percent removal of toluene vapor as a function of permeate pressure is also illustrated in figure 3.26. Feed flow rate was fixed at 60 cc/min. and permeate pressure as well as feed toluene vapor concentrations were changed. Percent removal of toluene vapor decreased nonlinearly with an increase of permeate pressure. Compared to almost 98-99 % removal at very low permeate pressures, percent removal was reduced to around 30 % at a permeate pressure of 25 cm Hg (corresponding to -20.0 in Hg). The dependency of vapor permeation on the permeate pressure appears to be very strong; it was also extremely sensitive at high vacuum levels. Small increase in the permeate pressure for a high vacuum level reduced the vapor permeation much.

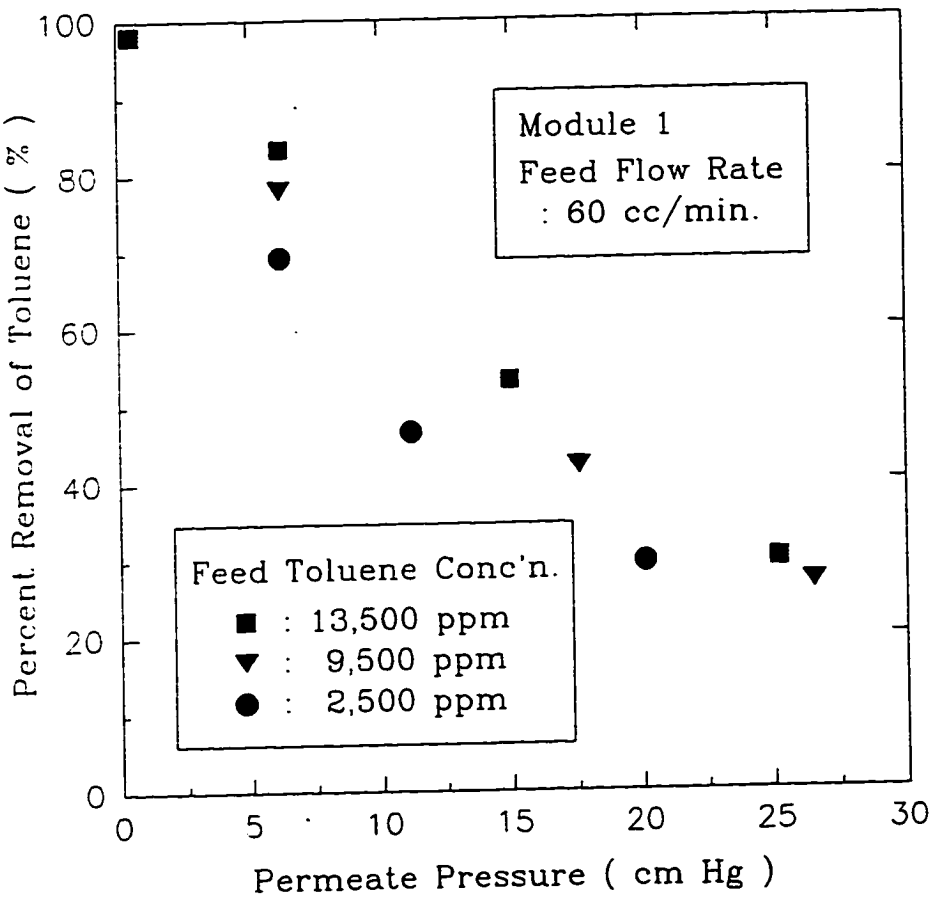

Figure 3.26 Percent Removal of Toluene vs. Permeate Pressure at Different Feed Toluene Concentration

3.4 Conclusions

Common VOCs such as toluene and methanol were removed successfully from N_2 at atmospheric pressure using the novel silicone-coated hollow fiber membrane module. This novel membrane is a thin film composite (TFC) and was highly efficient in removing VOCs selectively from an air/N_2 stream. This membrane had some innate advantages over other silicone-based membranes. The selective barrier (silicone coated layer) where the actual separation was taking place was ultrathin (~1 μm) and the porosity of the polypropylene substrate was high which leads to a low permeation resistance. The substrate was very strongly bonded to the coating layer by plasma polymerization and can withstand a very high pressure. The VOCs permeated preferentially through this membrane to form the VOC-depleted nitrogen stream on the feed side and VOC-enriched stream on the permeate side by application of vacuum on the permeate side.

A small hollow fiber module having a length of 25 cm and 50 fibers could remove 96-99 % of toluene as well as methanol vapors when the feed flow rate was up to 60 cc/min. The percent removal of VOCs were even higher when the feed inlet concentration was higher; 50,000 ppmv feed inlet methanol concentration was reduced to only 370 ppmv at a 60 cc/min. feed flow rate which amounts to more than 99 % removal. Therefore this process is especially suitable for treating streams having a low flow rate and high VOC concentration.

With a feed methanol vapor concentrations below 1 %, the enriched methanol vapor concentration on the permeate was around 20 %; in the case of high feed methanol vapor concentration around 5 %, the enriched permeate methanol concentration was as high as 80 %. The permeances of VOCs through this membrane was in the range of 4-30 x 10^{-9} gmol/sec.cm^2.cm Hg for both toluene and methanol and nitrogen permeance was in between 3-9 x 10^{-10} gmol/sec.cm^2.cm Hg. High separation factor (defined by the ratio of VOC permeance to nitrogen permeance) between 10-55 for toluene and 15-125 for

methanol were obtained depending on the feed flow rate ranges and feed VOC concentration levels.

In the case of methanol vapor, decreasing nitrogen flux was observed at a high concentration of feed methanol vapor; this may be explained in terms of substrate pore blocking phenomenon. The process using this novel silicone-coated hollow fiber membrane module is believed to have a great potential for treating VOC-laden air stream.

CHAPTER 4

REMOVAL OF VOCs FROM AN INERT GAS USING A MICROPOROUS CERAMIC MEMBRANE

4.1 Introduction

4.1.1 Pore Condensation Phenomenon

Transport of gases and vapors through a solid nonporous polymeric membrane occurs by solution-diffusion mechanism where the species dissolve in the upstream interface of the membrane and diffuse through it and finally desorb at the downstream interface of the membrane (Stern and Frisch, 1981). When the membrane has micropores or pores, the mechanisms of Knudsen diffusion or surface diffusion or pore condensation or Poiseuille flow or molecular sieving or any combination of them are operative. In this case, the membrane material may be polymeric or inorganic. The transport regime is determined amongst others by the nature of the gas, the pressure, the temperature and the nature of the membrane both in terms of its pore structure and chemical interaction characteristics. The highest selectivity is usually achieved by molecular sieving conditions in ultra-microporous membranes.

All vapors and gases except helium are adsorbed to varying extents on the surface of membrane pores; this leads to surface diffusion mode of species transport. In case of condensible vapors, there is a strong possibility of multilayer adsorption under appropriate conditions. In membranes with small pore diameters, it is possible to have multilayer adsorption and ultimately pore condensation leading to pore blockage by the condensed film of the vapor. Such pore blockage could drastically reduce the flux of noncondensible gases present in the feed gas mixture. Pore condensation separation of species does offer the possibility of a large separation factor.

When the partial pressure of the species is below that necessary for pore condensation, the separation factor is determined by the relative diffusion rates (gaseous as well as surface) of the two species. In the case of pore condensation, the transport of the non-condensible species through the pore is determined by its permeability in that condensed liquid. Since the permeation of non-condensible species through the condensed liquid film is much lower than the transport of that liquid by the appropriate driving force, permeate obtained will be highly enriched in the condensible vapor species. Since the separation factor is determined by the relative permeabilities of the two species, very high separation factor can usually be obtained by this mechanism.

One of the earliest examples is provided by Ash et al. (1973) who studied the transport and separation of NH_3 and He or H_2 or N_2 at 233 °K through a microporous carbon (carbolac) plug used as a membrane. Under conditions of pore condensation and complete pore blockage by NH_3, the separation factor between NH_3 and N_2 at 233 °K was in excess of 1,000 when that due to Knudsen flow (i.e. $(M_{N2} / M_{NH3})^{0.5}$) is only around 2. The separation of gases and vapors using microporous membranes has been extensively investigated by Hwang et al. (1975, 1986, 1991) using the microporous Vycor glass membrane which has 40 Å pore. Most recently, Qiu and Hwang (1991) constructed a continuous porous membrane permeator (CPMP) using a microporous Vycor glass membrane which was used to remove acetone and ethanol vapors from their mixtures with nitrogen gas. They also developed a mathematical model to describe the CPMP performance under various design and operating conditions.

Sperry et al. (1991) investigated the separation of CH_3OH from a H_2/CH_3OH mixture using a NaOH-poisoned γ-alumina membrane with 4 nm diameter pores. They observed CH_3OH condensation in the pores for certain pressure range between the temperature of 373 and 473 °K, and preferentially removed it through the pores. They also observed the capillary condensation of CH_3OH at pressures much lower than those predicted by the Kelvin equation and indicated the possible causes for the deviations.

Uhlhorn et al. (1990) separated C_3H_6/N_2 mixtures using γ-Al_2O_3 membranes having 2.5 nm pore diameter by preferential permeation of C_3H_6. They modified the membrane to decrease the pore size using MgO, and with that modified membrane, they obtained separation factors as high as 80. They also observed hysteresis in the separation factors as a function of C_3H_6 partial pressure. Tamon et al. (1981) interpreted the flow mechanism of adsorbable gas through the porous adsorbent in the presence of capillary condensation. They derived a new transport model by separately taking account the hopping behavior of adsorbed molecules in the adsorbed phase and the viscous flow of capillary condensate. Portions of surface flow and capillary condensate flow were separately calculated and the overall permeability of condensed phase was derived as the sum of surface permeability and condensate permeability.

Way and Roberts (1991) measured pure gas (He, H_2, CO_2, N_2, CO) permeabilities using microporous silica hollow fiber membranes as a function of temperature. They showed that the transport mechanism for the gas permeation is clearly non-Knudsen since several heavier gases permeate faster than lighter gases. They obtained an excellent correlation between permeability and kinetic diameter of the penetrant and also proposed the mass transport mechanisms as a combination of surface diffusion and molecular sieving.

This study explores the possibility of using pore condensation-cum-surface diffusion phenomenon to remove condensible organic vapors from gas streams, specifically, volatile organic compounds (VOCs) of importance in pollution control. Additional systems of interest are removal of natural gas liquids from natural gas. The membrane used was an inorganic microporous γ-alumina membrane.

4.1.2 Microporous Ceramic Membrane

Most polymeric membranes have limited resistance to high temperature and pressure as well as harsh chemical environments compared to inorganic membranes. While the pore

size distribution of a polymeric membrane is generally quite broad, current inorganic membranes have often a very narrow pore size distribution. Inorganic membranes are made from materials such as metals, ceramics, or inorganic polymers. Porous inorganic membranes are generally superior to organic (or polymeric) membranes in thermal, mechanical, structural stability, chemical and/or microbiological resistances and ease of cleaning and regeneration (Hsieh, 1988). The other advantage of inorganic membranes over polymeric membranes is their consistent quality and very narrow pore size distribution. Various materials can be used for making inorganic membranes and so far silica, alumina and zirconia are the most popular materials. Inorganic membranes have been explored for a variety of gas/vapor separations such as acid gas removal or hydrogen recovery from petrochemical industry and CO/H_2 ratio adjustment in the production of oxychemicals (Way and Roberts, 1991).

In this study, a tubular microporous ceramic membrane was used for the separation of organic vapors (generally VOCs) from inert N_2 by the pore condensation mechanism. This ceramic membrane tube known as Membralox^R was obtained from ALCOA separations technology company (Warrendale, PA). This tubular ceramic membrane is comprised of a rigid body of α-alumina support which has a coarse porosity and pore size (10-15 μm) and a γ-alumina membrane skin having 50 Å pore diameter in the inner surface layer. The membrane covers the inner surface and is bonded to the support by strong ceramic bonds. This membrane will not de-laminate or swell since the strength of the bond is very high. This membrane is compatible with harsh solvent environments; it can endure high temperature and pressure conditions (up to 500 °F and 25 atm) and can be operated over a wide pH range. Toluene and p-xylene was selected to represent two of the frequently used industrial solvents. The membrane was composed of three layers of porous ceramic having a well-defined texture made from γ-alumina. The layer with the finest porosity formed the free surface of the membrane and performed the separations.

4.2 Theoretical Background

4.2.1 Transport Mechanism through a Microporous Ceramic Membrane

Figure 4.1 illustrates schematically four separation (or transport) mechanisms of gases/vapors by microporous membranes (Asaeda and Du, 1986): (i) Knudsen diffusion; (ii) surface diffusion; (iii) capillary condensate flow; (iv) molecular sieving. The transport mechanisms are determined by the relative values of the mean free path λ of the gas molecules and the membrane matrix opening diameter. When the pore size of a porous membrane is much smaller than the mean free path of the gas molecule ($r_p / \lambda < 0.05$, r_p : pore radius, λ : mean free path), Knudsen diffusion is predominant. On the other hand, when the pore size is much greater than the mean free path of the gas molecules ($r_p / \lambda > 50$), viscous (or Poiseuille) flow is predominant (Sengupta and Sirkar, 1986). In the case of Knudsen diffusion, the molecules collide much more frequently with the pore wall than with each other. The diffusion rate is greatly reduced in this flow regime. The lower molecular weight component will diffuse faster than the higher molecular component and will be enriched in the permeate stream. The permeability ratio (or the ideal separation factor), however, is only limited to the square root of the molecular weight ratio of the two components. This is a theoretical maximum selectivity. So when the feed gas/vapor mixture has almost similar molecular weights, the separation factor will be close to 1.0 which means very little separation.

Surface diffusion takes place due to the adsorption of gas molecules on the walls of the pores and this adsorbed species are assumed to be in equilibrium with the bulk gas phase being convected through the pores. Since the pore gas pressure (or partial pressure) is usually decreasing in the direction of transport, the concentration of adsorbed gas species in the pore walls also decreases and this creates the concentration gradient of surface adsorbed species. In addition, molecules adsorbed on the surface of the pores may have considerable mobility. So surface diffusion is caused by the migration of this adsorbed gas molecules along the inner surface of the pores due to the concentration

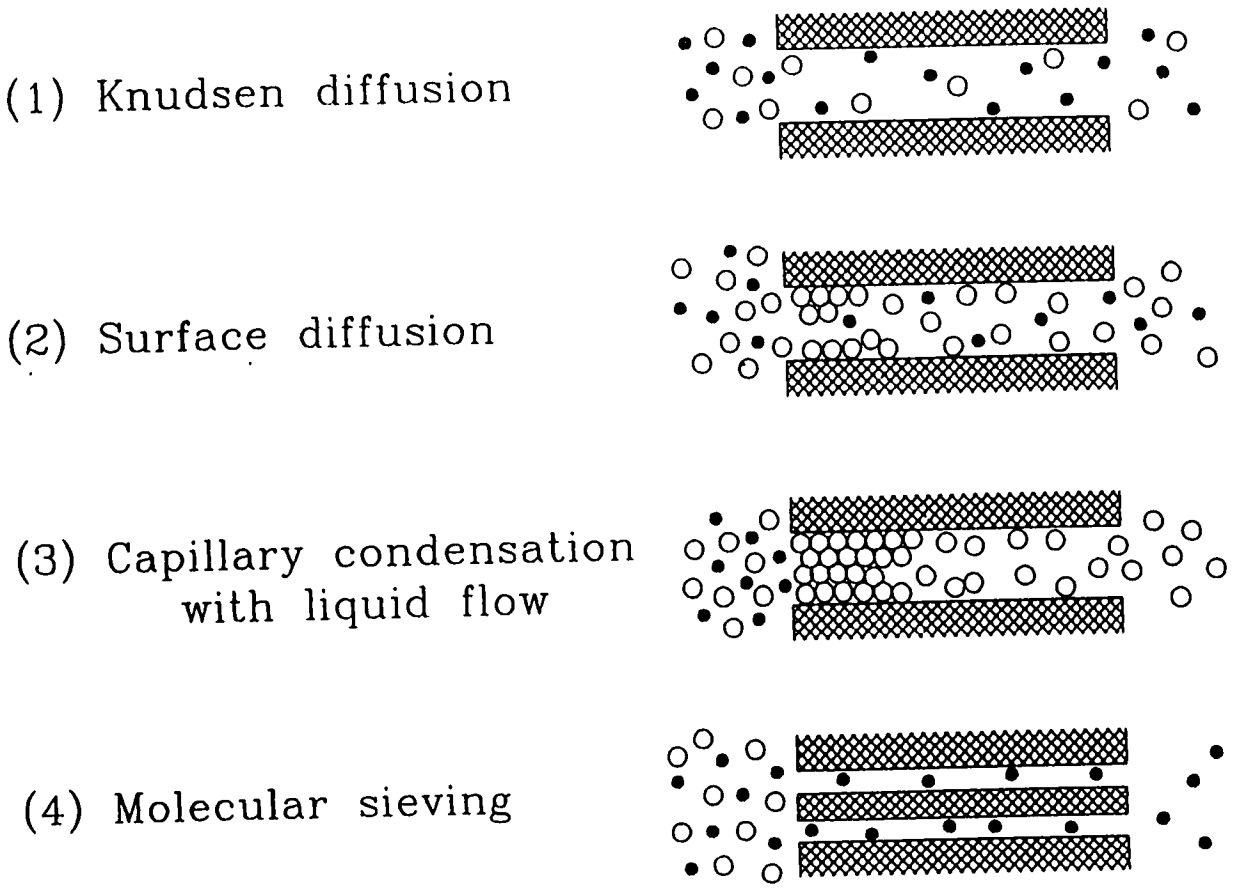

Figure 4.1 Trasnport Mechanisms of Gases/Vapors through Microporous Membrane

gradient in the adsorbed phase. The rate of surface diffusion is generally proportional to the amount of adsorption and the surface diffusivity of the adsorbed species; this mechanism is likely to be much more useful for gas/vapor separation than Knudsen diffusion.

When the partial pressure of the adsorbable gas is low, monolayer adsorption of the gas molecule occurs. As the partial pressure increases, the adsorption gradually increases to multilayer and finally capillary condensation starts to occur in the pores of the membrane when the partial pressure of the gas is approaching the pore condensation pressure. When the partial pressure of the vapor is higher than the capillary condensation pressure of a vapor, the vapor will be condensed inside the pores of the membrane. If all the pores are filled with condensate, it will block the passage of the non-condensible component which eventually will yield a high separation factor.

When the pore size of the membrane is in a range similar to that of the gas molecular size (ultramicropore range), molecular sieving mechanisms prevails. In this mechanism, molecules having a small size (or a particular shape) can pass through the pores of the membrane, while molecules having a bigger size (or a different shape) are blocked by the pore. The separation occurs due to the differences in size and shape in interstices. Molecular sieving behavior can be found in zeolites and materials like molecular sieve carbons. A molecular sieve carbon membrane (MSCM) which contains no pores greater than those of molecular dimensions can be produced by pyrolysis of some organic compounds such as cellulosic and phenolic resins (Koresh and Sofer, 1983). Among these four different transport mechanisms, high solvent permeability along with large selectivity through the enhanced condensate flow combined with the reduction of the non-condensible flow can be obtained by the pore condensation mechanism.

4.2.2 Kelvin Equation

There are a number of theoretical aspects of considerable degrees of complexity in pore condensation separation of a vapor from a gas mixture. These include pore condensibility criterion, flux and selectivity of different species, site-competition between different vapor species, permeation and permeator models. Prior to undertaking an extensive theoretical effort, it is important to find out what is the purification capability of a separation process based on pore or capillary condensation.

In capillaries having as small diameter as those in silica gel, a vapor would condense at pressures far below the normal vapor pressure of that liquid. This phenomenon was the basic formulation of the capillary condensation theory (Brunauer, 1943). If the liquid is confined in a small pore (or capillary), the vapor pressure over the meniscus is lower than the normal vapor pressure of the liquid. In other words, the saturation vapor pressure for capillary condensation is much lower than that of an ordinary condensation process. The smaller the radius of the pore, the greater the vapor pressure lowering and the relation between the saturated vapor pressure P_o of species i over a planar interface to that pressure (P_i) in a capillary of radius r_p is given by the Kelvin equation :

$$\frac{\rho R T}{M} \ln \frac{P_i}{P_o} = - \frac{2 \gamma \cos \theta}{r_p} \qquad (4.1)$$

Here, ρ is the density of the condensate, R is the gas constant and T is the absolute temperature, M is the molecular weight of the condensate. γ , θ , and r_p represent the interfacial tension, contact angle and the radius of the pore, respectively. If the pore size distribution is uniform and the pore size is known, the capillary condensation pressure of a vapor can be estimated using the above Kelvin equation. Capillary condensation starts

to occur from fine pores to the larger pores according to the Kelvin equation as the partial pressure of the gas increases. Therefore, the pores which are exposed to the higher partial pressure of the gas can be filled with capillary condensate more easily.

When all capillaries are filled with the condensate, the saturation vapor pressure of that liquid inside the pores is reduced and a new driving force caused by the action of surface tension at the meniscus arises. This is called capillary suction pressure or capillary force (P_c) and this pressure can be calculated by a force balance at one end of a cylindrical pore filled with a condensate as follows :

$$\begin{aligned} (2\pi r_p)\,\gamma\cos\theta &= -P_c(\pi r_p^2) \\ P_c &= -\frac{2\gamma\cos\theta}{r_p} \end{aligned} \qquad (4.2)$$

This equation is known as Laplace equation. Combining equation (4.2) with the previous Kelvin equation (4.1), one gets

$$P_c = \frac{\rho RT}{M}\ln\frac{P_t}{P_o} \qquad (4.3)$$

Here the new driving force for the capillary condensate flow inside the pore is the capillary pressure drop (ΔP_c) or sometimes called capillary potential (Carman, 1952) :

$$\Delta P_c = \frac{\rho RT}{M}\left(\ln\frac{P_1}{P_0} - \ln\frac{P_2}{P_0}\right) = \frac{\rho RT}{M}\ln\frac{P_1}{P_2} \qquad (4.4)$$

Here P_1 and P_2 are gas phase pressures at upstream and downstream side respectively. If there is a gradient of the gas-phase total pressure, both the gradients of the capillary force and the gas-phase total pressure act as driving forces in the transfer of the capillary condensate and the flow of capillary condensate is like a viscous flow. The capilllary pressure drop (ΔP_c) is several hundred times greater than the gas phase pressure drop applied (Lee and Hwang, 1986).

At room temperature, the normalized vapor pressure, which is the ratio of the pore condensation vapor pressure to the saturated vapor pressure on a planar interface, can be calculated as a function of the pore radius by the Kelvin equation. Figures 4.2 and 4.3 represent the normalized vapor pressure as a function of the pore radius for toluene and xylene (which were selected as VOCs in this study) respectively based on this equation. Physical properties of gas/vapors used in this study are represented in table 4.1. Here the contact angle between the condensate and the pore wall was assumed 0, so cos θ was 1.0. The normalized vapor pressure, which is a measure of vapor pressure lowering when the vapor is confined in the pore, is decreasing as the pore size of the membrane decreases. In other words, the vapor pressure lowering is more severe at smaller pores.

Theoretical pore condensation pressure which is a minimum vapor pressure for the pores to have condensation is a function of the physical properties of the condensate as well as the interaction properties between the condensate and pore walls as shown in figures 4.2 and 4.3. It is also a very strong function of pore size. In both cases (toluene and xylene), the normalized vapor pressure increases drastically as the pore size is increasing and if the pore radius approaches approximately 100 Å , the normalized vapor pressure becomes about 0.8. Pore condensation pressure becomes close to saturated vapor

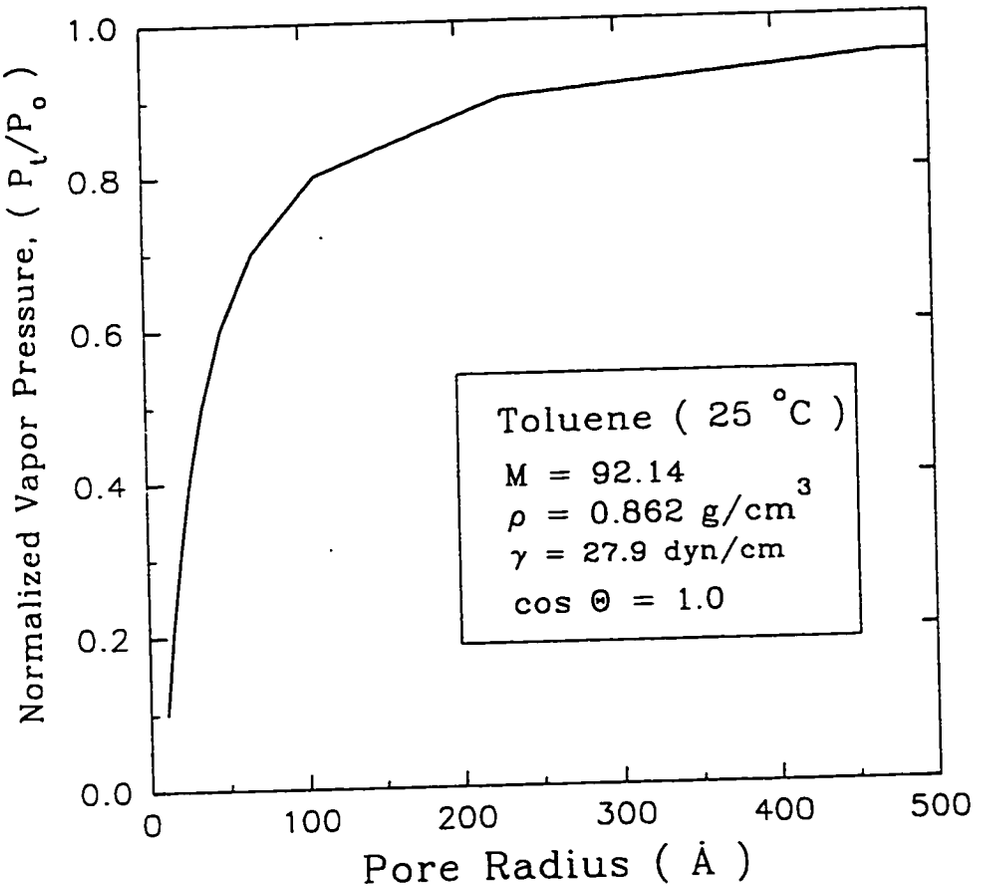

Figure 4.2 Normalized Vapor Pressure vs. Pore Radius for Toluene

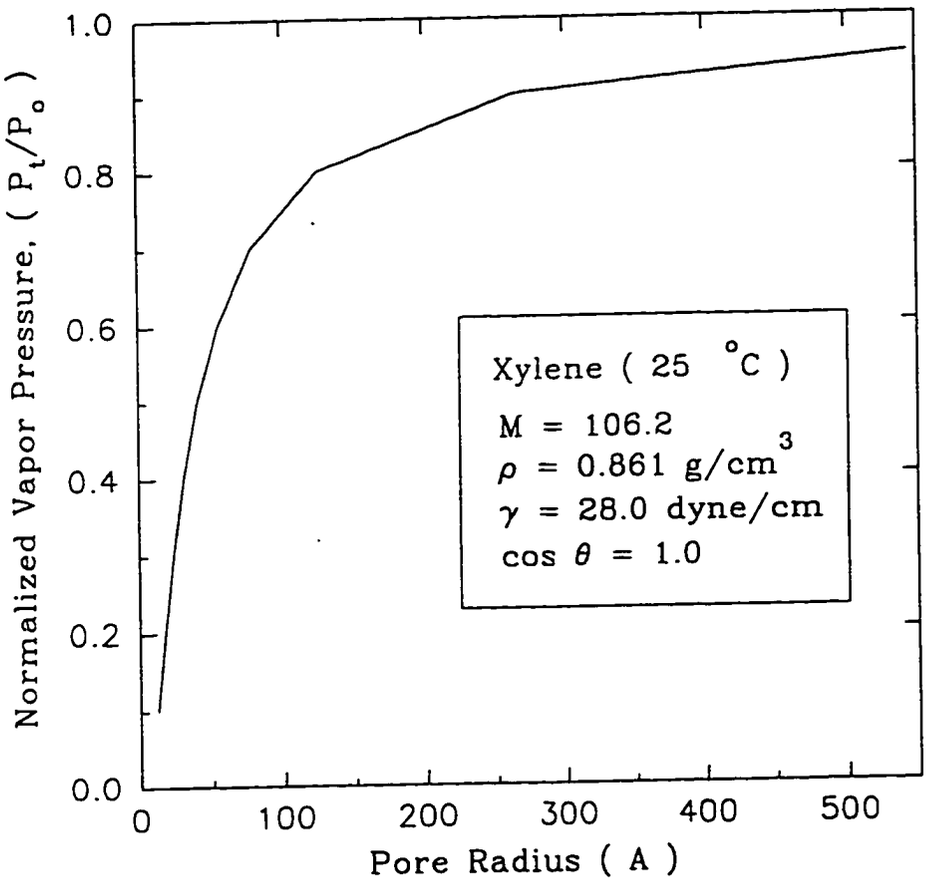

Figure 4.3 Normalized Vapor Pressure vs. Pore Radius for Xylene

Table 4.1 Physical Properties of Gas and Vapors

Gas/Vapors	Molecular Weight	Boiling Point (°C)	Vapor Pressure (mm Hg)	Liquid Density (g/cm^3)	Surface Tension (dyne/cm)	Normalized Vapor Pressure (P_i/P_o)[1]
Nitrogen	28.0	-195.8	-	-	-	-
Toluene	92.1	110.6	28.4	0.862	27.9	0.382
p-Xylene	106.2	138.4	8.76	0.861	28.0	0.328

1 : Calculated based on Kelvin Equation at 25 °C

pressure as the pore radius is over 200 Å; in this case it is difficult to expect pore condensation to occur unless the VOC partial pressure is high. Pore condensation pressure is the minimum pressure required so that pore condensation can occur and this pressure may be calculated using the Kelvin equation. If the partial pressure of the organic solvent in the feed gas is greater than this pore condensation pressure, vapor will be continuously condensed in the pores of the membrane.

4.3 Experimental

4.3.1 Microporous Ceramic Membrane Module

The specifications of ALCOA tubular ceramic membrane used in the experiments are shown in table 4.2a; the specifications of the two modules used in the experiments are shown in table 4.2b. The effective length of the two ceramic tubes were 60 mm and 225 mm respectively and its I.D./O.D. was 7.0/10.0 mm. The finest pore size was 50 Å. The short module (module # 1) was supplied 225 mm long at the beginning; due to breakage, a short length of 60 mm became available.

The long ceramic membrane tube (225 mm) was inserted compactly into the stainless steel housing which was also obtained from ALCOA (light industrial housing with Viton); the short ceramic membrane tube (60 mm) was inserted into a Teflon shell specially made as the housing for this membrane. The active membrane areas were calculated based on the logarithmic mean radius of the ceramic tube and it turned out to be 15.9 cm^2 and 59.5 cm^2 for modules 1 and 2 respectively. Figure 4.4 shows a photograph of the tubular ceramic membrane and the modules used in this experiments.

4.3.2 Materials, Chemicals and Equipment

The following materials, chemicals and equipment were used for the experiments:

Ceramic membrane (Alcoa Sep. Tech. Inc., Warrendale, PA)

Housing (light industrial housing with Viton, Alcoa Sep.Tech.Inc., Warrendale, PA)

Toluene (Certified ACS grade, Fisher Scientific, Springfield, NJ)

p-Xylene (Certified ACS grade, Fisher Scientific, Springfield, NJ)

Mass Flow Transducer (Model 8141, Matheson, E. Rutherford, NJ)

Mass Flow Controller (Model 8250, Matheson, E. Rutherford, NJ)

Table 4.2a Specifications of Alcoa Tubular Ceramic Membrane

	Layer	Material	Pore Diameter (μm)	Porosity (%)	Thickness (μm)
Membrane	1	γ - Al_2O_3	0.005	50	5
	2		0.2	35	30
	3		0.8	40	50
Support		α - Al_2O_3	10 - 15	40 - 45	1500

Table 4.2b Specifications of the Two Modules Used

Module Number	Inside Diameter (mm)	Outside Diameter (mm)	Wall Thickness (mm)	Effective Length (mm)	Surface Area (cm^2)
1	7.0	10.0	1.5	60.0	15.9
2	7.0	10.0	1.5	225.0	59.5

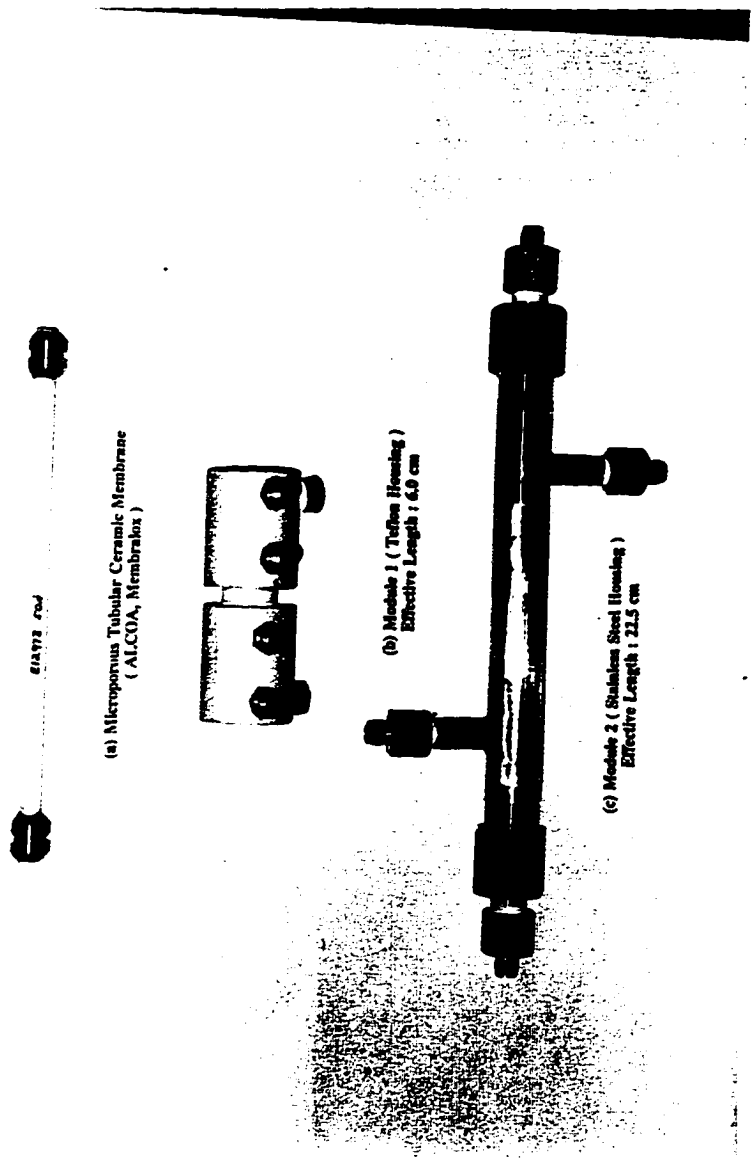

Figure 4.4 Photograph of the Tubular Ceramic Membrane and Modules

Gas Chromatograph (GC) (Hewlett Packard Model 5890A)

Integrator (Hewlett Packard Model 3392A)

Cold Trap (Model 8640, Pope Scientific, Inc., Menomonee Falls, WI)

Bubble Flow Meter (Varian, CA)

Vacuum Pump (Model 1410, Welch Scientific Inc., Skokie, IL)

Back Pressure Regulator (Model 10, Fairchild, Winston Salem, NC)

Nitrogen Extra Dry, Air Zero, Hydrogen Zero, Nitrogen Zero (Matheson, E. Rutherford, NJ).

4.3.3 Experimental Apparatus

The experimental setup for vacuum mode of operation is shown in figure 4.5. Pure nitrogen from a cylinder was introduced into a bubbler which contained pure toluene (or xylene) at a controlled rate using an electronic mass flow transducer-controller. The VOC-containing nitrogen stream (which simulates a feed of VOC-laden industrial waste air stream) was then passed through the tube side of the tubular ceramic membrane module via a rotameter.

All experiments were done at room temperature. A vacuum pump was connected at both ends of the shell side to provide the necessary pressure driving force for organic vapor permeation. In this case, feed side was maintained at atmospheric pressure and various degrees of vacuum (-5.0 in Hg to -25.0 in Hg) were applied to the shell side. Since the inner diameter of the tubular ceramic membrane is large (7.0 mm), there was no pressure drop in the tube side. Permeated organic solvents were collected in the cold trap.

In the high pressure mode of operation, a back pressure regulator which controlled the upstream (feed) pressure was placed after the membrane module to create the proper pressure level and therefore the driving force. The nitrogen stream containing VOCs was passed through the tube side of the membrane module. The feed side pressure was varied

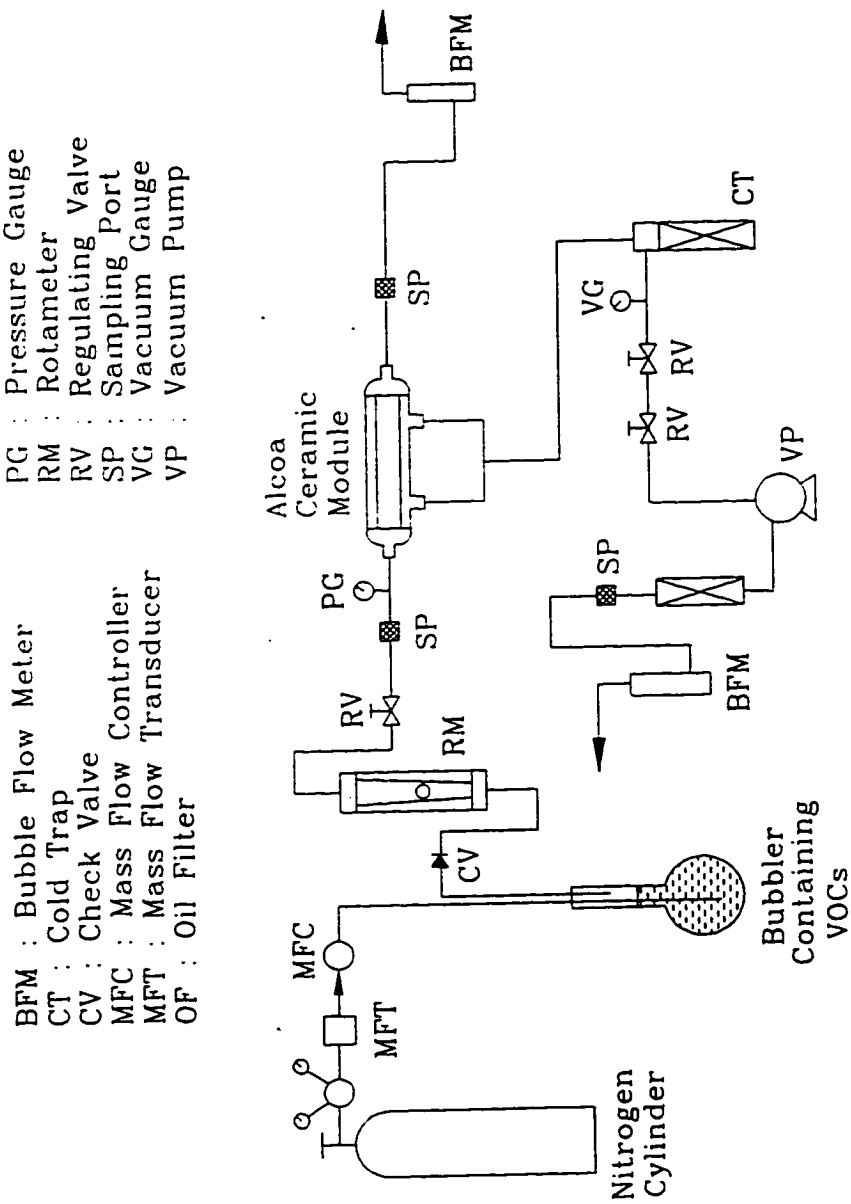

Figure 4.5 Experimental Setup for Vacuum Mode of Operation

from 10 to 30 psig and the shell side was maintained at atmospheric pressure. A pressure gauge was used to measure the applied feed side pressure. The experimental setup for the high pressure mode is shown in figure 4.6.

4.3.4 Experimental Procedure

4.3.4.1 GC Calibration for Toluene and Xylene

For toluene calibration, isopropyl alcohol was used as a diluent. Eight different volumes of toluene and isopropylalcohol were mixed together to represent different levels of toluene concentration. One μl of each sample was taken with microsyringe and injected into the GC (Hewlett Packard Model 5890A). This was repeatedly done until steady GC peak areas were obtained. Chromosorb W-HP column (Alltech, Deerfield, IL) and a flame ionization detector were used for the analysis of the solvents used in this experiments.

The injector and detector temperatures were set to 150 °C. The number of moles of toluene in 1.0 μl sample was calculated and plotted with the corresponding GC peak areas. The total number of moles in one c.c. of gas sample when the sample was taken during the experimental runs can be calculated using the ideal gas law. The number of moles of toluene in one c.c. of gas sample can also be calculated thereby from the calibration curve. The ratio of these two values will give the mole fraction (or the concentration) of toluene. Table 4.3 shows the number of moles of toluene vs. peak area and it is plotted in the figure 4.7. For xylene calibration, pentane was used as a diluent. Six different concentrations of xylene were prepared and the calibration procedures were similar to that for toluene calibration. Only difference was that 0.5 μl of sample was taken in the case of xylene. Table 4.4 and figure 4.8 represent the data and plot for the xylene calibration.

4.3.4.2 Removal of VOCs from Inert N_2 in Vacuum Mode of Operation

The solvent-containing nitrogen feed gas was passed through the tube side of the

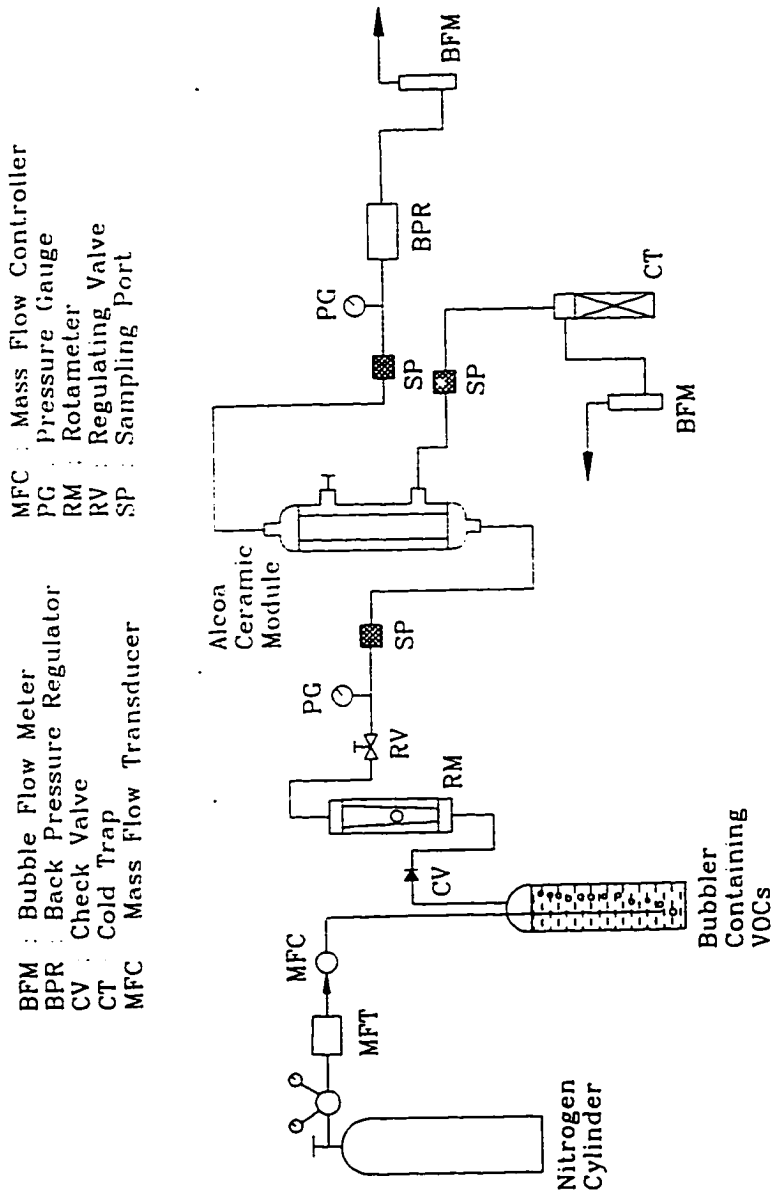

Figure 4.6 Experimental Setup for High Pressure Mode of Operation

Table 4.3 Concentrations of Toluene vs. GC Peak Area

Volume (ml)		Toluene Conc'n. (gmol/l)	No.of Moles of Toluene in 1.0 μl (x 10^7)	GC Peak Area
Toluene	Isopropyl Alcohol			
0.3	119.7	0.0233	0.233	270,950
0.3	59.7	0.0467	0.467	576,190
0.3	29.7	0.0933	0.933	1,202,300
0.6	29.4	0.187	1.87	2,221,200
1.2	28.8	0.373	3.73	4,548,500
1.8	28.2	0.560	5.60	6,912,900
2.4	27.6	0.750	7.50	8,923,200
3.0	27.0	0.937	9.37	10,829,000

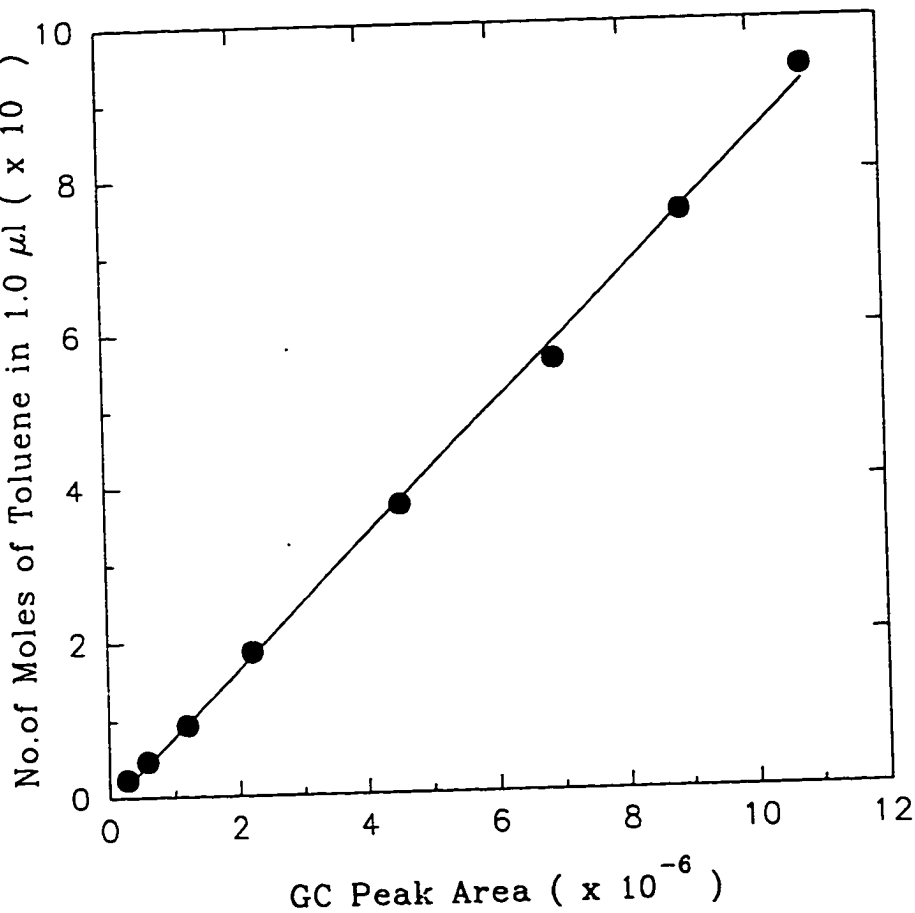

Figure 4.7 Calibration Curve for Toluene

Table 4.4 Concentrations of Xylene vs. GC Peak Area

Volume (ml)		Xylene Conc'n. (gmol/l)	No.of Moles of Xylene in 0.5 μl (x 10^7)	GC Peak Area
Xylene	Pentane			
0.5	16.0	0.246	1.23	809,820
0.5	8.0	0.477	2.39	1,651,750
1.0	8.0	0.901	4.51	2,518,600
1.0	4.0	1.62	8.11	3,656,900
2.0	4.0	2.70	13.5	5,449,350
4.0	4.0	4.06	20.3	7,651,450

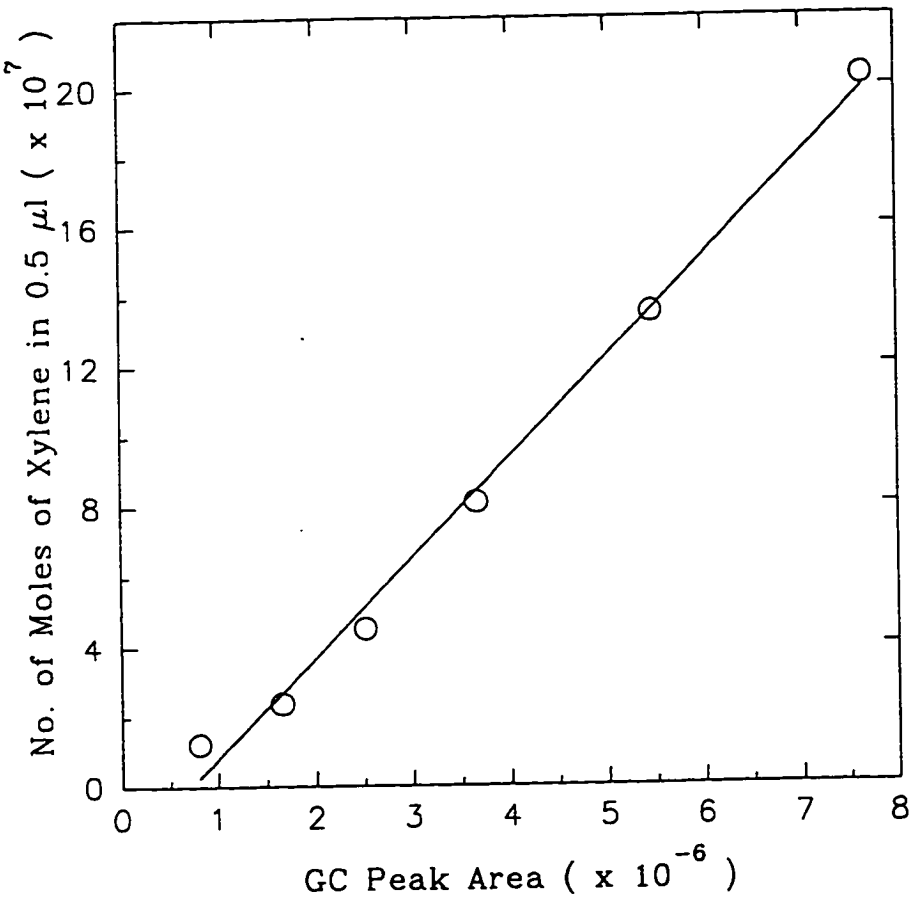

Figure 4.8 Calibration Curve for Xylene

membrane module at the desired flow rate for about 10-20 minutes. A mass flow transducer and controller with digital readout devices was used to adjust the feed flow rate. As the nitrogen flow rate was increased, the feed solvent vapor concentration was also increased slightly but still it did not reach the saturation concentration of solvent. Initially the vacuum line which was connected to both ends of the shell side was completely closed and then the vacuum line valve was opened very slowly. As time went on (as the pores were filled with the solvent), the feed outlet flow rate was stabilized to a certain level at a given applied vacuum. The feed inlet flow rates were changed from 20 to 220 cc/min. and the shell side vacuum levels were varied from -5.0 in Hg upto -25.0 in Hg. Tube side pressure was kept constant at atmospheric pressure. If the shell side vacuum was suddenly increased, the pores were opened suddenly and in this case the degree of vacuum applied was decreased immediately and there was no flow at the feed outlet side. So it was important to increase the shell side vacuum levels very slowly in order not to open the pores. Once the feed side flow and the desired vacuum level on the shell side were achieved (it usually took 2 hours), one c.c. of feed inlet and outlet samples were taken periodically with GASTIGHT syringe and injected into the GC (Hewlett Packard Model 5890A) until steady values were obtained. A flame ionization detector (FID) and a Chromosorb W-HP column were used for the analysis of solvent vapor concentration. The condensible solvent vapors which were transferred to the shell side were collected in a cold trap. Feed inlet flow rate was calculated from the calibrated rotameter readings and the feed outlet flow rate was measured periodically using a bubble flow meter.

4.3.4.3 Removal of VOCs from Inert N_2 in High Pressure Mode of Operation

The solvent-containing feed nitrogen stream was allowed to flow through the tube side of the membrane module at a desired flow rate and atmospheric pressure for about 5-10 minutes. A stainless steel vessel was used for bubbling nitrogen through the solvents.

Then the tube side pressure was increased very slowly using the back pressure regulator (so that the pores would not be open) to a certain level; in this case there was no vacuum applied to the permeate side. Permeate side was kept constant at atmospheric pressure.

During the pressure buildup at a certain setting of the back pressure regulator, there was no flow in the feed outlet side; once the pressure build up was finished, there was normal feed outlet flow. Feed inlet flow rates were changed between 20 to 200 cc/min. range and three different feed pressures (10, 20, 30 psig) were applied to the tube side of the membrane module by the back pressure regulator. One end of the shell side was closed so that the permeate flow is countercurrent to that of feed flow; one c.c of the feed inlet and outlet as well as the permeate samples were analyzed using a GC (Model : HP 5890A, Column : Chromosorb W-HP) and samples were taken every 20-25 minutes. The feed inlet flow rate was calculated based on electronic mass flow meter readings and the feed outlet flow rate was measured regularly by a bubble flow meter. One experimental run lasted usually 3-4 hours. The experimental feed concentration ranges were slightly higher than theoretical pore condensation concentration in both solvents. Table 4.5 provides the experimental feed concentration ranges for two solvents used in the experiments.

Table 4.5 Experimental Feed Solvents Concentration Ranges

Solvents	Saturated Concn. (ppmv)	Pore Condensation Concn. (ppmv)	Exp.Feed Concn. Range (ppmv)
Toluene	37,421[a]	14,300[b]	15,000 - 29,000
p-Xylene	11,526	3,779	4,000 - 6,000

a : Calculated using Saturated Vapor Pressure Data (Perry & Green, 1984)

b : Calculated based on Kelvin Equation at room temperature (25 °C)

4.3.5 Performance of the Membrane Module

The performance of this membrane separation system was examined in terms of the percent removal of solvent and separation factor. The percent removal of solvent is a ratio of the permeate side solvent flow rate to the feed inlet solvent flow rate.

The separation factor is sometimes defined as the permeate side mole fraction ratio divided by the reject side mole fraction ratio so that the value is larger than 1.0. When the pressure ratio is very small (permeate side pressure is very small compared to the reject side pressure), separation factor approaches the ideal separation factor which is the ratio of the permeabilities of the two components. The basis for calculation of percent removal and separation factor are given below:

$$\text{Percent removal of VOC (\% R)} = (1 - F_o.x_o / F_i.x_i) \times 100 \qquad (4.5)$$

$$\text{Separation factor } (\alpha) = [\, x_p / (1-x_p) \,] / [\, x_o / (1-x_o) \,] \qquad (4.6)$$

where x_i, x_o and x_p are feed inlet, feed outlet and permeate mole fraction of VOCs, respectively.

4.4 Results and Discussion

The results of pore condensation-based separation studies are presented in the following order. First, the effect of varying levels of permeate side vacuum is studied for the removal of toluene from N_2. Next, separation in the same system is studied when the feed is at a higher pressure and the permeate is essentially at atmospheric pressure. The results of separation of xylene from N_2 are illustrated at the end.

The experimental data using the vacuum mode of operation for toluene in N_2 are shown in tables 4.6 to 4.8 for changing shell side pressure levels. In this case, feed side pressure was kept constant at atmospheric pressure while the permeate side pressures was reduced in subsequent experimental runs by increasing the level of vacuum. In most cases, the percent removal of toluene as well as the separation factor was decreased as the total feed flow rate was increased at a particular shell side pressure. Inlet toluene concentration levels used here (around 27,000 ppmv) were higher than that predicted by Kelvin equation for pore condensation (14,300 ppmv).

In the module 2, the difference between the feed inlet and outlet flow rates was increased as the feed inlet flow rate increased. As the total flow rate increased, more nitrogen was passing through the pores which will reduce the separation factor. The percent removal of toluene was increased as the permeate side pressure was lowered. The higher removal rate is most likely due to the increased partial pressure driving force of toluene. The percent removal of toluene in module 1 (short module) was always 2-3 times higher than that of a module 2 (long module) at a given operating condition (see figure 4.9). But the separation factor was significantly less in module 1 compared to module 2. This was mainly due to the much higher flux of both toluene and nitrogen through the pores in module 1 under same operating conditions.

As the shell side pressure was decreased (increasing vacuum), percent removal of toluene was increased but the separation factor was even more reduced in both modules.

Table 4.6 Percent Removal of Toluene Vapor and Separation Factor in Vacuum Mode of Operation
(Feed Side : Atmospheric, Shell Side Pressure : 55.7 cm Hg)

Module #	Feed Inlet		Feed Outlet		Percent Removal of Toluene	Separation Factor
	Flow Rate (cc/min.)	Mole Fraction of Toluene	Flow Rate (cc/min.)	Mole Fraction of Toluene		
1	26.3	0.0205	20.4	0.0083	68.5	7.9
	43.4	0.0228	36.7	0.0139	48.5	6.7
	69.3	0.0281	62.6	0.0189	39.5	5.5
	103.0	0.0271	94.3	0.0224	24.4	3.7
	143.5	0.0296	126.3	0.0257	23.5	2.3
2	26.3	0.0217	25.4	0.0161	28.1	13.1
	43.4	0.0286	42.7	0.0262	9.7	7.7
	69.3	0.0264	66.0	0.0249	10.4	6.6
	103.0	0.0284	100.1	0.0263	9.9	4.1
	143.5	0.0268	132.7	0.0256	11.5	2.4

Table 4.7 Percent Removal of Toluene Vapor and Separation Factor in Vacuum Mode of Operation
(Feed Side : Atmospheric, Shell Side Pressure : 37.9 cm Hg)

Module #	Feed Inlet		Feed Outlet		Percent Removal of Toluene	Separation Factor
	Flow Rate (cc/min.)	Mole Fraction of Toluene	Flow Rate (cc/min.)	Mole Fraction of Toluene		
1	16.2	0.0241	5.3	0.0038	94.9	3.9
	44.6	0.0251	32.3	0.0081	76.8	2.8
	86.1	0.0267	77.9	0.0167	43.5	2.5
	143.5	0.0288	121.1	0.0214	37.3	1.4
2	19.8	0.0258	18.3	0.0197	29.4	5.5
	44.6	0.0260	43.2	0.0238	11.2	4.2
	89.4	0.0280	87.7	0.0261	8.4	2.8
	143.5	0.0273	133.1	0.0262	11.0	1.6

Table 4.8 Percent Removal of Toluene Vapor and Separation Factor in Vacuum Mode of Operation
(Feed Side : Atmospheric, Shell Side Pressure : 15.0 cm Hg)

Module #	Feed Inlet		Feed Outlet		Percent Removal of Toluene	Separation Factor
	Flow Rate (cc/min.)	Mole Fraction of Toluene	Flow Rate (cc/min.)	Mole Fraction of Toluene		
1	43.4	0.0297	17.6	0.0017	97.7	2.7
	69.3	0.0303	45.8	0.0050	89.0	2.2
	103.0	0.0300	81.9	0.0092	75.7	1.7
	143.5	0.0293	116.6	0.0127	64.8	1.2
2	69.3	0.0247	63.4	0.0145	46.2	4.8
	103.0	0.0252	95.7	0.0179	34.2	2.5
	143.5	0.0279	129.6	0.0216	30.2	1.3

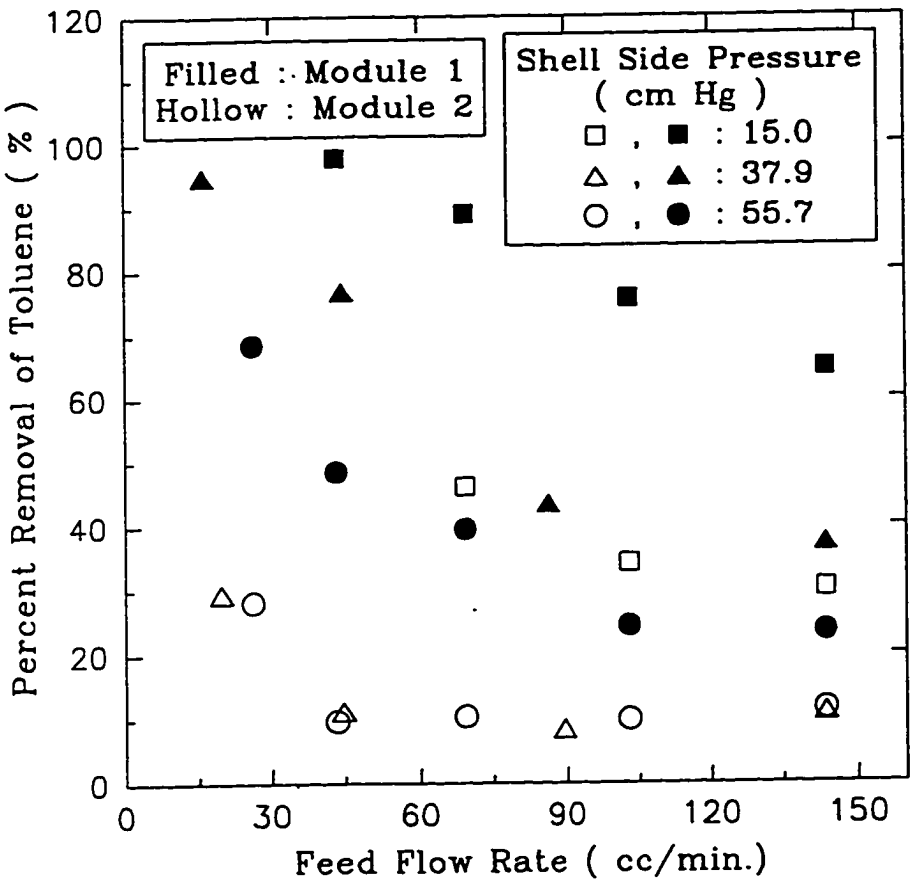

Figure 4.9 Percent Removal of Toluene vs. Feed Flow Rate at Different Shell Side Pressures

At 15 cm Hg shell side pressure (corresponding to -24.0 in Hg), percent removal of toluene was over 90 % at a small feed flow rate but the separation factor was limited to around 2.0 only due to a high flux of nitrogen.

If all pores are completely filled with the solvent and the continuous evaporation of solvent at permeate side by proper driving force is compensated by continuous condensation of solvent at feed side, the pores will be always filled with the solvent during the experimental runs. In this case, nitrogen can only pass through the pores by its permeation through the solvent inside the pores; the resulting N_2 flux is usually not a high value.

In module 2, permeator outlet toluene concentration was in most cases higher than the theoretical pore condensation concentration which means the vapor transport mechanism can be considered as pore condensation. However, the nitrogen flux through the pores are still considerably high especially when the permeate side pressure is very low. In other words, there are some pores in the membrane partially or totally open which allows nitrogen permeation through them. It is likely that the membrane pores near the inlet portion of the permeator are more easily filled with the solvent and the pores near the exit section of the permeator will be opened as the solvent concentration is depleted along the permeator.

In module 1, percent VOC removal was very high compared to module 2. The separation factor, however, was usually lower than that of module 2. Figure 4.10 shows the separation factor in both modules as a function of the feed flow rate. In addition, the permeator outlet toluene concentration in most cases was much lower than the theoretical pore condensation concentration. Due to this reason, the nitrogen permeation was always more compared to that in module 2 which also reduces the separation factor. Note that this module 1 was previously used in solvent extraction experiments. The pores may have been modified with some chemicals. It is difficult to assume the existence of pore condensation in module 1 since the theoretical separation factor in the Knudsen flow

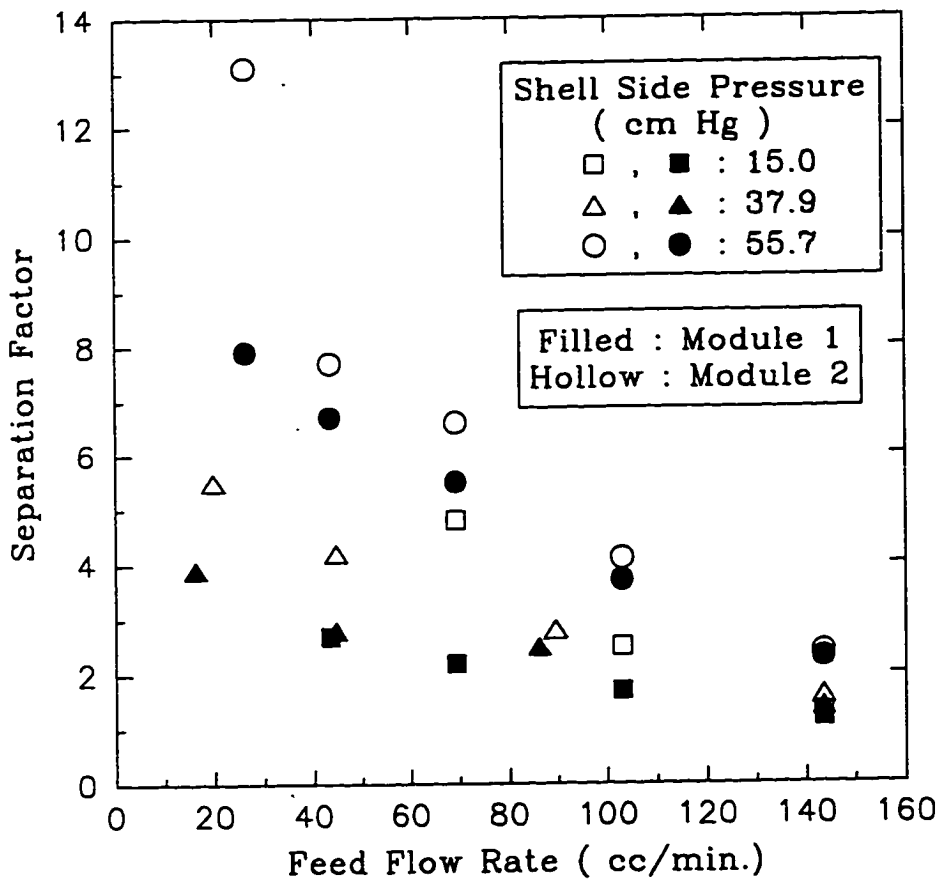

Figure 4.10 Separation Factor (toluene/N_2) vs. Feed Flow Rate at Different Shell Side Pressures

regime is about 1.8 which is similar to some of the results here.

In the pressure mode, the feed toluene concentration was generally lower than that in the vacuum mode at a similar total feed flow rate; the feed toluene concentration was even lower at higher feed side pressure. In this case, permeate side was maintained at atmospheric pressure while the feed side was pressurized using the back pressure regulator up to 30 psig. This mode of operation would be useful for processes where the vapor contaminated air is at a high pressure. Table 4.9 shows the experimental results for module 2.

The effect of feed side pressure on the separation performances is shown in figures 4.11 and 4.12. Module 2 was used in this case. As shown in figure 4.11, increasing feed pressure improved the percent removal of the solvent by increasing the driving force. The effect of feed side pressure on the separation factor is illustrated in figure 4.12. A higher feed pressure generally yielded lower values of separation factor. For the same permeate side pressure, a higher feed pressure in the feed side allowed more solvent and nitrogen permeation through the non-blocked portion of the membrane module. Since the feed solvent concentration was even lower than pore condensation concentration in some cases (especially at higher feed side pressure, 20-30 psig), it is reasonable to assume that there were blocked and non-blocked portion of the membrane module with solvent. In general, an increase in membrane effective length (of effective surface area) reduces the ratio of the blocked to the non-blocked portion of the membrane module which reduces the separation performance. The range of the separation factor shown in table 4.9 is around 1.5 - 3.5. These results also imply that pore condensation is not the main transport mechanism in this case. Possible explanations for these behavior are too low feed solvent concentration for pore condensation to occur and too long a module to block all pores of the membrane. Such a behavior is due to a combination of surface flow and pore condensate flow or even Knudsen flow.

Higher separation factor can be obtained with a high feed solvent concentration

Table 4.9 Percent Removal of Toluene Vapor and Separation Factor at Different Feed Side Pressures
(Module # 2, Shell Side : Atmospheric)

Feed Side Pressure (psig)	Feed Inlet		Feed Outlet		Percent Removal of Toluene	Separation Factor
	Flow Rate (cc/min.)	Mole Fraction of Toluene	Flow Rate (cc/min.)	Mole Fraction of Toluene		
10	50.5	0.0156	43.0	0.0131	15.4	3.3
	82.9	0.0174	75.4	0.0158	7.7	3.2
	119.6	0.0180	108.6	0.0162	6.1	3.1
	163.0	0.0206	150.1	0.0192	4.4	3.1
20	50.5	0.0133	38.5	0.0093	35.1	2.3
	82.9	0.0139	72.0	0.0108	22.6	2.3
	119.6	0.0143	104.0	0.0115	16.4	2.2
	163.0	0.0151	146.3	0.0132	11.8	2.2
30	119.6	0.0101	98.7	0.0062	27.2	1.6
	163.0	0.0100	141.8	0.0070	21.4	1.6

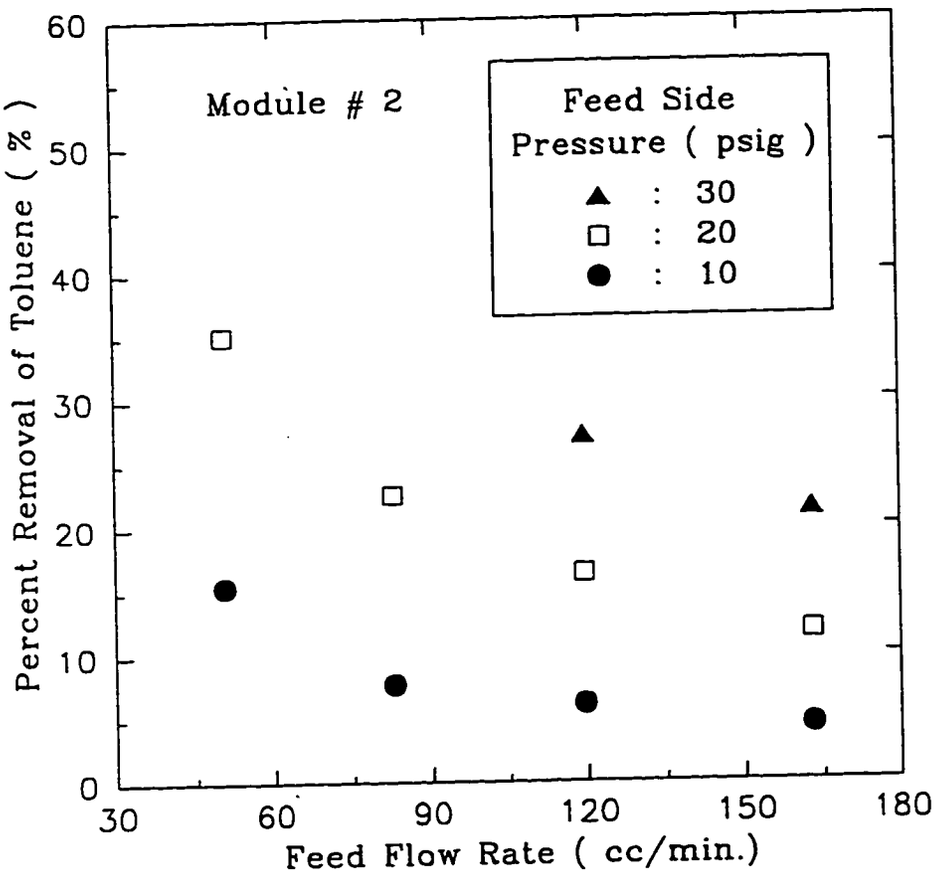

Figure 4.11 Percent Removal of Toluene vs. Feed Flow Rate at Different Feed Side Pressures

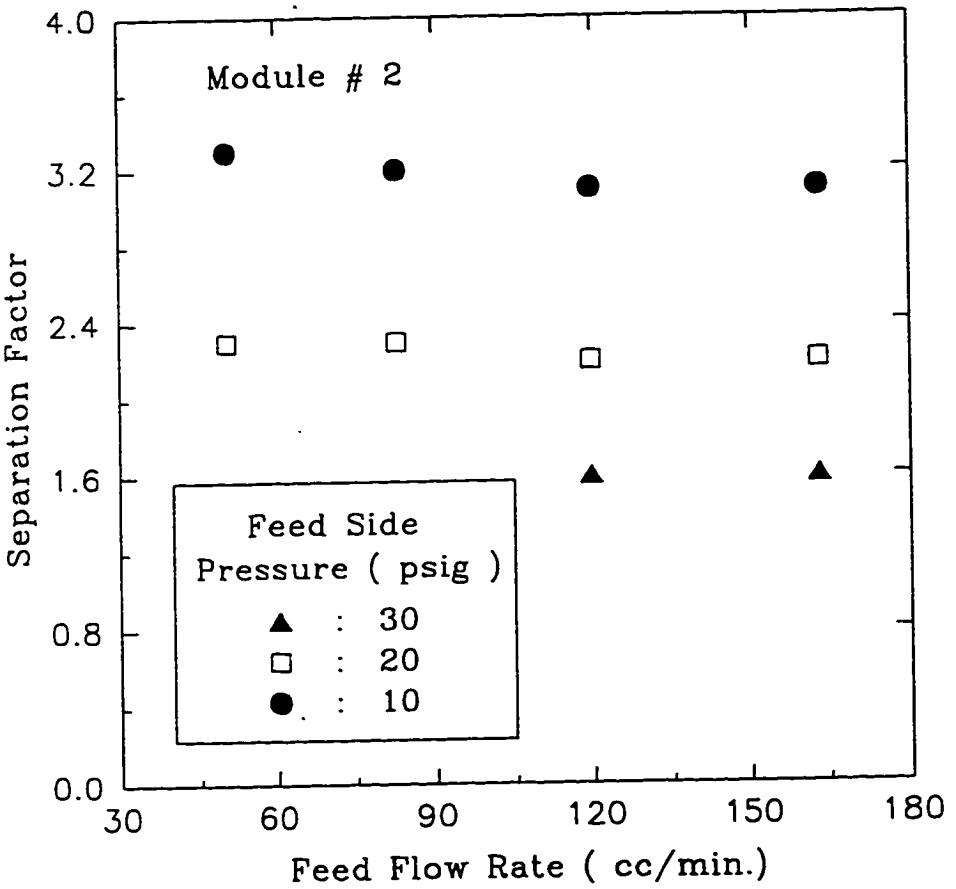

Figure 4.12 Separation Factor vs. Feed Flow Rate at Different Feed Side Pressures

and a relatively shorter membrane module. For the pressure mode of operation, the toluene permeance found to be in the range of 10^{-9} gmol/sec.cm^2.cm Hg.

Similar experiments were made with xylene using two modules and experimental results are represented in tables 4.10 and 4.11. Feed solvent concentrations were above the concentration required for the pore condensation. Three different levels of permeate side vacuum were applied; the tube side was maintained at atmospheric pressure. Percent removal of xylene was generally higher in module 1 compared to moduie 2 and separation factor was smaller in module 1 as was found for toluene. Nitrogen flux in module 1 was quite high which was similar to that for toluene; however, the nitrogen flux in module 2 was considerably reduced compared to the case of toluene vapor. Figures 4.13 and 4.14 show the percent removal of xylene and separation factor as a function of feed flow rate. The blocked fraction of the membrane tube length can be considered much higher in this case compared to that for toluene.

In module 1, percent removal was relatively high, but separation factor was still poor due to the nitrogen leakage through the pores. This is similar to that observed for toluene. It can be assumed that some pores of the module 1 were partially open through which the nitrogen was leaking. In the case of module 2, percent removal of xylene was of similar level as toluene, but the separation factor was enhanced much by less permeation of nitrogen through the membrane. From the values of separation factor obtained here, it is still difficult to assume that all pores in the membrane are filled with condensate. Of course, the pore size distribution is very narrow in ceramic membranes; there is still a possibility that some bigger pores may not be completely filled with the condensate at a particular partial vapor pressure. Therefore, the vapor species may be transferred partially as a pore condensate and also partially as a surface flow.

From the experimental data, it can be concluded that the pore condensation phenomenon is more favored in the case of xylene than toluene. First of all, pore condensation concentration predicted by Kelvin equation is much lower for xylene

Table 4.10 Percent Removal of Xylene and Separation Factor at Different Shell Side Pressure
(Feed Side : Atmospheric, Module # 2)

Shell Side Pressure (cm Hg)	Feed Inlet		Feed Outlet		Percent Removal of Xylene	Separation Factor
	Flow Rate (cc/min.)	Mole Fraction of Xylene	Flow Rate (cc/min.)	Mole Fraction of Xylene		
55.7	24.3	0.00375	22.0	0.00113	72.8	26.5
	40.3	0.00401	38.3	0.00205	51.3	21.4
	70.0	0.00406	66.7	0.00270	36.7	13.9
	103.2	0.00411	99.2	0.00278	34.9	11.9
	139.0	0.00407	132.6	0.00274	35.8	11.8
37.9	45.7	0.00434	43.3	0.00146	68.2	40.5
	94.3	0.00477	91.6	0.00247	49.6	28.9
	139.1	0.00434	136.1	0.00309	30.3	22.6
	160.0	0.00477	157.7	0.00368	24.0	21.0
25.2	103.2	0.00559	97.4	0.00195	67.2	37.1
	139.0	0.00430	130.1	0.00202	56.1	19.3

Table 4.11 Percent Removal of Xylene and Separation Factor at Different Shell Side Pressure
(Feed Side : Atmospheric, Module # 1)

Shell Side Pressure (cm Hg)	Feed Inlet		Feed Outlet		Percent Removal of Xylene	Separation Factor
	Flow Rate (cc/min.)	Mole Fraction of Xylene	Flow Rate (cc/min.)	Mole Fraction of Xylene		
55.7	26.6	0.00370	13.8	0.00097	86.4	6.8
	41.5	0.00389	29.2	0.00198	64.1	4.3
	72.9	0.00465	57.5	0.00310	47.4	3.4
	106.0	0.00514	92.3	0.00392	33.6	3.4
	139.8	0.00415	126.7	0.00346	24.4	3.1
37.9	47.1	0.00514	33.6	0.00206	71.4	6.3
	97.3	0.00510	80.2	0.00337	45.5	3.9
	139.8	0.00465	123.7	0.00353	33.0	3.8
	169.3	0.00502	151.3	0.00393	30.1	3.6
25.2	40.3	0.00458	26.5	0.00137	80.3	17.9
	70.0	0.0048	54.5	0.00141	77.2	12.1
	103.2	0.00465	87.6	0.00215	60.7	8.9
	139.0	0.00407	122.5	0.00214	53.8	8.8

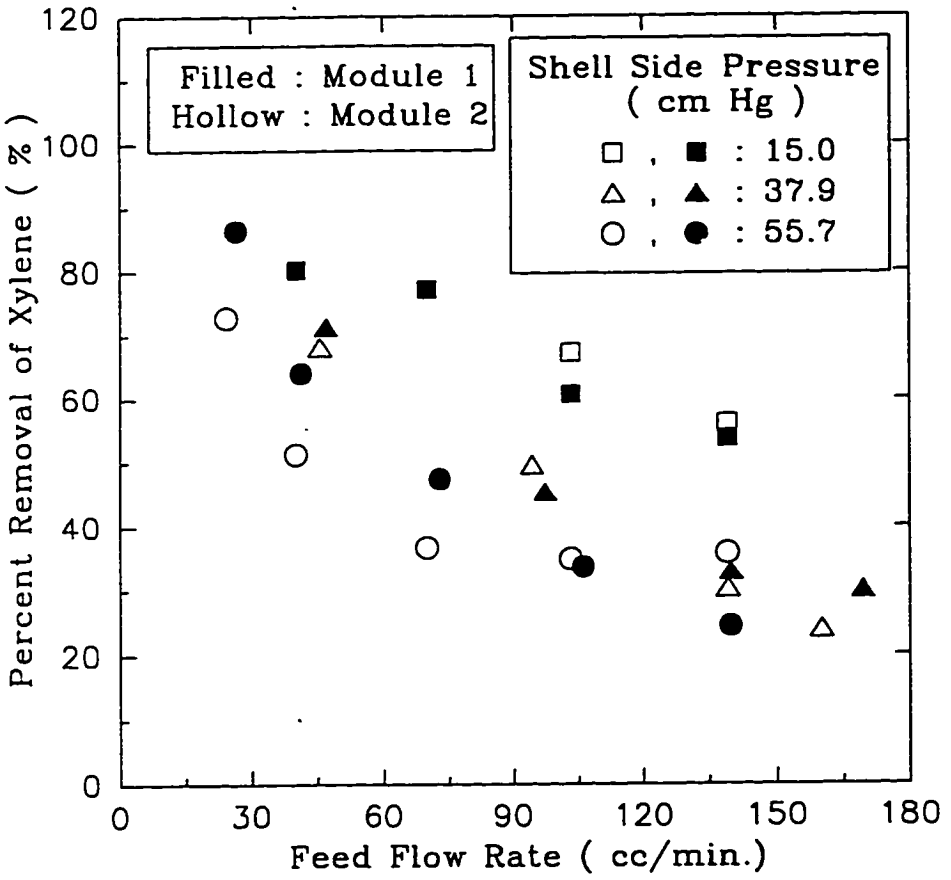

Figure 4.13 Percent Removal of Xylene vs. Feed Flow Rate at Different Shell Side Pressures

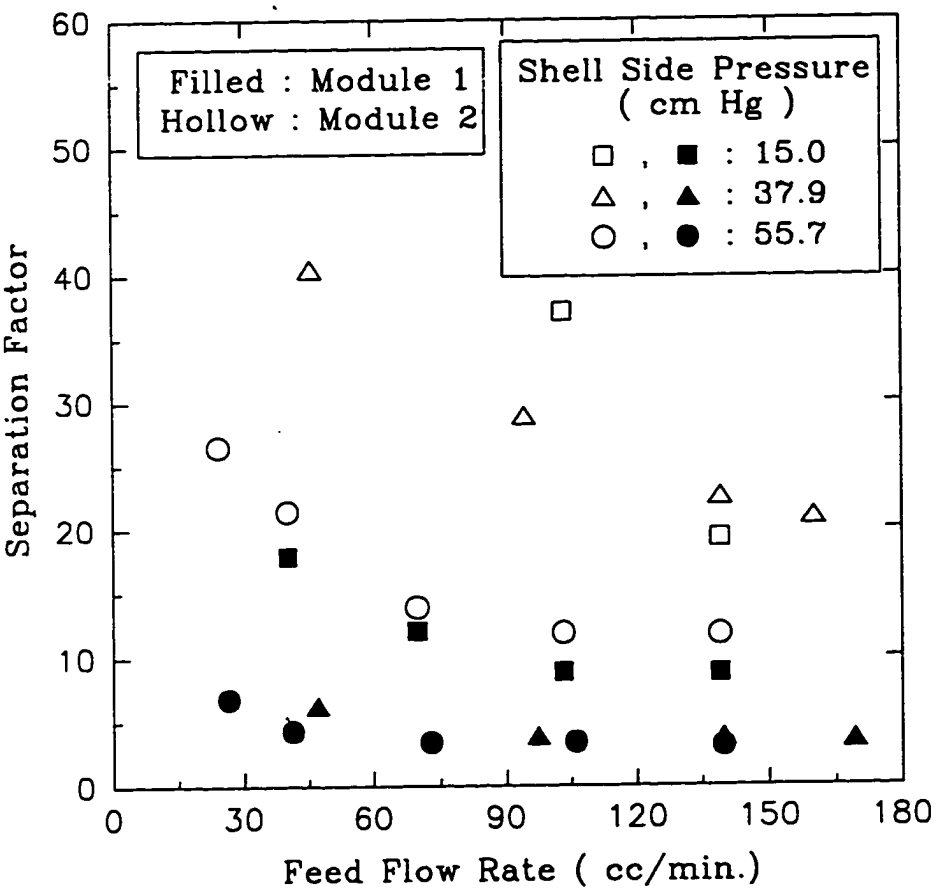

Figure 4.14 Separation Factor (xylene/N_2) vs. Feed Flow Rate at Different Shell Side Pressures

compared to that for toluene. Further slightly bigger size of the xylene molecule compared to toluene may result in pore filling with fewer adsorption layers. The site-competition between the two different vapor species with the γ-alumina pore surface will definitely affect the separation performances. In addition, the condensibility of xylene is geater than that of toluene.

Some experiments were also performed at constant values of feed flow rate, tube and shell side pressures for approximately 8 hours. Percent removal and separation factor were plotted in figures 4.15 and 4.16 respectively as a function of elapsed time. Experimental data showed that a constant value of solvent removal and separation factor could be obtained after 4-5 hours.

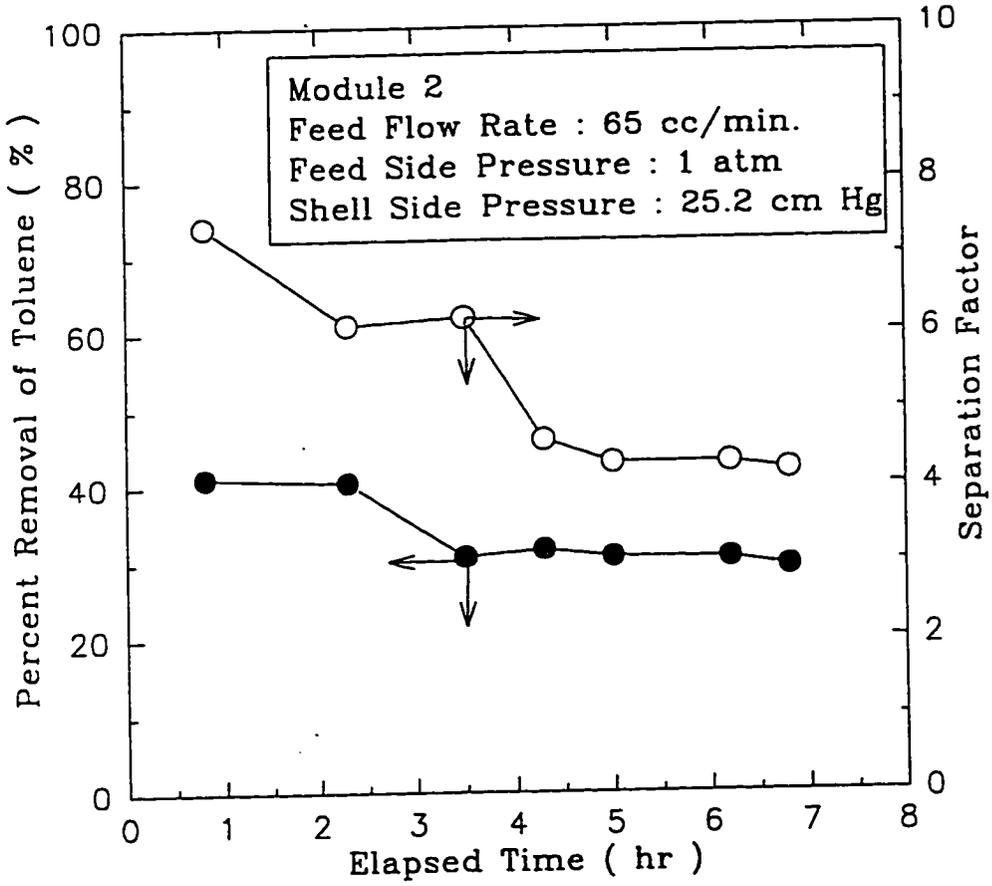

Figure 4.15 Percent Removal of Toluene and Separation Factor vs. Elapsed Time

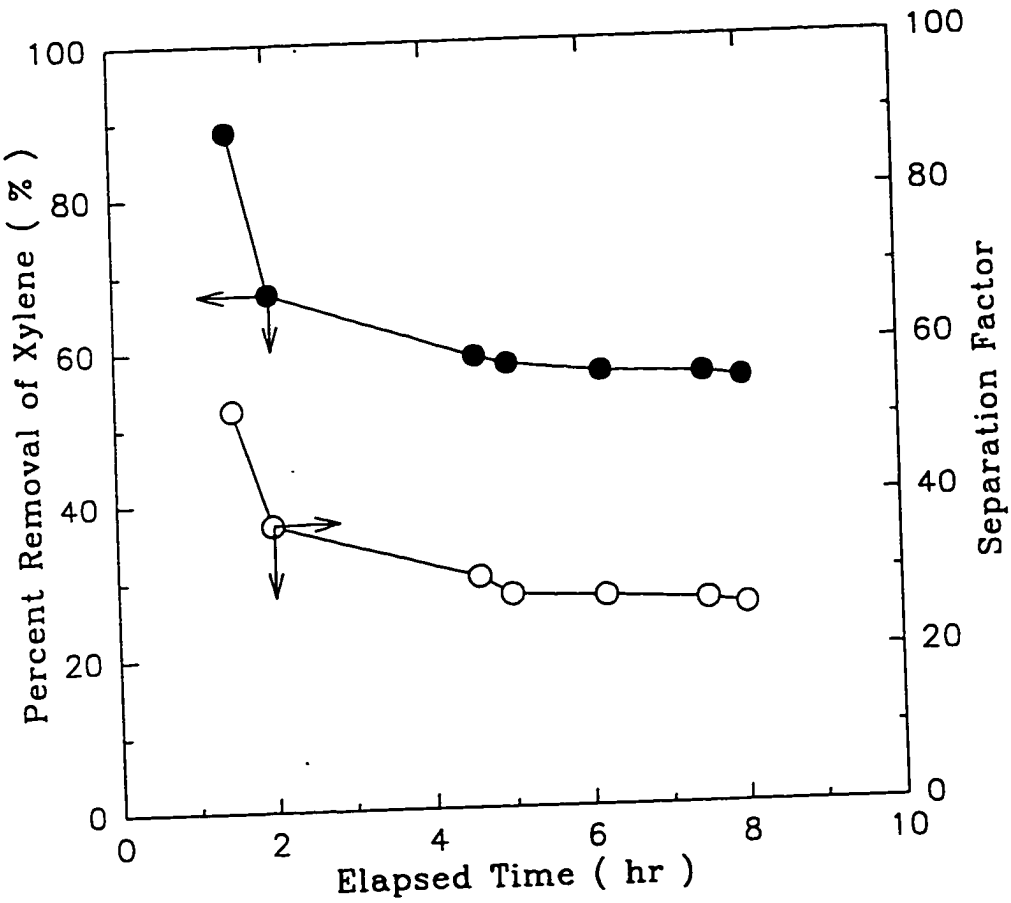

Figure 4.16 Percent Removal of Xylene and Separation Factor vs. Elapsed Time

4.5 Conclusions

Pore condensation-based separation of toluene and xylene from a nitrogen stream was studied. From pore condensibility point of view, many factors affect how pores may be filled completely with organic solvent. The performance of the membrane module is usually examined in terms of product removal as well as the selectivity. These two factors are generally contradictory.

Toluene and xylene removal rate by a microporous ceramic membrane was generally enhanced by increasing the partial pressure difference across the membrane; the selectivity was reduced accordingly due to higher flux of nitrogen in the case of increasing partial pressure difference. This was found in the vacuum mode of operation as well as pressure mode of operation.

Pore condensation separation can theoretically yield a very high separation factor of VOCs over nitrogen if all pores are totally blocked with condensed VOCs. The nitrogen permeation in this case would be essentially very small. The experimental results from this study suggest that nitrogen permeation was not negligible and that some pores are partially open. It seemed that pores near the inlet portion of the module were filled with the organic solvent while the pores near the exit section of the module were opened as the solvent concentration was depleted along the module. The transport mechanism was most likely a combination of surface flow and pore condensation.

The removal rate and separation factor of xylene in module 2 were quite high compared to those for toluene. Nitrogen permeation in the case of xylene was reduced considerably compared to that in the case of toluene resulting in a much higher separation factor. Condensibility of xylene appears to be higher than that of toluene; the possibility of pore condensation-based separation of xylene is also higher than that for toluene.

CHAPTER 5

CONCLUSIONS AND RECOMMENDATIONS

The feasibility of membrane applications for removing water vapor as well as VOCs from air/N_2 stream was studied systematically using three different types of membranes in this thesis.

Studies on removal of water vapor and VOCs like toluene and methanol from N_2 by a Cuprophan hollow fiber hydrogel membrane suggest the following conclusions :

1. Depending on the feed flow rate and partial pressure of the water vapor in the feed, water vapor removal of 20-80 % was easily achieved in a small hollow fiber permeator. Increasing partial pressure of water vapor in the feed yielded higher removal rate of water vapor. Depending on the level of the feed partial pressure of water vapor, high separation factors in the range of 20-250 were obtained between water vapor and N_2.
2. The permeance of water vapor was observed to vary exponentially with its partial pressure. A simple mathematical model taking into account this partial pressure dependent permeance behavior was developed to describe the permeator behavior. Experimentally obtained module performances, such as flux, percent removal and module-averaged permeance of water vapor were well described by the model developed.
3. Water vapor removal was considered as primary when the feed was a mixture of water vapor and some VOCs like toluene and methanol. Removal rate of water vapor was at least an order of magnitude higher than that of toluene. The removal rate of a hydrophilic polar VOC like methanol was 4-10 times larger compared to that of a hydrophobic VOC like toluene through this hydrogel membrane.
4. This process is especially useful for recovering moisture from humid space cabin atmosphere for drinking purposes since the moisture removal rate decreases

drastically at low relative humidities. It is also likely to be useful for recovering moisture from spent air being discharged from a building into fresh air entering a building.

5. This membrane-based technology for water vapor removal can be operated in a stable and continuous manner.

The following conclusions can be drawn from the studies of VOC removal from N_2 in a permeator containing novel silicone-coated hollow fiber composite membranes :

1. The novel silicone-coated hollow fiber module was very efficient in removing VOCs such as toluene or methanol from N_2 stream. More than 96 % of VOCs were removed from a feed stream of 60 cc/min. using a small module having 50 fibers of length 25 cm when the permeate side was subjected to a high vacuum. These membranes were especially suitable for higher feed VOC concentrations since the permeance of VOC appears to increase very rapidly with increasing VOC concentration.
2. The permeances of VOCs were at least an order of magnitude higher compared to nitrogen permeance yielding a high separation factor in the range of 10-125 depending on the feed flow rate, VOC and VOC concentration levels.
3. Highly VOC-enriched permeate stream (up to 80 %) could be obtained from a N_2 feed containing a relatively high concentration (5 %) of methanol vapor.
4. The innate advantages of this membrane compared to other membranes used in VOC removal and its optimal operational modes have resulted in a highly efficient performance for removing VOCs selectively from a N_2 stream.

A mathematical model-based work was avoided in chapter 3 of this thesis due to the difficulty of obtaining a concentration dependent permeance equation. Two possible suggestions are being made to solve this problem.

First, a very short module (e.g. effective fiber length : 6 cm ; # of fibers : 15)

may be used for the measurement of permeance of VOC as a function of its partial pressure. Since the membrane surface area is quite low in this case, the partial pressure of VOC along the module length can be maintained almost constant if the feed flow rate is maintained relatively high. Further the permeate vacuum level can be high. Secondly, permeance may also be measured using a high flow rate of helium sweep gas on the permeate side ; the flux of the VOC as well as that of N_2 through the membrane may be measured directly by means of a GC.

Further studies on VOC removal using this type of hollow fiber membrane should focus on :

(a) single VOC removal experiments for other VOCs such as acetone, methylene chloride and hydrocarbons in the vacuum mode of operation so that a broader performance spectrum is developed ;

(b) carrying out experiments with N_2 containing multiple VOCs ;

(c) exploration of VOC-separation employing a high pressure feed N_2 containing VOC on the shell side and permeate on the tube side.

Experimental pore condensation-based separation studies for the removal of VOCs from N_2 by a microporous γ-alumina ceramic membrane suggest the following conclusions :

1. Increasing partial pressure difference across the membrane yields a higher removal rate of VOCs but lower separation factor in vacuum as well as pressure modes of operation.
2. Transport mechanism of gas/vapor through this microporous ceramic membrane can be considered as a combination of surface flow and pore condensate flow.
3. Condensibility of xylene appeared to be higher than that of toluene leading to much better performance.

The following suggestions can be made for further studies of pore condensation-based separation for VOC removal from N_2 :

(a) explore pore condensation by modifying/reducing of ALCOA ceramic membrane pore size ;

(b) explore pore condensation with other membranes having a smaller pore size (< 20 Å) such as PPG glass fiber membrane.

This study showed that particular vapors (VICs or VOCs) can be removed selectively and preferentially by the nature of the membranes used. For example, when the feed contained water vapor (a VIC) and toluene (a VOC) together, Cuprophan hydrogel membrane which is highly hydrophilic by nature, could preferentially separate water vapor over toluene with a high selectivity. Similarly, this membrane was highly selective for water vapor over N_2. Flux of water vapor through Cuprophan membrane was an order of magnitude higher (14-88 times) than that of toluene (see table 2.9). On the other hand, hydrophobic silicone rubbery membrane could remove VOCs preferentially over water vapor. Permeance of methanol vapor through silicone-coated membrane was also an order of magnitude higher (24 times) than that of water vapor (see table 3.4). VOC selectivity over N_2 through this membrane was in the range of 10-125.

The permeance of the VOC toluene (figure 3.12) through the hydrophobic silicone-coated fiber was much higher than that of water vapor through the hydrogel Cuprophan membrane (figure 2.10). A major part of this must be ascribed to the thick homogeneous Cuprophan membrane (~10 μm wall thickness) compared to the ultrathin (~1 μm) silicone coating in the thin film composite membrane. However, one cannot also ignore the rubbery nature of the silicone membrane having a high chain mobility compared to the Cuprophan membrane having a cellulosic backbone and residual crystallinity.

Vapors appear to affect drastically the permeance of nonglassy polymeric membranes. Whether it is a hydrogel hydrophilic Cuprophan membrane exposed to water vapor or a hydrophobic silicone membrane exposed to solvent vapors, the permeance of

the membrane increases exponentially with the vapor concentration (figures 2.10 and 3.12). In this respect, both polymeric membranes, although fundamentally different, display similar permeation-based behaviors. Interestingly, the selectivity of the vapor vis-a-vis the inert gas N_2 increases with vapor concentration in both types of membranes. This is unlike the more conventional glassy polymeric membranes where plasticization or swelling reduce the selectivity considerably. If, however, the inert gas has a high solubility in the condensed vapor, one may not observe increased selectivity with increased vapor concentration (consider CO_2 and water vapor, figure 2.13).

Permeation through the Cuprophan membrane and the silicone-coated membrane continues regardless of the level of the partial pressure of the vapor. However, that is not true for pore condensation-based membrane (in the ceramic substrate) which does not exist unless the vapor partial pressure is significant. Thus for high levels of VOC and VIC removal from air/N_2, pore condensation does not appear to be attractive. Both permeation-based membranes are good in this respect. One has to temper this judgement by holding open the option that pore condensation may be a viable strategy provided the pores are sufficiently small.

APPENDIX A

PROGRAM FOR OBTAINING PERMEATOR OUTLET MOLE FRACTION OF WATER VAPOR

This computer program calculates the permeator outlet mole fraction of water vapor by solving the equation (2-9) provided in chapter 2.

```
c       This program calculates the feed outlet mole fraction of water vapor
        by solving the equation (2-9) provided in chapter 2.

        implicit real*8 (a-h,o-z)

c       Q = a * exp(b x), where Q is the permeance of water vapor, x is
        the average mole fraction of water vapor in the feed side and aa and
        b are regression coefficients, dlm is the logarithmic mean diameter
        of the fiber, zl is the effective fiber length of the module.
c       p is the total pressure of feed side which is 1 atmosphere.

        a=4.763e-10
        b=161.3
        pi=3.14159
        dlm=0.02108
        p=76
        zl=16.5

c       Read the experimental data from cha.dat. cl is the molar flow rate,
        mol/sec, xi and xfe are the feed inlet and feed outlet mole fractions
        of water vapor respectively.

        open (1,file='cha.dat',status='old')
        open (2,file='model.dat',status='new')
        do 10 i=1,16
        read (1,*) cl,xi,xfe

c       ck is a constant and the number of fibers are 50.
       cal subroutine calculate the estimated z value from a, b, ck,
        and zi

        ck=pi*dlm*P*50.0/cl
        call cal(a,b,ck,xi,zi)

c       The following program estimates the mole fraction of
        water vapor in the permeator outlet end

        xf=0.0
   70   xave=(xi+xf)/2.0
        call cal(a,b,ck,xave,zf)
        dz=(zf-zi)*(-1.0)-zl
        print *,xave,dz
        if (abs(dz).lt.0.001) goto 80
        if (dz.gt.0.0) then
        xf=xave
        else
        xi=xave
        endif
        go to 70

c       Print estimated results
c
  80    write (2,*) xf,xfe
        print *,'estimated feed outlet mole fraction = ',xf,xfe
  10    continue
        close (1,status='keep')
        close (2,status='keep')
        stop
        end
c
c       Subroutine to calculate lnx + bx/1/1! + (bx)**2/2/2! + (bx)**3/3/3! + ..
        subroutine cal(a,b,ck,x,z)
        implicit real*8 (a-h,o-z)
        integer*4 i,j,k,l
        zl=dlog(x)
c
```

```
c       Calculate bx/1/1! + (bx)**2/2/2! + (bx)**3/3/3! + .......
c
        v1=(-1.0)*b*x
        z2=0.0
        k=1
        do 20 j=1,500
        k=k*j
        v2=(v1**j)/j/k
        z2=z2+v2
        rat=v2/z2
c       print *,v2,z2
        if (abs(rat).lt.0.001) goto 50
   20   continue
c
c
   50   z=(z1+z2)/ck/a
        return
        end
```

APPPENDIX B

SAMPLE CALCULATIONS

Sample calculations for the performances of different membrane medules in terms of flux, percent removal, module-averaged permeance and separation factor are provided here.

1. Calculation of Flux, Percent Removal, Module-averaged Permeance of Water Vapor, and Water-N_2 Separation Factor for a Cuprophan Hollow Fiber Membrane Module

(a) Module Specifications (Module # 1)

# of Fibers : 50

Effective Fiber Length : 16.5 cm

I.D. of the Fiber : 200 μm

O.D. of the Fiber : 220 μm

Effective Surface Area (A) of the Module Based on Logarithmic Mean Diameter of the Fiber : (3.14) x [(220-200)/ln(220/200)] x 10^{-4} x (16.5) x (50) = 54.6 cm^2

(b) Experimental Data (Taken from Table 2.5)

Room Temperature : 21.7 °C

Vapor Pressure of Water at 21.7 °C : 19.47 mm Hg

F/I Flow Rate : 21.7 cc/min.

F/I Molar Flow Rate (F_i) : (1 atm) x (0.0217 l/min.)/[(0.082 atm.l/gmol.°K) x (273.15 + 21.7 °K)] = 8.975 x 10^{-4} gmol/min.

F/I Relative Humidity : 88.9 %

F/I Mole Fraction of Water Vapor (x_i) : (19.47) x (0.889)/760 = 0.02277

F/O Flow Rate : 21.2 cc/min.

F/O Molar Flow Rate (F_o) : 8.768 x 10^{-4} gmol/min.

F/O Relative Humidity : 34.3 %

F/O Mole Fraction of Water Vapor (x_o) : (19.47) x (0.343)/760 = 0.008786

Permeate molar flow rate (F_p) and mole fraction of water vapor (x_p) was calculated by mass balance :

$F_p = F_i - F_o = 8.975 \times 10^{-4} - 8.768 \times 10^{-4} = 2.07 \times 10^{-5}$ gmol/min.

$x_p = (F_i.x_i - F_o.x_o) / F_p = [(8.975 \times 10^{-4}) \times (0.02277) - (8.768 \times 10^{-4}) \times (0.008786)] / (2.07 \times 10^{-5}) = 0.6165$

* Flux of Water Vapor

$= F_p.x_p / A = (2.07 \times 10^{-5}) \times (0.6165) / (54.6) = 2.337 \times 10^{-7}$ gmol/min.cm^2

* Percent Removal of Water Vapor

$= (1 - F_o.x_o / F_i.x_i) \times 100$

$= [1 - (8.768 \times 10^{-4}) \times (0.008786) / (8.975 \times 10^{-4}) \times (0.02277)] \times 100$

$= 62.3\%$

* Module-averaged Permeance of Water Vapor (Q_w/δ_m)

Partial pressure difference of water vapor across the membrane $(\Delta p)_w$: permeate side partial pressure of water vapor was neglected due to very high vacuum level in the permeate side

$(\Delta p)_w = [(76) \times (0.02277) + (76) \times (0.008786)] / 2 = 1.199$ cm Hg

Permeance (Q_w/δ_m) = (Flux, gmol/min.cm^2) / [60 x $(\Delta p)_w$] = $(2.337 \times 10^{-7}) / (60 \times 1.199) = 3.249 \times 10^{-9}$ gmol/sec.cm^2.cm Hg

Corresponding nitrogen permeance (Q_{N2}/δ_m) by a similar calculation

$= 3.232 \times 10^{-11}$ gmol/sec.cm^2.cm Hg

* Separation Factor

$= (Q_w / Q_{N2}) = (3.249 \times 10^{-9}) / (3.232 \times 10^{-11}) = 100.5$

2. Calculation of Flux, Percent Removal, Module-Averaged Permeance, and Toluene-N_2 Separation Factor for Silicone-Coated Hollow Fiber Membrane Module

(a) Module Specification (Module # 2)

# of Fibers : 50

Effective Fiber Length : 25 cm

I.D. of the Fiber : 240 μm

O.D. of the Fiber : 290 μm

Effective Surface Area (A) of the Module Based on Logarithmic Mean Diameter of the Fiber : (3.14) x [(290-240) / ln (290/240)] x 10^{-4} x (50) x (25) = 103.76 cm^2

(b) Experimental Data (Taken from Table 3.5)

Temperature : 30 °C

Feed Side Pressure : 76 cm Hg

F/I Flow Rate : 58.9 cc/min.

F/I Molar Flow Rate (F_i) : (1 atm) x (0.0589 l/min.) / [(0.082 atm.l/gmol.°K) x (303.15 °K)] = 2.369 x 10^{-3} gmol/min.

F/I Mole Fraction of Toluene Vapor (x_i) : 0.01078

F/O Flow Rate : 54.2 cc/min.

F/O Molar Flow Rate (F_o) : (1 atm) x (0.0542 l/min.)/[(0.082 atm.l/gmol.°K) x (303.15 °K)] = 2.180 x 10^{-3} gmol/min.

F/O Mole Fraction of Toluene Vapor (x_o) : 0.000455

* Permeate Molar Flow Rate (F_p)

$$F_p = F_i - F_o = 2.369 \times 10^{-3} - 2.180 \times 10^{-3} = 1.89 \times 10^{-4} \text{ gmol/min.}$$

* Permeate Mole Fraction of Toluene Vapor (x_p)

$$x_p = (F_i.x_i - F_o.x_o) / F_p = [(2.369 \times 10^{-3}) \times (0.01078) - (2.18 \times 10^{-3}) \times (0.000455)] / 1.89 \times 10^{-4} = 0.13$$

* Flux of Toluene Vapor

$$= F_p.x_p / A = (1.89 \times 10^{-4}) \times (0.13) / 103.76$$

$$= 2.368 \times 10^{-7} \text{ gmol/min.cm}^2$$

* Percent Removal of Toluene Vapor

$$= (F_p.x_p / F_i.x_i) \times 100$$

$$= (1.89 \times 10^{-4}) \times (0.13) / [(2.369 \times 10^{-3}) \times (0.01078)] \times 100$$

$$= 96.2\ \%$$

* Module-Averaged Permeance of Toluene Vapor (Q_t/δ_m)

partial pressure difference of toluene vapor across the membrane

$$= [(76 \times 0.01078) + (76 \times 0.000455)] / 2 = 0.427 \text{ cm Hg}$$

$Q_t/\delta_m = (2.368 \times 10^{-7}) / (60 \times 0.427) = 9.243 \times 10^{-9}$ gmol/sec.cm^2.cm Hg

Corresponding nitrogen permeance by a similar calculation

$Q_{N2}/\delta_m = 3.444 \times 10^{-10}$ gmol/sec.cm^2.cm Hg

* Separation Factor (α)

$$\alpha = (Q_t / Q_{N2}) = 9.243 \times 10^{-9} / 3.444 \times 10^{-10} = 26.8$$

3. Calculation of Percent Removal of Toluene Vapor and Separation Factor in the Vacuum Mode of Operation using Microporous Tubular Ceramic Membrane

(a) Module Specifications (Module # 2)

I.D. of Membrane : 0.7 cm

O.D. of Membrane : 1.0 cm

Effective Length : 22.5 cm

Effective Surface Area : (3.14) x [(1.0-0.7) / ln (1.0/0.7)] x (22.5) x (1)

= 59.5 cm^2

(b) Experimental Data (Taken from Table 4.6)

Temperature : 25 °C

F/I Flow Rate : 26.3 cc/min.

F/I Molar Flow Rate (F_i) : (1 atm) x (0.0263 l/min.)/[(0.082 atm.l/gmol.°K) x (298 °K)] = 1.0763 x 10^{-3} gmol/min.

F/I Mole Fraction of Toluene Vapor (x_i) : 0.02167

F/O Flow Rate : 25.4 cc/min.

F/O Molar Flow Rate (F_o) : 1.039 x 10^{-3} gmol/min.

F/O Mole Fraction of Toluene Vapor (x_o) : 0.01614

Permeate molar flow rate (F_p gmol/min.) and mole fraction of toluene vapor (x_p) was calculated by mass balance :

$F_p = F_i - F_o = 1.0763 \times 10^{-3} - 1.039 \times 10^{-3} = 3.69 \times 10^{-5}$ gmol/min.

$x_p = (F_i.x_i - F_o.x_o) / F_p = [(1.0763 \times 10^{-3}) \times (0.02167) - (1.039 \times 10^{-3}) \times (0.01614)] / (3.69 \times 10^{-5}) = 0.1774$

* Percent Removal of Toluene Vapor

$$= (F_p.x_p / F_i.x_i) \times 100 = 28.1\ \%$$

* Separation factor was defined as a mole fraction ratio of toluene vapor and nitrogen in the permeate divided by that in the feed outlet :

$$\alpha = [x_p/(1-x_p)] / [x_o/(1-x_o)] = [x_p \cdot (1-x_o)] / [x_o \cdot (1-x_p)]$$

$$= (0.1774) \times (0.98386) / [(0.01614) \times (0.8226)] = 13.1$$

REFERENCES

Asaeda, M., and Du, L.D., "Separation of Alcohol/Water Gaseous Mixtures by Thin Ceramic Membrane", J. Chem. Eng. Japan, Vol.19, No.1, 1986, 72-77.

Ash, R., Barrer, R.M., Lawson, R.T., "Transport of single Gases and of Binary Gas Mixtures in a Microporous Carbon Membranes", J. Chem. Soc., Faraday Trans. I, 69, 1973, 2166-2178.

Baker, R.W., "Process for Recovering Organic Vapors from Air", United States Patent, 4,553,983, Nov. 18, 1988.

Baker, R.W., Yoshioka, N., Mohr, A.M., and Khan, A.J., "Separation of Organic Vapors from Air", J. Memb. Sci. 31, 1987, 259-272.

Barrie, J.A., Water in Polymers, Chapter 8 in Diffusion in Polymers, Crank, J., and Park, G.S. (Ed), Academic Press, London, 1968.

Behling, R.O., Ohlrogge, K., and Peinemann, K.V., "The Separation of Hydrocarbon from Waste Vapor Stream", AIChE Symp. Series. 85, (272), 1989, 68-73.

Blume, I., Schwering, P.J.F., Mulder, M.H.V., and Smolders, C.A., "Vapor Sorption and Permeation Properties of poly(dimethylsiloxane) Films", J. Memb. Sci. 61, 1991, 85-97.

Bonne, U., Deetz, D.W., Lai, J.H., Odde D.J., and Zook, J.D., "Membrane Dehumidification", U.S.P. 4,915,838, Apr.10. 1990.

Brunauer, S., The Adsorption of Gases and Vapors, Princeton Univ. Press, Vol.C-1, 1943.

Carman, P.C., "Diffusion and Flow of Gas and Vapors through Micropores", IV. Flow of Capillary Condensate", Proc. Roy. Soc. Ser., A211, 1952, 526-535.

Chern, R.T., Koros, W.J., and Fedkiw, P.S., "Simulation of a Hollow-Fiber Gas Separator: The Effect of Process and Design Variables", Ind. Eng. Chem. Process Des. Dev. 24, 1985, 1015-1022.

Collins, M.C., "Mass Transport through Polymeric Membranes", J. Phys. Chem. 89, 1985, 312-319.

Cussler, E.L., Wang, K.L., and McCray, S.H.,"Air Drying with Hollow Fibers", AIChE Preprints, Nov. '92, Florida, 1992, 866-870.

REFERENCES
(Continued)

Feng, X., Sourirajan, S., Tezel, F.H., and Matsuura, T., "Separation of Organic Vapor from Air by Aromatic Polyimide Membranes", J. Appl. Pol. Sci., 43, 1991, 1071-1079.

Feng, X., Sourirajan, S., Tezel, F.H., Matsuura, T., "Separation of Volatile Organic Compound/ Nitrogen Mixtures by Polymeric Membranes", Ind. Eng.Chem. Res. 32, 1993, 533-539.

Filho, G.R., Bueno, W.A., "Water State of Cuprophan (Hemodialysis Membrane)", J. Memb. Sci. 74, 1992, 19-27.

Gilliland, E.R., Baddour, R.F., and Russel, J.L., "Rates of Flow Through Microporous Solids", AIChE J. 4, No.1, 1958, 90-96.

Henis, J.M.S., and Tripodi, M.K., "Composite Hollow Fiber Membranes for Gas Separation : the Resistance Model Approach", J. Memb. Sci., 8, 1981, 233-246.

Hsieh, H.P., Inorganic Membranes, Sirkar, K.K., Lloyd, D.R.(Eds), New Membrane Materials and Processes for Separation, AIChE Symp. Series 261, Vol.84, 1988, 1-18.

Kim, S.S., Cha, J.S., Kim, J.J., Kim, E.Y., "Morphological Studies of Cellulose Acetate Hollow Fiber Membranes", J. Memb. Sci. 37, 1988, 113-129.

Kimmerle. K., Bell, C.M., Gudernatsch, W., and Chmiel,H., "Solvent Recovery from Air", J. Memb. Sci. 36, 1988, 477-488.

Koresh, J.E., Sofer, A., "Molecular Sieve Carbon Permselective Membrane. Part I. Presentation of a New Device for Gas Mixture Separation", Sep. Sci. & Tech., 18(8), 1983, 723-734.

Koros, W.J., Gas Separation, in "Membrane Saparation Systems : A Research Needs Assessment - Final Report", DOE/ER/30133-H1, Vol.2 of 2, 1990.

Krishnamoorthy, B., Saraf, D.N., "Study of Water Transport in Swelling Membranes", Indian Journal of Technology, 10, 1972, 59-62.

Lee, K.H., and Hwang, S.T., "The Transport of Condensible Vapors through a Microporous Vycor Glass Membrane", J. Colloid. Interface. Sci. 110, 1986, 544-555.

REFERENCES
(Continued)

Matson. S.L., Lopez, J., and Quinn, J.A., "Separation of Gases with Synthetic Membranes", Chem. Eng. Sci., Vol.38, No. 4, 1983, 503-524.

Notley,N.T., "Permeability to Oxygen of Cellophan Laminates", J. Appl. Chem., Lond., 13, 1963, 107-111.

Pan, C.Y., Jensen, C.D., Bielech, C., and Habgood, H.W., "Permeation of Water Vapor through Cellulose Triacetate Membranes in Hollow Fiber Form", J. Appl. Poly. Sci., 22, 1978, 2307-2323.

Papadopoulos, H., "Further Studies on Hollow Fiber Contained Liquid Membrane Separation of Gas and Liquid Mixtures", Ph.D. Dissertation, Stevens Inst. of Tech., Hoboken, NJ 1992.

Paul, H., Philipsen, C., Gerner, F.J., and Strathmann, H., "Removal of Organic Vapors from Air by Selective Membrane Permeation", J. Memb. Sci., 36, 1988, 363-372.

Peinemann, K.V., Mohr, J.M., Baker, R.W., "The Separation of Organic Vapors from Air", AIChE. Symp.Series, 82 (250), 1986, 19-26.

Perry, R. H., Green, D. W., Perry's Chemical Engineers Handbook, 6th ed., 1984, 3-99.

Pilar, F.L., "The Flow of Gases through High Polymer Films in Equilibrium with Sorbed Vapors", J. Polym. Sci. 45, 1960, 205-215.

Qiu, M., and Hwang, S.T., "Continuous Vapor-Gas Separation with a Porous Membrane Permeation System", J. Memb. Sci., 59, 1991, 53-72.

Rhim, H., and Hwang, S.T., "Transport of Capillary Condensate", J. Colloid Interface Sci., 52, 1975, 174-181.

Ruddy, E.N., and Carroll, L.A.,"Select the Best VOC Control Strategy", Chem. Eng. Prog., July, 1993, 28-35.

Sander, U., Janssen, H., "Industrial Application of Vapor Permeation", J. Memb. Sci. 61, 1991, 113-129.

Sengupta, A., and Sirkar, K.K., Membrane Gas Separation, in Progress in Filtration and Separation 4, 289-415, Wakeman, R.J. (Ed.), Elsevier Science Publishers, Amsterdam, 1986.

REFERENCES
(Continued)

Sperry, D.S., Falconer, J.L., and Noble, R. D., "Methanol-Hydrogen Separation by Capillary Condensation in Inorganic Membranes", J. Memb. Sci., 60, 1991, 185-193.

Stamm, A.J., "Diffusion of Water into Uncoated Cellulose, II. From Steady-State Diffusion Measurements", J. Phys. Chem. Wash., 60, 1956, 83-86.

Stern, S. A., Frisch, H. L., "The Selective Permeation of Gases through Polymers", Ann. Rev. Mater. Sci., 11, 1981, 523.

Strathmann, H., Bell, C.M., and Kimmerle, K., "Development of Synthetic Membranes for Gas and Vapor Separation", Pure & Appl.Chem. 58, No.12 1986, 1663-1668.

Tamon, H., Okazaki, M., and Toei, R., "Flow Mechanism of Adsorbate through Porous Media in Presence of Capillary Condensation", AIChE J. 27 No.2, 1981, 271-277.

Uhlhorn, R.J.R., Keizer, K., and Burggraaf, A.J., "Gas Transport and Separation Properties of Ceramic Membranes with Pores of Molecular Dimensions", Proceedings of ICOM '90, 1990, 451-453.

Urquhart, A.R., Moisture in Textiles, Hearle, J.W.S., and Peters, R.H. (Eds.), Butterworths, London, 1960, p.14.

Valentine, L., "Studies on the Sorption of Moisture by Polymers I.Effect of Crystallinity", J. Polym. Sci. 27, 1958, 313-333.

Ward, R.A., Feldhoff, P.W., and Klein, E., Membrane Materials for Therapeutic Applications in Medicine, Lloyd, D.R. (Ed.), Materials Science of Synthetic Membranes, ACS Symp.Series 269, Washington, 1985, 99-118.

Way, J.D., and Roberts, D.L., "Hollow Fiber Inorganic Membranes for Gas Separations", Sep. Sci.& Tech., 1991.

Wijmans, J.G., and Helm, V.D., "A Membrane System for the Separation and Recovery of Organic Vapors from Gas Streams", AIChE Symp. Series 272. 85, 1989, 74-79.

Yasuda, H., and Stannett, V., "Permeation, Solution, and Diffusion of Water in Some High Polymers", J. Polym. Sci. 57, 1962, 907-923.